FRAGILITY BASED ASSESSMENT OF LOW–RISE AND MID–RISE REINFORCED CONCRETE FRAME BUILDINGS IN TURKEY

A THESIS SUBMITTED TO
THE GRADUATE SCHOOL OF NATURAL AND APPLIED SCIENCES
OF
MIDDLE EAST TECHNICAL UNIVERSITY

BY

BEKİR ÖZER AY

IN PARTIAL FULFILLMENT OF THE REQUIREMENTS
FOR
THE DEGREE OF MASTER OF SCIENCE
IN
CIVIL ENGINEERING

AUGUST 2006

Approval of the Graduate School of Natural and Applied Sciences

_____

Prof. Dr. Canan ÖZGEN
Director

I certify that this thesis satisfies all the requirements as a thesis for the degree of Master of Science.

_____

Prof. Dr. Erdal ÇOKÇA
Head of Department

This is to certify that we have read this thesis and that in our opinion it is fully adequate, in scope and quality, as a thesis for the degree of Master of Science.

_____

Asst. Prof. Dr. Murat Altuğ ERBERİK
Supervisor

Examining Committee Members

Prof. Dr. Haluk Sucuoğlu	(METU, CE)	_____
Asst. Prof. Dr. Murat Altuğ Erberik	(METU, CE)	_____
Assoc. Prof. Dr. Dede Sinan Akkar	(METU, CE)	_____
Assoc. Prof. Dr. Ahmet Yakut	(METU, CE)	_____
Dr. Mustafa Tolga Yılmaz	(METU, ES)	_____

I hereby declare that all information in this document has been obtained and presented in accordance with academic rules and ethical conduct. I also declare that, as required by these rules and conduct, I have fully cited and referenced all material and results that are not original to this work.

Name, Last name: Bekir Özer Ay

Signature :

ABSTRACT

FRAGILITY BASED ASSESSMENT OF LOW–RISE AND MID–RISE REINFORCED CONCRETE FRAME BUILDINGS IN TURKEY

Ay, Bekir Özer
M.S., Department of Civil Engineering
Supervisor: Asst. Prof. Dr. Murat Altuğ Erberik

August 2006, 145 pages

In this study, structural vulnerability of reinforced concrete frame structures by considering the country–specific characteristics is investigated to manage the earthquake risk and to develop strategies for disaster mitigation. Low–rise and mid–rise reinforced concrete structures, which constitute approximately 75% of the total building stock in Turkey, are focused in this fragility–based assessment. The seismic design of 3, 5, 7 and 9–story reinforced concrete frame structures are carried out according to the current earthquake codes and two dimensional analytical models are formed accordingly. The uncertainty in material variability is taken into account in the formation of structural simulations. Frame structures are categorized as poor, typical or superior according to the specific characteristics of construction practice and the observed seismic performance after major earthquakes in Turkey. The demand statistics in terms of maximum interstory drift ratio are obtained for different sets of ground motion records. The capacity is determined in terms of limit states and the corresponding fragility curves are obtained from the probability of exceeding each limit state for different levels of

ground shaking. The results are promising in the sense that the inherent structural deficiencies are reflected in the final fragility functions.

Consequently, this study provides a reliable fragility–based database for earthquake damage and loss estimation of reinforced concrete building stock in urban areas of Turkey.

Keywords: RC frame structures, structural deficiencies, fragility curve, seismic demand, material variability, seismic intensity.

ÖZ

TÜRKİYE'DEKİ AZ VE ORTA KATLI BETONARME ÇERÇEVELİ BİNALARIN HASARGÖREBİLİRLİĞİNİN İNCELENMESİ

Ay, Bekir Özer
Yüksek Lisans, İnşaat Mühendisliği Bölümü
Tez Yöneticisi: Yrd. Doç. Dr. Murat Altuğ Erberik

Ağustos 2006, 145 sayfa

Betonarme çerçeveli yapıların hasargörebilirliği, deprem riskinin tahmini ve olası etkilerinin hafifletilmesi için yerel yapı karakteristiği ve bina envanteri göz önüne alınarak belirlenmiştir. Bu hasargörebilirlik çalışması, ülkemizdeki yapı stokunun yaklaşık %75'ini oluşturan ve genellikle konut amaçlı kullanılan az ve orta katlı betonarme çerçeveli yapı sistemlerinin değerlendirilmesini içermektedir. 3, 5, 7 ve 9 katlı betonarme çerçeveli yapıların mevcut deprem yönetmeliklerine uygun olarak sismik tasarımı yapılmış ve bu yapılara ait iki boyutlu analitik modeller hazırlanmıştır. Malzeme değişkenliğindeki belirsizlikler yapı simülasyonlarının oluşturulmasında göz önüne alınmış, bu modeller ülkemize özgü yapı karakteristikleri ve büyük depremler sonrası elde edilen sismik performans gerçekleri doğrultusunda yetersiz, olağan veya iyi kalitede olmak üzere sınıflandırılmıştır. Yapıların farklı deprem grupları için hesaplanmış talep istatistikleri katlararası ötelenme oranı ile ifade edilmiştir. Yapısal kapasite ise hasar sınırları ile tanımlanmıştır. Hasargörebilirlik eğrileri her bir yapı sınıfı için oluşturulmuştur. Ortaya çıkan sonuçların ışığında çerçeveli betonarme

sistemlerinin doğasındaki yapısal zayıflıklar hasar potansiyeli fonksiyonları ile yansıtılmıştır.

Sonuç olarak bu araştırma projesi önümüzdeki dönemde ülkemizde özellikle kentsel alanlarda yapılacak deprem hasar ve kayıplarının tahminine ilişkin çalışmalar için güvenilir bir hasar potansiyeli veri tabanı oluşacaktır.

Anahtar Sözcükler: Betonarme çerçeveli yapılar, yapısal zayıflıklar, hasargörebilirlik eğrisi, sismik talep, malzeme değişkenliği, sismik şiddet.

To My Parents

ACKNOWLEDGMENTS

This study was carried out under the supervision of Asst. Prof. Dr. Murat Altuğ Erberik. I gratefully appreciate his guidance, criticism, advice, encouragements and understanding throughout this study.

I want to thank Assoc. Prof. Dr. Dede Sinan Akkar for his invaluable support during this research.

I also owe thanks to Soner Baş, Hazım Yılmaz and Deniz Toz for their friendship and support whenever I needed.

Başak Türkeç deserves special thanks for her patience and understanding in the most difficult period of this study.

This study was supported by The Scientific Research and Technical Council of Turkey (TUBİTAK), Project No: 104M565.

Finally, I would like to express my deepest appreciation to my parents Hasan Hüseyin Ay and Güler Ay for their love, encouragement, support, and understanding throughout my whole life.

TABLE OF CONTENTS

LIST OF TABLES

LIST OF FIGURES

CHAPTER 1

INTRODUCTION

1.1 GENERAL

The earthquakes that have occurred in Turkey within the last ten years caused much tragic life and monetary losses. Due to these earthquakes, cost of damage have scaled up with the loss in production and resulted in strokes for Turkish economy. The high population density near or on the fault zones is an indicator of potential future disasters. Hence a multidisciplinary and comprehensive study should be conducted in order to estimate possible earthquake hazard and develop strategies to mitigate losses. The part of such a study related to structural engineering is fragility assessment of Turkish building stock.

Earthquake hazard identification and structural vulnerability evaluation are the main components of earthquake risk assessment. Earthquake hazard identification is out of the scope of this study. Structural vulnerability evaluation is the subject of civil engineering and city planning disciplines and aims to determine, classify, and assess the fragility of existing building stock and other structures (dams, bridges, power plants, etc.).

For disaster management purposes, a fragility based assessment that considers local structural properties is required. However, local conditions are usually ignored and vulnerability based assessment studies for structures in different countries are adapted to earthquake hazard estimation and disaster mitigation projects in Turkey.

Unfortunately, differences in structural characteristics cause significant deviations on damage and loss estimation by influencing the resulting fragility curves.

The aim of this study is to provide fragility information to inquire effects of ground motion parameters and Turkish construction practice state on structural vulnerability. After the devastating earthquakes that occurred within the last decade, a well organized and comprehensive database for reinforced concrete (RC) residential buildings in Turkey has been gathered. The data regarding damaged structures during earthquakes is collected particularly since this information is planned to be used for statistical surveys afterwards. Making use of this comprehensive database, this study is deemed to be a benchmark for future studies on earthquake damage and loss estimation in urban areas in Turkey.

1.2 GENERAL STATE OF TURKISH CONSTRUCTION PRACTICE

Despite the popularity of steel structures due to the up rising passion of humankind, RC with the ease of application for ordinary structures, in–site forming ability, and raw material abundance, is the most popular construction technique of the 21st century, not only in Turkey but also all over the world. Moreover, due to inexperienced staff and cursory workmanship in Turkey, it turns into a fast and cheap construction technique.

Fast growing population, urbanization endeavor, and insistent need for residential structures have caused an increase both in population that lives on seismic areas and in poor quality building stock that is constructed without any regulations or supervision. People that immigrate to urban areas have used RC as a cheap construction material to build residential houses without any earthquake resistance considerations. Expecting a satisfactory earthquake behavior from structures that are built by inexperienced and unqualified people with such a mentality is impossible. Also, there are examples of collapses due to even gravity loads in Turkey (Karaesmen, 2002).

Besides inconsiderate owners and supervisors, the governments, for consideration of vote, have declared amnesties to legalize buildings which do not obey current code regulations. In turn, these encouraged non–engineered and seismically unsafe construction in all earthquake prone regions of Turkey. The investigation of severely damaged or collapsed RC structures that have caused loss of lives and money after earthquakes in Turkey revealed that most of them do not fulfill code requirements and have both architectural and structural issues. Figure 1.1 and 1.2 show examples of mid–rise structures collapsed during 1999 Kocaeli Earthquake.

Figure 1.1 Air photo after 17 August 1999 Kocaeli Earthquake (courtesy of, METU–GISAM)

RC structures in Turkey are usually moment resisting frames with inadequate lateral resistance and strength; poor reinforcement detailing against earthquake forces and low quality, low strength concrete. Moreover, most of these structures have soft stories, weak stories, short columns and strong beam weak–column joints that cause a building stock vulnerable to seismic action (Özcebe et al., 2002).

Figure 1.2 Almost fully collapsed avenue during 17 August Kocaeli Earthquake (courtesy of, METU–GISAM)

Structural deficiencies of RC building stock in Turkey can be classified in three groups: Design deficiencies, detailing deficiencies and constructional deficiencies (Tankut, 1999).

Design Deficiencies: In Turkey, in rural and even in urban areas, it is sometimes difficult to encounter engineered structures. Unfortunately, most of the engineers and architects are not familiar with earthquake resistant design. The deficiencies due to improper choice of architectural and structural systems can be listed as follows:

- Low lateral resistance and redundancy
- Irregularities in plan and elevation
- Soft story, weak story
- Short Column
- Overhangs
- Strong beam–weak column joints etc.

Among these deficiencies, soft story formation is the most common problem regarding the existing building stock in Turkey. Furthermore, sudden changes in stiffness and/or strength in the elevation or in the plan of the structure cause concentrations of high inelastic deformations around the region of discontinuity. Such excessive deformations cause damage and even lead to local instability problems. Another issue is the inadequacy of the lateral resistance of the structure so that it cannot withstand the earthquake forces. Lack of redundancy is also a related problem which hinders the redistribution of earthquake lateral forces within the structure in the case of a local failure. Strong beam–weak column concept leads to undesired hinging mechanisms in the structure which cause excessive deformations and damage in critical members. The field observations after recent earthquakes have revealed the fact that almost all the buildings that were severely damaged or collapsed have one of the aforementioned deficiencies or a combination of them.

Detailing deficiencies: The basic principle of detailing is to provide the necessary strength and ductility at critical sections of structural members and at beam-column joints (Özcebe et al., 2003). Detailing deficiencies occur mostly due to tendency to violate the code provisions about detailing of members or to disregard the detailing in the design drawings both intentionally and due to ignorance. These deficiencies can be listed as follows:

- Insufficient transverse reinforcement
- Insufficient spliced length of bars
- Insufficient beam–column joint reinforcement etc.

Constructional deficiencies: Incorrect site applications due to the lack of supervision and careless contractors result in structures different than initial architectural and engineering design. Some of the constructional deficiencies in Turkish RC build stock are:

- Unqualified workmanship and inferior material quality
- Addition of new members which are not considered in the design stage
- Omission of some structural members that have been considered in the design stage and that are critical for the lateral resistance of the structural system
- Different member sizes that does not comply with the original design drawings
- Insufficient and wrong reinforcement applications etc.

1.3 LITERATURE SURVEY

Fragility curves are structural response functions that yield the probability of exceeding a limit state at a given seismic hazard level. These curves are frequently used tools of performance–based seismic design methods which have been developed recently for designing new buildings and assessing performance of existing buildings in many earthquake prone regions of the world.

There are various ways from simple to complex to obtain fragility curves. Certainly, using simple methods gives approximate fragility information whereas complex methods result in realistic and more definite fragility curves.

One of the simplest methods of obtaining fragility curves is to use expert opinion. The most systematic study using this method is conducted by Applied Technology Council (ATC) in the USA and the results are submitted in ATC–13 report (Applied Technology Council, 1985). Fragility curves of 40 different structural types are obtained with opinion of 58 experts. Basically, the estimations of experts about the damage states of the structures at different seismic hazard levels are obtained and the results are submitted as probability matrices. Apparently, the disadvantage of this method is the subjective data based on personal opinion of experts. The subjectivity of expert opinion is included besides the randomness of the ground motion and the uncertainty in the structural response. In spite of this

disadvantage, several studies (Cardona and Yamin, 1997; King et al., 1997) not only followed this method but also used the fragility curves given in ATC–13. Most significant of these studies is HAZUS Earthquake Loss Estimation Methodology (National Institute of Building Sciences, 1999). The only difference between HAZUS and the former ATC–13 is that HAZUS is based on expert opinion and it uses spectral acceleration and displacement as the ground motion parameter instead of Modified Mercalli Intensity scale employed in ATC–13.

Another way of obtaining fragility information is to observe the actual post–earthquake structural damage. Hence the information concerning observed damage can be collected and statistically converted to fragility curves. This approach is suitable for structures with little engineering intervention like masonry structures. One of the early studies that was based on this method investigated the structural damage of 5–story buildings after the San Fernando earthquake, 1971 in California. This study obtained fragility curves based on the actual statistical structural damage database (Whitman et al., 1974). In 1989, a similar study was conducted by Swiss Insurance Company, investigating the 1978 Albstadt (Germany) and the 1985 Chile earthquakes (Porro and Schraft, 1989). In a recent fragility research, damage of RC structures after 19 different earthquakes has been observed and used (Rossetto and Elnashai, 2003). However, researchers stated the difficulties about systematic grouping of the structural responses observed by different expert groups after each earthquake, although they have a comprehensive database.

Using experimental data is an alternative way of obtaining fragility curves. Recently, the increasing possibilities of testing big scale and realistic experimental models have caused research interest to shift toward experimental data. However, big scale realistic experiments have both time and economic limitations and difficulties. Since testing numerous models is not practically feasible, parametric study is nearly impossible. Consequently, experimental studies are performed to establish the vulnerability of structural elements (RC column, beam, shear wall,

masonry wall) rather than assessing the vulnerability of structures (Chong and Soong, 2000; Constantinou et al., 2000).

Most common way of obtaining fragility curves is to use analytical models and structural simulations. In the absence of experimental or observational data and expert opinion, the only way of investigating structural vulnerability is to use analytical methods. The advantage of employing analytical methods is the possibility of executing numerous structural analyses. In the case of analytical methods, structural simulations and corresponding algorithms are important. The simplest structural model is single–degree–of–freedom (SDOF) system. Simple SDOF model with only few parameters enables the computation of numerous analyses in a short period of time. Hence SDOF models have been used by many researchers (Ibarra, 2003; Jeong and Elnashai, 2004). Figure 1.3 shows fragility curves of brick infilled RC frame structures obtained by Mosalam et al. (1997) using similar analytical methods.

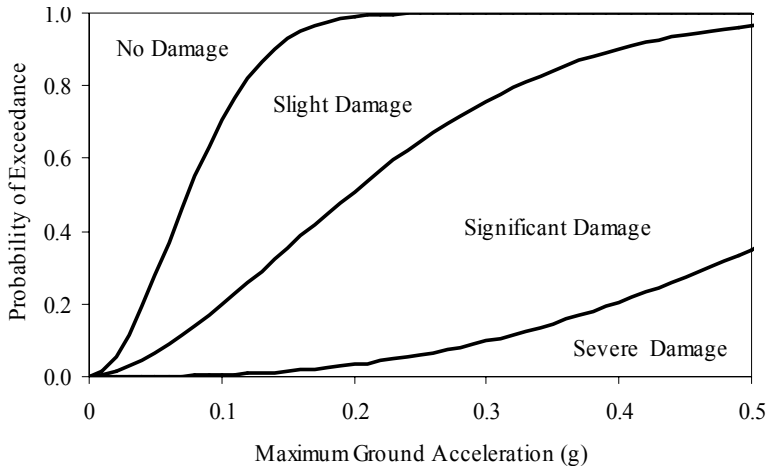

Figure 1.3 Fragility curves of brick infilled RC Structures (Mosalam et al., 1997)

Although it is easy to obtain huge response statistics in a short period of time by using simple models (such as SDOF models), inspection of real structural response

and damage distribution is not possible. Usually, detailed models and finite element programs are employed to obtain the response of a structure that does not show simple frame behavior or has particular properties. It is usually preferred to conduct elastic or inelastic time–history analysis in such cases. Studies about flat–slab structures that behave different than usual frame structures are such examples (Erberik and Elnashai, 2004; Hueste and Bai, 2004). Fragility curves obtained by Erberik and Elnashai are given in Figure 1.4. Moreover, such detailed models and analysis methods have been recently used to obtain fragility information for low, mid, and high–rise structures that have properties similar to buildings in USA (Wen et al., 2003; Hwang and Huo, 1997; Singhal and Kiremidjian, 1997). However, time–history analysis is very complicated and time consuming. Such difficulties make the researchers tend to use methods based on spectral analysis. Most popular one of the spectral methods is Capacity Spectrum Method. In Capacity Spectrum Method, static pushover results of the structure are used together with elastic (or inelastic) spectrum results in order to obtain a target performance level for the structure (Sinozuka et al., 2000; Barron–Corvera, 2000).

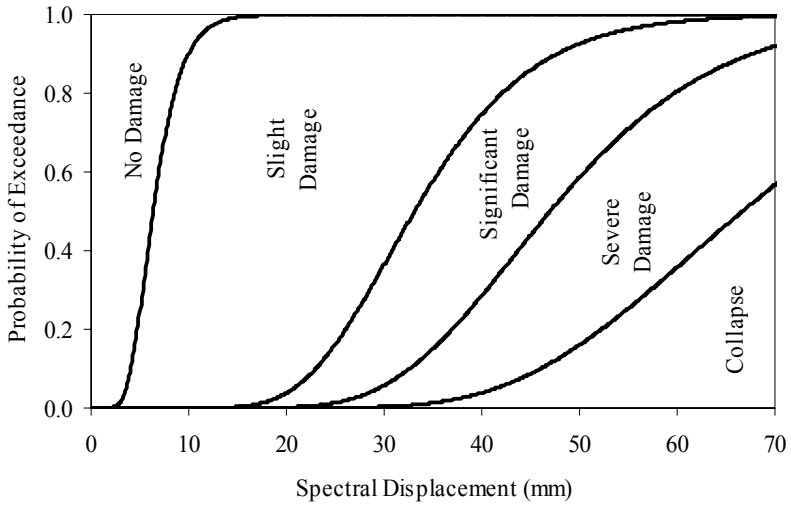

Figure 1.4 Fragility curves of mid–rise RC flat–slab structures (Erberik and Elnashai, 2004)

There are also some analytical fragility studies conducted recently in Turkey. In terms of SDOF analysis, Akkar et al. (2005) utilized 32 sample buildings to represent the general characteristics of 2–story to 5–story Turkish substandard RC building stock. In this study, field data are employed to obtain building capacities, and time–history analyses are used to calculate dynamic responses in order to obtain fragility information of ordinary RC buildings in Turkey. Erberik and Çullu (2006) investigated the sensitivity of different parameters and approaches on the fragility of low–rise and mid–rise RC frame structures with story number between 2 and 6 from the same field database. A similar fragility study using SDOF models is conducted for 5–story RC moment resisting frames to assess the vulnerability of buildings in Turkey at different levels of damage with respect to the site class (Baykal and Kırçıl, 2006). Fragility analyses based on multi–degree–of–freedom (MDOF) systems have also been employed by some researchers. The study of Kırçıl and Polat (2006) aimed to obtain fragility curves for mid–rise RC frame buildings in Istanbul, and employed MDOF models of 3, 5, and 7–story buildings.

1.4 OBJECTIVE AND SCOPE

Earthquake damage and loss estimation studies in Turkey usually refer to international research results since generation of realistic fragility data for building structures is a complicated and demanding task. International studies are directly adapted to estimate the fragility of Turkish building stock or some simple approaches are applied to transform the fragility data to meet the structural requirements of RC frame construction in Turkey. However the problem is that, there exist significant differences between structural characteristics in Turkey and countries for which these fragility curves are generated. Hence considering inherent structural characteristics in Turkey and obtaining fragility curves in accordance with these is compulsory to estimate earthquake damage and loss in Turkey.

Taking into account the results and limitations of previous research as discussed in the literature survey, this study aims at generating the fragility curves for low–rise

and mid–rise RC residential frame buildings in Turkey. The frame buildings are classified as poor, typical and superior according to the inherent characteristics and deficiencies of construction practice and the observed post–earthquake seismic performance. Planar analytical models are employed to represent the frame buildings considered since they are symmetric and regular in plan and elevation. The analysis method to obtain the response statistics is time–history analysis. The material variability is also taken into account in the formation of structural simulations. The fragility curves generated at the final phase of the study provide a reliable database for earthquake damage and loss estimation of RC concrete building stock in Turkey.

The study is composed of seven chapters. First chapter gives a general overview of the study and includes a literature survey on fragility of RC frame buildings.

Chapter 2 describes fragility analysis of RC moment resisting frames in a general manner. Parameters affecting fragility of individual buildings and sources of structural uncertainty are given accompanying with sampling techniques and limit states.

Design and analysis considerations of the selected RC buildings are given in Chapter 3. Furthermore, current code requirements and qualifications are presented in this chapter.

Chapter 4 summarizes building subclass definitions with respect to material properties and structural parameters. In this chapter determination of hysteretic behavior and material variability are given.

Chapter 5 presents fragility curve generation in terms of ground motion selection and characterization, structural simulation, limit state attainment, and determination of the probability of exceedance of each limit state at a given hazard intensity.

The fragility information generated for damage estimation studies of actual RC frame structures is employed in Chapter 6. The selected study region is the Fatih district in Istanbul.

Finally, Chapter 7 is devoted to summary and conclusion of fragility information obtained. Recommendations for future studies are also given in this chapter.

CHAPTER 2

FRAGILITY ANALYSIS

2.1 DEFINITION OF FRAGILITY

In most basic terms, fragility is a measure of the proneness of a structure to be damaged (Corvera, 2000). Determination of fragility includes the investigation of the seismic performance of a class or population of buildings when subjected to ground motion records with a wide range of characteristics. Since neither the characteristics of potential near future earthquakes nor the actual performance of structures under consideration are exactly known, fragility analysis has to be performed in a probabilistic way that involves record–to–record ground motion variability along with a probabilistic evaluation of response.

Fragility represents the probability that the response of the structure "R" exceeds the limit state "LS" given the hazard intensity "HI" on an individual structure or a population of structures. This statement can be written in mathematical form as follows:

$$\text{Fragility} = P\left[R \geq LS \middle| HI\right] \tag{2.1}$$

In Equation 2.1, "R" is the selected response parameter (deformation, force, velocity, etc.) and "LS" stands for the limiting value of the response parameter that is correlated with damage. The abbreviation "HI" is the hazard intensity, which is obtained from the seismic hazard on site.

There are two approaches in order to express the probability of exceeding the limit states (i.e. fragility): Damage Probability Matrix (DPM) or fragility curve. DPM is the tabular presentation of distribution of damage and it specifies the discrete probabilities of reaching a damage state at different ground motion intensities. DPM type of fragility representation is out of the scope of this study. On the other hand, fragility curves provide graphical information of the damage distribution. In other words, fragility curves provide the same information as a DPM does but the only difference is that fragility represents the cumulative distribution of damage specifying the continuous probability that the limit state under consideration is satisfied or exceeded.

2.2 PARAMETERS CONTRIBUTING TO FRAGILITY OF STRUCTURES

To define the fragility of structures, three types of parameters are involved. These parameters are as follows:

1. The ground motion (or hazard) parameters,
2. Structural input parameters,
3. Response (damage) parameters, indicating performance of structural capacity subjected to a specific demand.

The limit states, which represent different levels of damage, should also be in terms of the response parameter. The most commonly used hazard, input and response parameters are introduced next.

2.2.1 GROUND MOTION (HAZARD) PARAMETERS

The selection of the fragility hazard parameter is an important issue since the selected parameter should describe the potential ability of the motion to cause structural damage. In a general perspective, it is appropriate to classify hazard parameters as descriptive and quantitative. Quantitative parameters can further be

classified as peak value, energy and spectral parameters as suggested by Mostafa (2003).

Modified Mercalli Intensity (MMI) is one of the most common examples of descriptive parameters. It is a qualitative measure regarding the size of the earthquake in terms of observed damage and human reactions. The advantage of using MMI is that an extensive damage database in terms of this parameter is available since it has been used for a long time. On the other hand, it involves uncertainties, because it is a highly subjective measure and depends on personal judgment to a great extent.

Peak ground acceleration (PGA) and peak ground velocity (PGV) are well known peak value parameters. It is very easy to obtain them directly from time history records. Both of these ground motion parameters are frequently used in fragility analysis. However PGV is considered as a more reliable indicator of strong motion intensity than PGA (Sucuoğlu and Erberik, 1998). The observations indicate that PGV is more capable of reflecting the deformation demands on structures that behave in the inelastic range (Akkar and Özen, 2005).

Ratio of PGV to PGA (V/A) is still a simple parameter to obtain, but it is more enhanced when compared to PGA or PGV alone. For impulsive type of records, the ratio V/A indicates the average duration of the dominant acceleration pulse where the maximum values occur simultaneously and for harmonic type of records, it stands for the inverse of the dominant circular frequency (Sucuoğlu and Nurtuğ, 1995). However, it is not a well–established parameter to be used in fragility analysis.

Effective peak acceleration (EPA) is defined as the average of the spectral acceleration (S_a) in the period interval $0.1<T<0.5$ seconds, divided by a constant value 2.5, which is accepted as a global acceleration response amplification factor

for 5% damped SDOF systems in the acceleration–sensitive range of response spectra. Such a definition is obviously difficult to quantify.

Energy Index (EI) is based on total input energy as a measure of ground motion intensity or its damage potential. EI is obtained with the following expression (Sucuoğlu et al., 1999).

$$EI = \frac{1}{T_{max}} \int_0^{T_{max}} V_{eq}(T)dT \tag{2.2}$$

The parameter T_{max} in Equation 2.2 is an upper bound for the natural period of SDOF systems regarding the definition of the index and V_{eq} is the input energy equivalent velocity and it is defined by Equation 2.3.

$$V_{eq} = \sqrt{\frac{2E_i(T)}{m}} \tag{2.3}$$

In Equation 2.3, E_i represents the input energy of a linear viscously damped SDOF system and m denotes the mass of the system. Previous studies have shown that EI is an effective measure of the damage potential of ground motion records since it takes into account many basic ground motion characteristics. On the other hand, it is not an easy parameter to obtain and to employ in fragility analysis.

The duration of ground motion which contributes to the significant part of the vibratory response of SDOF systems is called the effective duration, t_{eff}. There exist various definitions of t_{eff}. The most commonly used definition is proposed by Trifunac and Brady (1975) and it is the time interval where 90% contribution of the Arias intensity (AI) takes place. The 90% contribution is selected as the time interval between 5% and 95% of the Husid plots that are used for computing AI. The parameter AI is described by Equation 2.4.

$$AI(t) = \frac{\pi}{2g}\int_0^t f^2(t)\,dt \qquad (2.4)$$

In Equation 2.4, f(t) represents the time history of ground acceleration. Effective duration has not been used before as the fragility hazard parameter, and it has been stated that the parameters based on strong motion duration show very low correlation with the observed damage (Mostafa, 2003).

Other than the parameters discussed above, spectral parameters like spectral acceleration (S_a) and spectral displacement (S_d) have also been used in fragility studies. However, since these are period dependent response parameters, their exact definition plays an important role in the interpretation of the resulting fragility curves. As an example, in the commonly used loss estimation software HAZUS (National Institute of Building Sciences, 1999), the fragility functions are based on damped elastic spectral displacement at the intersection of the pushover curve and the earthquake response spectrum, $S_d(T_c)$ whereas most of the other studies employ damped elastic spectral displacement at the fundamental period of the structure, $S_d(T_o)$. This discrepancy has been discussed elsewhere (Erberik and Elnashai, 2006) and may lead to misinterpretation in terms of the fragility functions obtained.

2.2.2 STRUCTURAL INPUT PARAMETERS

For an adequate estimation of the uncertainty in response, certain variables which are deemed to influence the fragility of structures should be taken as random input variables. Each of these parameters has its own statistical distribution. The selection of these input parameters is based on the fragility generation approach and output variable of interest.

For fragility estimation, two different approaches can be considered. In the first approach, fragility studies are conducted for a class or population of buildings by

using the statistical properties of that population. Simple SDOF models, that are equivalent to the complex structures, are employed in this approach. Hence there are only a few input parameters to be considered. The period and strength ratio are the main SDOF input parameters to simulate stiffness and strength of the equivalent structural model, respectively. Strength ratio is defined as the ratio of lateral yield strength to the total weight of the structure. This is a convenient parameter that is extensively used in seismic design practice. Secondary SDOF input parameters can be considered as the post elastic stiffness (or slope) as a fraction of the elastic stiffness, strength degradation and pinching parameters if a complex force–deformation relationship is used in the analysis. The advantage of equivalent SDOF model approach is that it is simple and feasible from computational time point of view. However, the results computed would be crude and the limitations of the models should be clearly understood. This approach has been used by different researchers (Jeong and Elnashai, 2004; Akkar et al., 2005; Erberik and Çullu, 2006).

In the second approach of fragility estimation, each building in the stock is investigated individually and the vulnerability of the building stock is obtained by combining the fragility information associated with each building. Very detailed planar or even three–dimensional models are employed; hence the results would be highly accurate. In the case of RC frame type of structures, the most important material parameters influencing the fragility are in terms of strength and stiffness (for concrete and reinforcement) characteristics of the structural components. In some cases, spatial distribution of material parameters may also affect the fragility analysis. For instance, spatial distribution of concrete strength may be considered since this is meaningful in real practice where an RC frame would be constructed story by story. If time–history analysis is employed for structural simulations, for a prescribed building geometry and member dimensions, building mass and viscous damping characteristics also play a significant role in the development of fragility information for structural systems. The consideration of material variability in building structures will be discussed in detail in Chapter 4.

2.2.3 RESPONSE (DAMAGE) PARAMETERS

Quantification of structural response and damage under seismic loading is a key factor in fragility analysis. Both the response statistics (representing demand) and limit states (representing capacity) are obtained in terms of the same response parameter. Hence the response parameter should be selected carefully for reliable fragility estimation.

There are two main categories of response parameters, local and global. Local response parameters are employed for specific locations or elements in the structure whereas global response parameters are employed in the estimation of overall response of the structure. Response parameters are further classified as maximum value based or cumulative value based parameters. Rotational ductility, curvature ductility and interstory drift are good examples of maximum displacement value based local response parameters. Among these parameters, interstory drift is very commonly used in fragility analysis of RC frame type of structures. Among cumulative value based parameters, Park and Ang Damage Index (Park and Ang, 1985) has been employed by Singhal and Kremidjian (1996). The index has two terms reflecting the influence of maximum deformation and absorbed hysteretic energy.

$$D_{PA} = \frac{\delta_m}{\delta_u} + \frac{\beta_{PA}}{F_y \delta_u} \int dE \qquad (2.5)$$

The parameter D_{PA} stands for Park and Ang's Damage index, δ_m is maximum deformation, δ_u is ultimate deformation under monotonic loading, β_{PA} is strength degradation parameter, F_y is yield strength and dE is incremental absorbed hysteretic energy in Equation 2.5. The advantage of D_{PA} is that it is an enhanced response parameter which includes both displacement and energy. However there is a significant arbitrariness in the selection of β_{PA} parameter, which is undesirable.

There are two main approaches regarding global response parameters. In the first approach, local response parameters are calculated for different elements of the structure and the global response parameter is obtained as a weighted average of them. However this approach is not very suitable for fragility analysis where thousands of structural simulations are required to construct the response statistics. The second approach is to relate the global response parameter to some performance measures of the structure that depend on the status of all components. Examples of such global response parameters are the global roof drift, and the vibrational characteristics of the structural system.

2.3 SAMPLING AND SIMULATION

In the absence of actually observed or experimental structural data, the viable alternative to obtain the response statistics that are vital for the generation of fragility curves is to utilize structural simulation. In the last two decades, analytical approaches have been used extensively for the generation of the required structural data due to advances in computational technology and analytical modeling capabilities. Another advantage of using analytical simulation and sampling techniques is that it becomes possible to quantify the numerous sources of uncertainties that are involved in structural design and analysis phases.

Sampling can be defined basically as the selection of members to reflect the whole population as good as possible. Sampling is preferable since it saves time, reduces the cost and controls the data when the population of main group makes the exact counting impossible. There are two main approaches in sampling: probability (random) and non–probability sampling. Random sampling approach enables the use of statistical methods and distributions to control whether the samples fairly generalize the whole population or not (Orhunbilge, 1997).

Assume a study simulating the outcome of a single continuous random variable with known distribution, to recognize how the outcome of a model depends on the

distribution of the random variable. It is possible to derive the relationship by examining the outputs of the model with randomly chosen variables. The way followed on that subject will be the random variable identification and model evaluation strategy.

Accepting the RC structure as a model and the response of the structure as the output leads to the determination of the analysis variables. In earthquake engineering, the main sources of response uncertainty for a RC moment resisting frame are the variability in structural properties and randomness in ground motion characteristics.

2.3.1 SAMPLING TECHNIQUES

In order to consider the uncertainty in structural input parameters, sampling based approaches are used in this study. Among these methods, The Monte Carlo (MC) method (Rubinstein, 1981) is the most commonly used one as a sampling approach. The MC method basically takes randomly generated values that follow a probability distribution to simulate a system of variables. As an alternative approach to MC simulation, Latin Hypercube Sampling (LHS) Method is developed (McKay et al., 1979). Instead of the randomly chosen samples in the MC simulation, the LHS method provides a constrained sampling technique (Ayyub and Lai, 1989).

2.3.1.1 THE MONTE CARLO METHOD

The MC sampling method provides a numerical process to evaluate an uncertain value that is a function of one or more other variables. The inputs are simulated; the outputs are derived and iterated to compile output statistics (Porter, 2002).

The MC method expresses random values in terms of deterministic values, often called samples. Therefore, the corresponding problem is symbolized into a group of

samples. The deterministic outputs are obtained from deterministic input values, and these deterministic outputs are converted into probabilistic or statistical forms (Lee and Mosalam, 2004).

Since the MC simulation is a powerful tool of sampling, it has been used in many studies in earthquake engineering field. Good examples are the studies conducted by Collins et al. (1996) and Wu and Wen (2000) who simulated ground motions by using available seismic data for the Los Angeles and Santa Barbara areas.

From algorithm point of view, the advantage of the MC method is its straightforward application. Although the method itself is not complex, it can be used for complex problems or systems that behave nonlinear. However, even for the simple systems, the need for a large sample size is the main disadvantage of the MC method. In the case of structural analysis, it is not feasible to conduct thousands of time–history analysis, especially if the investigated structure is large and complex. Besides, when problems like nonlinear or inelastic structural behavior including complex member responses are in consideration, then the computation requirement can easily get out of hand (Wen et al., 2003).

2.3.1.2 LATIN HYPERCUBE SAMPLING METHOD

The LHS is a stratified method. Basically, the input values are classified in terms of probabilistic ranges and random permutation of outputs are obtained. This method has been employed for numerous simulation based studies (Ayyub and Lai, 1989; Wyss and Jorgensen, 1998; Iman and Conover, 1982; Iman et al., 1981.a and b).

The advantage of the LHS method is the sample size required for a sufficiently accurate estimate. Rather than the MC method, LHS achieve the results with a smaller sample size (Ayyub and Lai, 1989). Because of this advantage, LHS method is preferred in this study to include the input variability in the models.

In LHS method, the samples are selected from all the possible ranges by providing a highly involved selection algorithm of sampling instead of random sampling. The sampled population is imposed to reflect the characteristics of the statistical distribution under consideration at each probability interval by using such a constrained sampling approach.

For a problem with k random variables $X_1 ... X_k$, the LHS method obtains n different values by dividing the range of each variable into n non–overlapping intervals. Since the area of each probability density function is equal to P(X) = 1/n, the same probability of occurrence is achieved. Figure 2.1 shows the cumulative distribution function and probability density function of a normally distributed variable in case n equals to 5. Here, n represents the sample size chosen for a desired accuracy level.

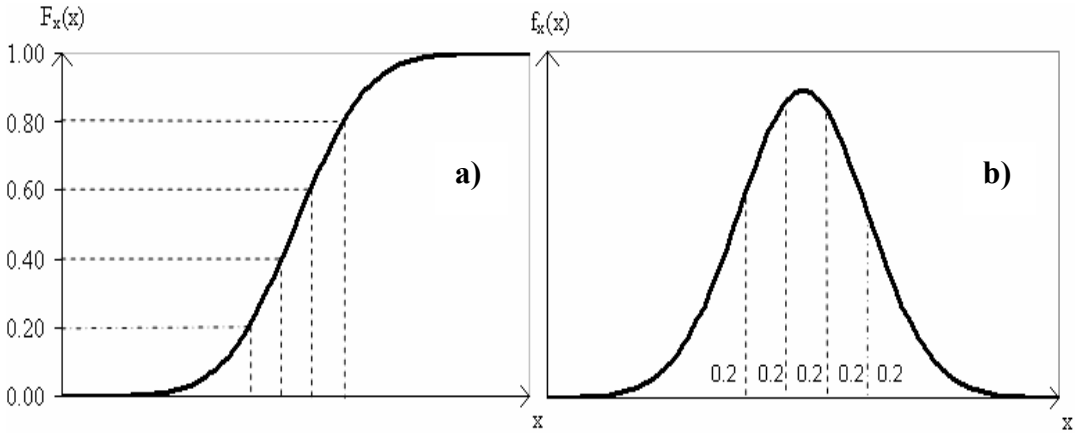

Figure 2.1 a) Cumulative distribution function (n = 5) b) Probability density function (n = 5)

Next, n different values between 0 and 1 are designated randomly for each sample. As a result, for a sample size of n, one randomly selected value per each n non–overlapping interval is obtained. Then, these randomly selected variables are

converted into cumulative probabilities for each of the n intervals by linear transformation given in Equation 2.6.

$$P_m = \left(\frac{1}{n}\right)U_m + \left(\frac{m-1}{n}\right) \tag{2.6}$$

In Equation 2.6, m is the integer interval numbers from 1 to n, P_m is the cumulative probability value for the m^{th} interval obtained from the randomly generated number, and U_m is the randomly generated number (between 0 and 1). Equation 2.7 shows that P_m (each generated value) falls into one of the n intervals.

$$\left(\frac{m-1}{n}\right) < P_m < \frac{m}{n} \tag{2.7}$$

Then, the inverse distribution function given in Equation 2.8 is used to produce the sampling values to be employed in the final sample space from randomly generated P_m.

$$X_{k,m} = F_x^{-1}(P_m) \tag{2.8}$$

Using Equation 2.8, $X_{k,m}$ is generated as the m^{th} sample value of the k^{th} random variable via the inverse cumulative distribution function (F_x^{-1}) of that specific random variable.

Final step is to obtain random pairs of the resulting values of each variable ($X_{k,m}$). To achieve this, n numbers corresponding to n generated values is paired by random permutation for each variable. After that, the sampling matrices are obtained by associating these different random permutations respectively (Erberik and Elnashai, 2003).

2.4 LIMIT STATES

Realistic and comprehensive limit state determination and thus performance level identification is one of the significant steps of fragility curve construction because these indicators affect resulting fragility curves directly (Erberik and Elnashai, 2004).

The limit state definitions that represent the performance of building structures mainly depend on three factors: functional considerations, social and economical aspects, and finally engineering issues. The functional considerations are important in the case of loss of function, which has considerable impact in the recovery of the region. A typical example for this case is the disruption of a hospital or a factory. The social and economical considerations refer to deaths and injuries, along with the number of homelessness and the monetary value of the direct physical damage to engineering structures and other facilities. The engineering issues are related to design considerations. For example in any design procedure, the strength and stiffness of the structure are proportional such that for different earthquake intensity levels the strength and the deformation are maintained at certain levels such that the damage to the structure and its contents is confined within prescribed limits (Corvera, 2000).

From engineering point of view, limit state is the point at which the system is no further capable of satisfying a performance level. There are different definitions of limit states for structural or nonstructural members in terms of both quantitative and qualitative expressions. To correlate post–earthquake condition of a structure to a performance parameter, strength degradation, damage, or possibility of repair can be employed. Usually, qualitative descriptions for structural performance levels are used in building codes. However, for design and analysis stages, the limit states should be given quantitatively in terms of either forces or deformations in structural or nonstructural members (Wen et al., 2003).

A comprehensive building provision, FEMA 356 (ASCE, 2000) defines 3 limit states qualitatively for structural members.

- Immediate Occupancy (IO) – Very limited or no damage has occurred after earthquake. Strength and stiffness of structural system and members have remained almost same as the prior state.
- Life Safety (LS) – Although significant damage has occurred, this has not resulted in collapse. The repair of structure is essential but not always feasible.
- Collapse Prevention (CP) – The structure is on the limits of instability, partial or total collapse. Strength and stiffness degradation is high, permanent deficiencies have occurred. Reuse of the structure is not safe.

In HAZUS Earthquake Loss Estimation Methodology (National Institute of Building Sciences, 1999), there are five damage states: None, Slight, Moderate, Extensive and Complete. Structural limit states are expressed in terms of spectral displacement whereas nonstructural damage states are expressed in terms of spectral acceleration. HAZUS limit states are determined for 36 different building classes and 4 different design deficiencies.

Alternatively, limit state can be described by structural behavior or possibility of repair. From behavior point of view, three performance levels as elastic, inelastic and collapse can be used. In terms of repair feasibility instead, Ghobarah (2004) defined five limit states as; no damage, repairable damage, irreparable damage, extreme, and collapse.

For the quantification of limit states, performance levels are generally expressed in terms of deformation. Accordingly, cracking of concrete, first steel yield, and wide concrete cracks are possible indicators of performance levels of ductile systems. Besides the damage level, these descriptions identify the feasibility of repairing and corresponding cost.

The drift or displacement of a structural system under earthquake forces should be monitored due to three reasons: 1) Structural stability, 2) Architectural integrity and potential damage to various non–structural components and 3) Human comfort while and after the building experiences the ground motion (Naeim, 1989).

Due to its simplicity, interstory drift is the most commonly used parameter in the literature for the determination of limit states and also suggested by seismic codes and guidelines.

However, drift or displacement based structural damage limits are an oversimplification because the damage level of the structure is based on several other factors like structural system, spatial damage distribution and loading effects.

Measures of structural damage as global or local can be used as performance level. A simple global measure is roof drift that is used frequently. In cases where the damage distribution through the height of the structure is important, interstory drift can be used as a damage indicator. Empirical observations and dynamic response analyses have indicated that there is a strong correlation between the interstory drift values and building damage potential.

At local level, member deformation plays an important role in the identification of damage. Member deformation is considered in terms of strain or curvature. Local criterion generally depends on yield or ultimate deformation stage of a member or a group of members. Yield state is generally established when the longitudinal reinforcement starts to yield whereas the ultimate state is established when the strain of extreme fiber of concrete reaches its ultimate value. Other suggested criteria for the attainment of ultimate local failure include buckling of longitudinal reinforcement bars and fracture of confining hoops.

Nonlinear pushover analysis is a commonly used tool for the attainment of quantitative limit state values. The pushover analysis is carried out by increasingly

applying lateral loads, or displacements, to the structure until it reaches collapse state. The results of pushover analysis are usually in terms of the relationship between roof displacement and base shear capacity or more specifically story drift and story shear capacity. Along the pushover curve, critical stages in the response can be identified, such as cracking and yielding in structural members, or the failure of a member, or the initiation of a collapse mechanism, etc (Corvera, 2000). Typical limit state definitions as shown in Figure 2.2 are as follows:

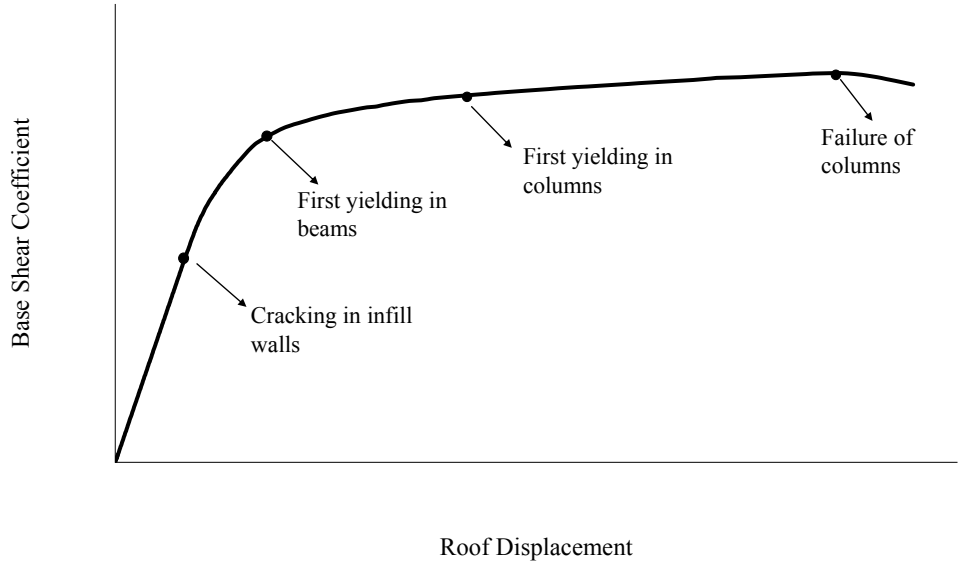

Figure 2.2 Pushover curve

- Cracking in Infill Walls (CI) – Deformation at which diagonal cracks in brick infill are initiated due to lateral loading.
- First Yielding in Beams (FYB) – Roof displacement value at which first yielding in beams occurred at a member of the story.
- First Yielding in Columns (FYC) – Roof displacement value at which first yielding in columns is initiated.

- Column Failure (CF) – Strength Degradation at a certain roof displacement value due to the effects of lateral load.

2.5 SOURCES OF UNCERTAINTY IN FRAGILITY ANALYSIS

Recent advances in earthquake engineering and computation technology have made it possible to predict the behavior and performance of complex structural systems with a certain degree of accuracy, provided that demands on the system and the capacity of the system to withstand those demands are known. However numerous sources of uncertainty arise in the analysis and assessment process. Some of these uncertainties are due to factors that are inherently random (or aleatory) at the scale of understanding in engineering whereas others arise from lack of knowledge, ignorance or modeling assumptions and are case–dependent (epistemic). The inevitable consequence of these uncertainties is the risk that the structure will fail to perform as expected or not (Wen et al., 2003).

Fragility estimation of structural systems involves the consideration of uncertainties associated in defining the hazard, the structural model and the limit states. Among these, the main source of uncertainty is the hazard or the seismic excitation. There are too many uncertain parameters within seismic hazard concept. Over a specified period of time, the threat of seismic excitation to a given system at a given site can come from events at different times and of different magnitudes, distances, focal depths and rupture surface geometries and features. Hence in fragility studies, hazard uncertainty and record–to–record variability are much more pronounced than the uncertainties associated with the capacity of the structural system (Erberik and Elnashai, 2003; Kwon and Elnashai, 2004; Mostafa, 2003).

Development of fragility curves for an individual building requires an accurate analytical representation of the model as discussed previously. It is obvious that the member and system capacity depend directly on the material strength which is

inherently uncertain. The uncertainty can be modeled by random variable with two statistical parameters, i.e. the mean and the standard deviation to describe the central value and the variability. Normal and lognormal distribution is commonly used for convenience.

The sources of both aleatory and epistemic uncertainty in identifying the various limit states for the structural system, nonstructural system, and the overall building system are many. In terms of the quantitative methods for determining limit states, some of the sources of aleatory uncertainty include the variability in material properties for both structural strength and stiffness, variability in sectional properties, and variability in construction stage. Some of the sources of epistemic uncertainty include the nonlinear models for the variety of structural materials and components, imposed loading distribution to identify critical response, effects of using monotonic response to represent capacity when actual earthquake demand is cyclic in nature, differences in analytical programs, etc (Wen et al., 2003). Thus the limit states should be described on a probabilistic manner. However they are often considered as deterministic values because the uncertainty in ground motion characterization is considerably larger than the limit–state uncertainty as stated previously.

CHAPTER 3

DESIGN AND ANALYSIS CONSIDERATIONS

3.1 GROUND MOTION RECORD SELECTION

Investigation of building fragility using analytical methods involves both structural capacity uncertainty and record–to–record ground motion variability. In this study, three different ground motion sets are selected to characterize different levels of seismic hazard. Each set contains 20 ground motion records. Peculiar records due to extreme near–fault (pulse–dominant) wave forms and very soft soil site effects are not included. Grouping of the records are based on PGV values which ranges between 0–20 cm/s, 20–40 cm/s, and 40–60 cm/s. Sixty ground motion records classified in three sets are given in Tables 3.1–3.3 along with their major ground motion parameters; moment magnitude (M_w), closest distance to fault (D), PGA and PGV. Considering the NEHRP site classification (Building Seismic Safety Council, 2000) that considers the sites as "Hard" (V_s>760m/s), "Medium" (360m/s<V_s<760m/s), and "Soft" (180<V_s<360m/s) in terms of shear wave velocity, V_s, it is observed that majority of the sites selected can be classified as "Soft" whereas none of them can be regarded as "Hard". This reveals the fact that the resulting fragility information should be used for building stocks located in regions with similar site characteristics (medium–to–soft soil site class).

For a more detailed examination of the characteristics of each ground motion data set, the mean value of each parameter and corresponding coefficient of variation (COV) value as a measure of dispersion are listed in Table 3.4.

Table 3.1 Ground motion records: Set I

EARTHQUAKE	STATION	COMPONENT	SITE	M_w	D (km)	PGA (cm/s^2)	PGV (cm/s)
Morgan Hill, 04/24/84	Gilroy #2	0	S	6.1	11.8	153.7	5.0
Morgan Hill, 04/24/84	Gilroy#3	90	S	6.1	10.3	189.8	11.9
Morgan Hill, 04/24/84	Gilroy#6	0	M	6.1	6.1	214.8	11.3
Morgan Hill, 04/24/84	Gilroy #7	90	M	6.1	7.9	111.5	5.8
Morgan Hill, 04/24/84	Gilroy – Gavilian College	67	S	6.1	13.2	95.0	3.4
Imperial Valley, 10/15/79	Calexico Fire Station	N45W	S	6.5	10.4	197.6	18.9
Imperial Valley, 10/15/79	Borchard Raxch El Centro Array #1	S50W	S	6.5	22.6	121.1	10.4
Imperial Valley, 10/15/79	Parachute Test Facility, El Centro	N45W	S	6.5	10.4	197.6	17.3
Imperial Valley, 10/15/79	Casa Flores, Mexicali	0	S	6.5	9.8	236.8	19.3
Coyote Lake, 08/06/79	Gilroy Array NO. 3 Sewage Treatment	50	S	5.7	6	252.4	16.9
Coyote Lake, 08/06/79	SJB Overpass, Bent 3	67	S	5.7	17.2	84.6	4.7
Livermore, 01/24/80	Livermore VA Hospital	128	M	5.5	–	121.7	17.4
Livermore, 01/24/80	Livermore VA Hospital	38	M	5.5	–	180.3	17.9
North Palm Springs, 07/08/86	Fun Valley	135	S	6.2	12.7	123.0	9.5
North Palm Springs, 07/08/86	Fun Valley	45	S	6.2	12.7	123.5	6.1
Whittier Narrows, 10/01/87	7420 Jaboneira, Bell Gardens	S27W	S	6.1	16.4	89.8	2.7
Whittier Narrows, 10/01/87	200 S. Flower, Brea, CA	N20E	S	6.1	22.2	109.4	7.1
Loma Prieta, 10/18/89	Gilroy #6 – San Ysidro	0	M	7	12.2	112.2	13.1
Loma Prieta, 10/18/89	Gilroy #6 – San Ysidro	90	M	7	12.2	166.9	13.9
Livermore, 01/27/80	Morgan Territory Park	265	M	5.8	8	242.7	11.0

Table 3.2 Ground motion records: Set II

EARTHQUAKE	STATION	COMPONENT	SITE	M_w	D (km)	PGA (cm/s^2)	PGV (cm/s)
Morgan Hill, 04/24/84	Halls Valley	240	S	6.1	2.5	305.8	39.6
Imperial Valley, 10/15/79	Keystone RD., El Centro Array #2	S40E	S	6.5	16.2	309.4	32.7
Imperial Valley, 10/15/79	Anderson RD., El Centro Array #4	S40E	S	6.5	8.3	480.8	38.1
Imperial Valley, 10/15/79	Community Hosp.,Keystone RD.,El Cenrto Array#10	S50W	S	6.5	8.7	117.3	22.9
Imperial Valley, 10/15/79	Aeropuerto Mexicali	315	S	6.5	3.2	249.9	23.9
Parkfield, 06/27/66	Cholame,Shandon, Array NO. 5	N85E	M	6.1	7.1	425.7	25.4
Coyote Lake, 08/06/79	Gilroy Array NO. 2	140	S	5.7	6.0	248.9	31.9
Imperial Valley, 10/15/79	Casa Flores, Mexicali	270	S	6.5	9.8	414.7	31.5
Whittier Narrows, 10/01/87	7420 Jaboneria, Bell Gardens	N63W	S	6.1	16.4	215.9	28.0
Northridge, 01/17/94	6850 Coldwater Canyon AVE., North Hollywood	S00W	S	6.7	12.5	296.0	23.1
Northridge, 01/17/94	Los Angeles, Brentwood V.A. Ho	195	S	6.7	23.1	182.1	24.0
Loma Prieta, 10/18/89	Saratoga – 1–Story School Gym	270	S	7	13.7	347.3	37.2
Loma Prieta, 10/18/89	Gilroy #2 – HWY 101/Bolsa RD	0	S	7	4.5	344.2	33.3
Loma Prieta, 10/18/89	Gilroy #2 – HWY 101/Bolsa RD	90	S	7	4.5	316.3	39.2
Loma Prieta, 10/18/89	Gilroy #3 – Gilroy Sewage Plant	0	S	7	6.3	531.7	34.5
Loma Prieta, 10/18/89	Gilroy – Gavilian Coll.	67	M	7	3.0	349.1	28.9
Loma Prieta, 10/18/89	Gilroy – Gavilian Coll.	337	M	7	3.0	310.0	23.0
Whittier Narrows, 10/01/87	Los Angeles – Obregon Park	360	S	6.1	14.2	420.1	21.8
Northridge, 01/17/94	Los Angeles – UCLA Grounds	90	M	6.7	22.9	272.4	22.0
Northridge, 01/17/94	Los Angeles – UCLA Grounds	360	M	6.7	22.9	464.6	21.9

Table 3.3 Ground motion records: Set III

EARTHQUAKE	STATION	COMPONENT	SITE	M_w	D (km)	PGA (cm/s^2)	PGV (cm/s)
Duzce, 11/12/99	Bolu	NS	S	7.1	20.41	722.1	55.2
Imperial Valley, 10/15/79	Bonds Corner	230	S	6.5	4.4	762.4	45.0
Imperial Valley, 10/15/79	Bonds Corner	140	S	6.5	4.4	578.0	44.3
Imperial Valley, 10/15/79	James RD., El Centro Array #5	S40E	S	6.5	5.2	539.8	49.7
Imperial Valley, 10/15/79	McCabe School, El Centro Array #11	S50W	S	6.5	12.4	362.5	45.2
Imperial Valley, 10/15/79	Dogwood RD., Diff. Array, El Centro	NS	S	6.5	5.6	473.6	41.1
Imperial Valley, 10/15/79	Aeropuerto Mexicali	45	S	6.5	3.2	284.9	42.0
Imperial Valley, 10/15/79	Community Hosp.,Keystone RD.,El Cenrto Array#10	N40W	S	6.5	8.7	226.6	46.0
Northridge, 01/17/94	7769 Topanga Canyon Blvd., Canoga Park	S16W	S	6.7	15.7	381.0	59.8
Chi–Chi, Taiwan, 09/20/99	Chiayi – Meishan School, CHY006	360	S	7.6	14.5	351.8	42.1
Loma Prieta, 10/18/89	Corralitos – Eureka Canyon RD	0	S	7	2.8	617.7	55.2
Kocaeli 8/18/99	Duzce	SN	S	7.4	17.06	307.8	50.7
Landers, 06/28/92	Joshua Tree – Fire Station	90	M	7.3	10	278.4	42.7
Northridge, 01/17/94	Pacoima – Kagel Canyon	360	M	6.7	10.6	424.2	50.9
Cape Mendocino, 04/25/92	Petrolia	0	S	7	9.5	578.1	48.3
Cape Mendocino, 04/25/92	Rio Dell – 101/Painter ST. Overpass	360	M	7	18.5	538.5	42.6
Chi–Chi, Taiwan, 09/20/99	Taichung – Chungming School, TCU051	360	S	7.6	7	230.0	40.6
Chi–Chi, Taiwan, 09/20/99	Taichung – Taichung City, TCU082	360	S	7.6	4.5	182.1	41.0
Northridge, 01/17/94	17645 Saticoy ST.	S00E	S	6.7	13.3	428.7	59.8
Northridge, 01/17/94	14145 Mulholland DR., Beverly Hills, CA	N09E	S	6.7	19.6	419.3	57.9

Table 3.4 Statistical properties of ground motion sets

	SET I		SET II		SET III	
	Mean	COV (%)	Mean	COV (%)	Mean	COV (%)
Magnitude (M_w)	6.2	7	6.6	6	6.9	6
Distance (km)	12.3	38	10.4	67	10.4	56
PGA (in g)	0.16	35	0.34	31	0.44	38
PGV (cm/s)	11.17	49	29.14	22	48	13

Table 3.4 indicates that the mean PGV values are in accordance with the intentional PGV–based classification of ground motion records in this study. It is observed that, shifting from Set I to Set III, as the mean PGV values increase, mean PGA values also increase significantly and there is a slight increase in mean magnitude value. Such a trend indicates that the damage potential of ground motion records in Set III is higher than the damage potential of records in Set I. The mean value of distance parameter seems to be nearly constant, so it can be stated that the ground motion sets have similar distance to the fault characteristics. The COV values of the ground motion parameters except magnitude are very high. This is an indicator of the pronounced hazard uncertainty, in the form of record–to–record variability, which generally dominates over other sources of uncertainty arising from structural characteristics, response and modeling in vulnerability studies.

3.2 DESIGN METHODOLOGY

Design of an earthquake–resistant structure is much more complicated than conventional design both from architectural and structural engineering point of view due to great sources of uncertainty that exist in the estimation of design loadings as well as structural demands and capacities in the inelastic range. Modern seismic codes and guidelines basically rely on the extensive knowledge database gathered from previous research and observed structural behavior during past earthquakes.

According to the general philosophy of earthquake resistant design, the primary goal is to provide a safe margin against collapse by requiring RC buildings to have sufficient strength and ductility in a severe, but infrequent earthquake. A secondary goal is to prevent structural damage and control nonstructural damage in moderate and more frequent earthquakes.

3.2.1 DESIGN SPECTRUM

In earthquake codes, the characterization of design earthquake is achieved in the form of acceleration response spectrum. In Turkish Seismic Code, the proposed design spectrum is based on four seismic zones obtained from broadly described geological conditions. Hence, major ground motion characteristics like distance to fault and magnitude are ignored. However, for probabilistic and deterministic vulnerability studies, design spectrum that depends on site–distance–magnitude parameters is more convenient (Kalkan and Gülkan, 2004).

A more elaborate method is introduced in FEMA 356 (ASCE, 2000) for the characterization of design earthquake and this approach is also used in this study. The sketch of FEMA design spectrum is illustrated in Figure 3.1. The spectrum parameters S_{xs}, S_{x1} and T_s are obtained from the mean response spectra of each set of ground motion records used. The short period, S_{xs}, value of the design spectrum is obtained as the response spectrum value at a period of 0.2 seconds, such that it is not less than 90% of the peak value obtained by response spectrum at any period. The design spectrum parameter S_{x1}, corresponds to response spectrum value at a period of 1.0 seconds. S_a values are obtained by using $S_a = S_{x1}/T$ such that at any period, the value of S_a obtained from the equation is not less than 90% of that which would be obtained directly from the spectra. T_0 is 20% of T_s and the value of T_s shall be determined by dividing S_{x1} to the S_{xs}.

Mean acceleration response spectra for the ground motion sets and the corresponding design spectra obtained by FEMA procedure is shown in Figure 3.2.

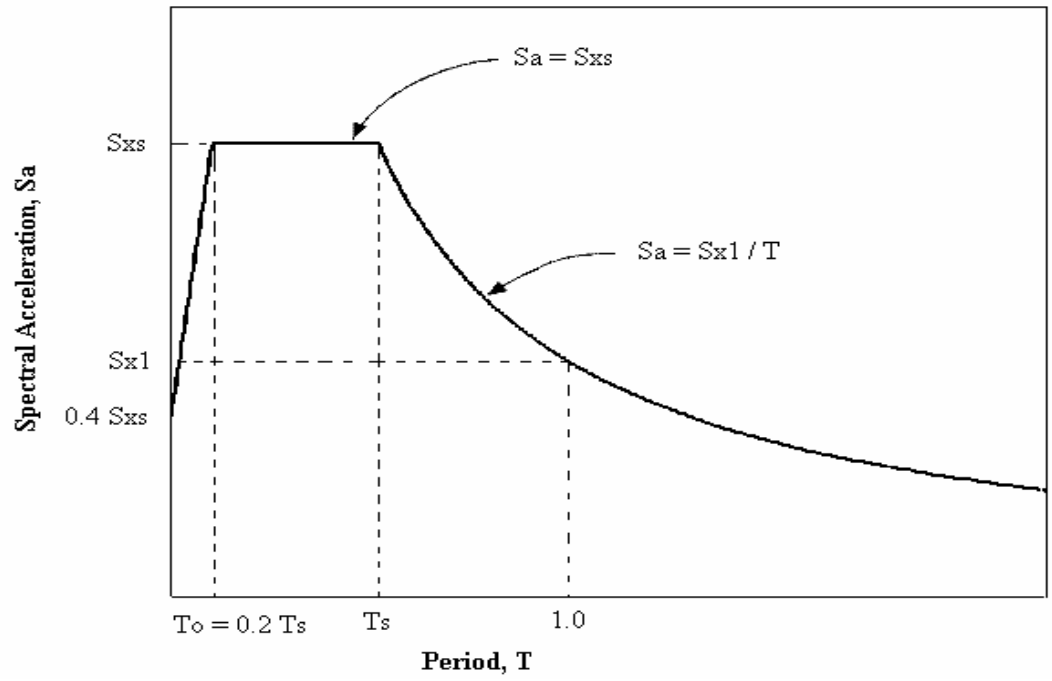

Figure 3.1 Design spectrum according to FEMA 356 (ASCE, 2000)

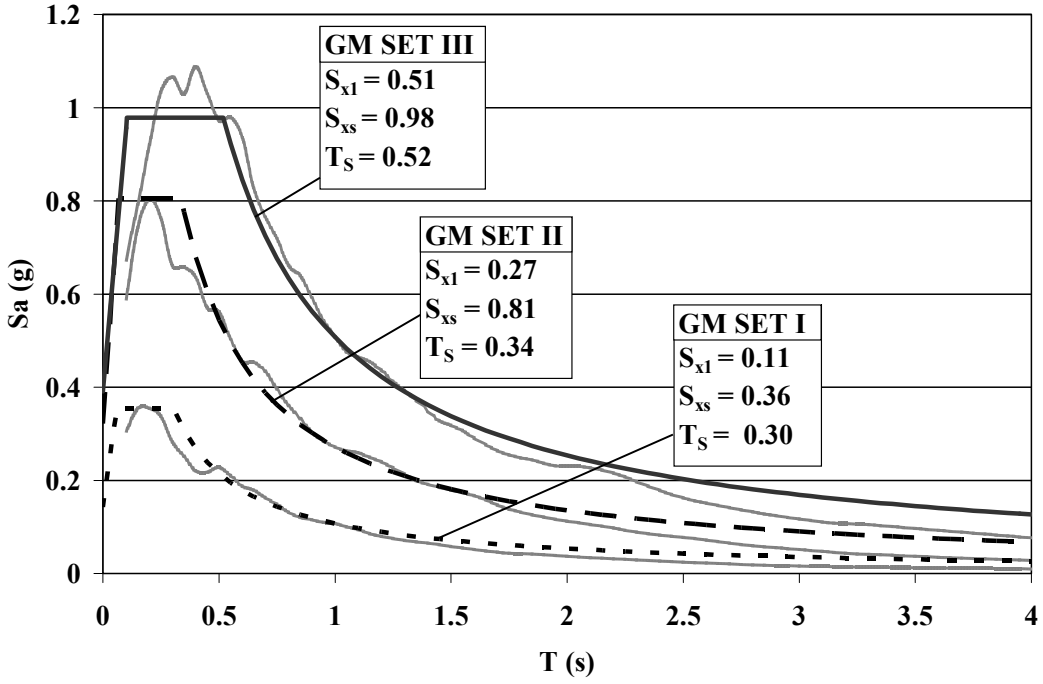

Figure 3.2 Comparison of mean response and design spectra of ground motion sets

3.2.2 DESIGN OF ANALYTICAL MODELS

This study refers to two national codes for the design of RC buildings. These are the latest versions of the Turkish Standards for Design and Construction of RC Structures, TS 500 (Turkish Standards Institute, 2000) and Turkish Seismic Code (Ministry of Public Works and Settlement, 1998) that states the minimum requirements for structures and structural components to be built in disaster areas. Furthermore, the dimensions of the structural members and reinforcement detailing in these members comply with ACI building code (ACI Committee 318, 2002).

Moment resisting frames are frequently used structural systems in Turkish construction practice. In a structural system, the beam and column members form the integral part of the frame system that sustain the lateral and gravity loads. Their detailing and dimensions are computed to confirm the design provisions. In conventional design, the infill and partition walls are not considered as load carrying members. This study that aim to reflect the earthquake performance of Turkish build stock chooses analytical models of which the lateral loads are resisted by ductile, in–situ cast moment resisting frames, without including the presence of infill walls due to the reasons explained above. Since number of stories is deemed to be important regarding the seismic response of RC frame structures, it is considered as a major parameter in this study. Hence 3, 5, 7, and 9–story planar frame models are constructed. The analytical models considered cover the low–rise and mid–rise RC frame structure population, which represents the majority of residential buildings in Turkey. Story height of 3 meters and bay width of 5 meters are assumed in accordance with the common practice. For simplicity, the buildings are assumed to be regular and symmetric in plan. This enables the use of planar models in both design and analysis.

During design stage, the gravity loads (dead and live loads) are calculated using the Design Loads for Buildings, TS 498 (Turkish Standards Institute, 1987). After the determination of dead and live loads, the story mass of the structural models is

calculated as 45.5 tons. The story mass computed is used for nodal weight computation. Since the analytic models are selected as regular 3 bay moment resisting frames; story weight is distributed equally at each of the four column–beam joints. Then, using the design codes and the design spectra calculated, the design forces are calculated and the corresponding structural member dimensions are determined. The cross sectional dimensions of columns are reduced with respect to increasing story number to be compatible with a frequent application in Turkish construction practice. For 3–story model, constant column cross section throughout the height is assumed and the models are designed accordingly whereas for the 5–story model a reduction in column dimensions is applied for the fourth and fifth stories. Hence in case of the 5–story model different column dimensions are selected for the first three stories and the remaining two stories. For 7–story and 9–story models three different column dimensions are obtained by reducing the structural member cross sections twice. The reduction is implemented at level four and six in the case of 7–story model whereas for the 9–story model, the column and beam sections are reduced at levels four and seven. Finally, for longitudinal reinforcement design, SAP 2000 (Computers and Structures Inc., 2002) is employed.

Main properties of the analytical models are listed in Table 3.5. The abbreviations used for the models provide information about the number of stories and the design level of the corresponding model. The models according to the story number (3S, 5S, 7S and 9S) are designed according to the three design spectra (D1, D2, D3) that are based on the previously described ground motion sets and 12 basic structural variants are obtained. For instance, 3SD1 refers to a three–story building that is designed according to the design spectrum representing the first set of ground motions. Remaining columns in the table give information about the beam and column dimensions (in centimeters) of the models. Table 3.5 also lists the fundamental period values corresponding to these models that are given next to the model abbreviation. In Figure 3.3, typical sketches of the analytical models are given.

Table 3.5 Different properties of model buildings

NO	MODEL	PERIOD (s)	SECTION	STORY	h (cm)	b (cm)
1	3SD1	0.65	BEAM3	1–2–3	45	25
			COL3	1–2–3	30	30
2	3SD2	0.52	BEAM3	1–2–3	45	30
			COL3	1–2–3	35	35
3	3SD3	0.42	BEAM3	1–2–3	50	30
			COL3	1–2–3	40	40
4	5SD1	0.93	BEAM2	1–2–3	45	25
			BEAM3	4–5	45	25
			COL2	1–2–3	35	35
			COL3	4–5	30	30
5	5SD2	0.72	BEAM2	1–2–3	50	30
			BEAM3	4–5	50	30
			COL2	1–2–3	40	40
			COL3	4–5	35	35
6	5SD3	0.64	BEAM2	1–2–3	50	30
			BEAM3	4–5	50	30
			COL2	1–2–3	45	45
			COL3	4–5	40	40
7	7SD1	1.06	BEAM1	1–2–3	50	30
			BEAM2	4–5	50	30
			BEAM3	6–7	45	25
			COL1	1–2–3	40	40
			COL2	4–5	35	35
			COL3	6–7	30	30
8	7SD2	0.89	BEAM1	1–2–3	55	30
			BEAM2	4–5	50	30
			BEAM3	6–7	50	30
			COL1	1–2–3	45	45
			COL2	4–5	40	40
			COL3	6–7	35	35
9	7SD3	0.81	BEAM1	1–2–3	55	30
			BEAM2	4–5	50	30
			BEAM3	6–7	50	30
			COL1	1–2–3	50	50
			COL2	4–5	45	45
			COL3	6–7	40	40
10	9SD1	1.19	BEAM1	1–2–3	55	30
			BEAM2	4–5–6	50	30
			BEAM3	7–8–9	45	25
			COL1	1–2–3	45	45
			COL2	4–5–6	40	40
			COL3	7–8–9	35	35
11	9SD2	1.04	BEAM1	1–2–3	55	30
			BEAM2	4–5–6	55	30
			BEAM3	7–8–9	50	30
			COL1	1–2–3	50	50
			COL2	4–5–6	45	45
			COL3	7–8–9	40	40
12	9SD3	0.93	BEAM1	1–2–3	60	30
			BEAM2	4–5–6	55	30
			BEAM3	7–8–9	50	30
			COL1	1–2–3	55	55
			COL2	4–5–6	50	50
			COL3	7–8–9	45	45

Figure 3.3a) 3 story model, b) 5 story model, c) 7 story model, d) 9 story model.

Fundamental period values in Table 3.5 are compared with the period values of previous studies and the results are given in Figure 3.4. Period values that have been obtained from planar analytical models of 3, 5, 7, and 9–story buildings considering three different design levels are represented by solid dots. The dotted lines represent lower bound, mean and upper bound of the first natural period versus story height relationship suggested by Goel and Chopra (1997) for RC frame structures. Continuous gray curve represents the period story height relationship given by Uniform Building Code (1997) in USA.

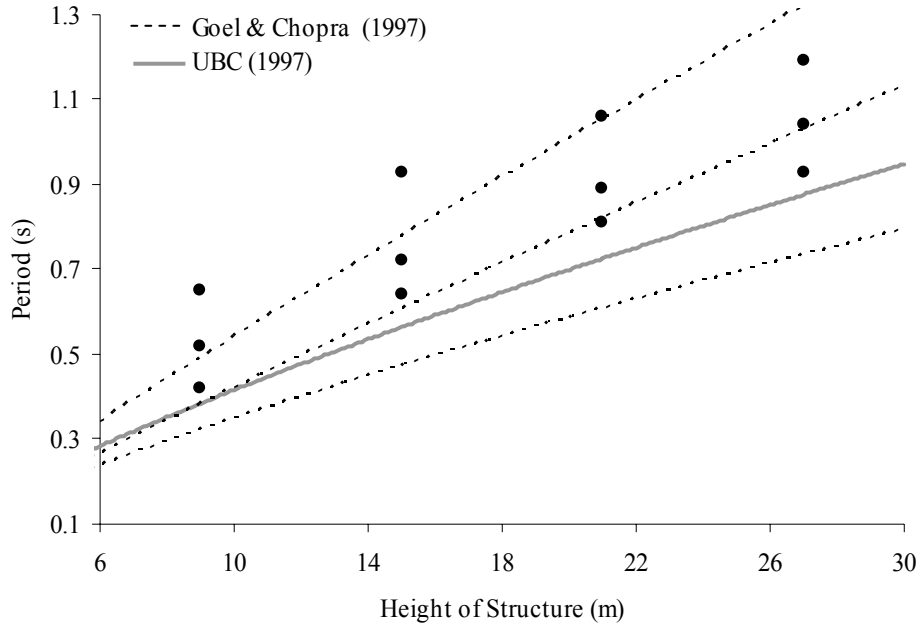

Figure 3.4 Period values of planar analytical models compared with empirical values suggested in literature.

Figure 3.4 indicates that the fundamental period values of the analytical models are slightly higher than the values proposed by other studies. However, it should be considered that, the suggested values by other studies are based on the RC frame structure databases in California, USA. Moreover, period values presented in this study are computed without considering the infill wall effects that have significant

contribution to the fundamental period. Hence models without infill walls are more flexible than the actual buildings. Besides, comparatively high period values, especially for the structures designed according to D1 spectrum, are due to minimum cross sectional dimensions allowed by the regulations to reflect local constructional characteristics. As described previously, most of the structures in Turkey are weak and have inadequate earthquake resistance. So, they tend to deform excessively due to lateral loads.

3.3 ANALYSIS CONSIDERATIONS

Estimating seismic response and capacity of structures is a challenging task due to inherent uncertainties of buildings and complexities of structural dynamics. The need for an accurate seismic performance assessment is closely related with the detailed methods and validated mathematical models. At the expense of computational time, the increasing computer power and knowledge in the field of earthquake engineering encourage the use of nonlinear dynamic analysis for MDOF models to estimate structural behavior in a more precise manner.

In order to investigate the seismic demand and the structural capacity of the buildings under concern, the analysis program IDARC–2D is used in this study. The computer program evaluates the inelastic response through damage analysis of members and of the global structure. Some significant features incorporated in the program could be summarized as distributed flexibility model to implement inelastic behavior in the macro–models that is more suitable for RC elements, built–in validated hysteresis models that are validated through tests, computational feasibility obtained by some simple assumptions like rigid floor diaphragms. Detailed information about the computational facilities and features of IDARC–2D can be found elsewhere (Valles et al., 1996).

Determination of seismic demand and the probability of exceedance of a limit state requires two types of analysis: nonlinear static pushover analysis for the estimation

of structural capacity and nonlinear time–history analysis for the computation of structural response. Since P–delta effects can not be reflected in the nonlinear static pushover results in IDARC–2D, it is not considered in this study.

In this study, force–controlled pushover analyses are conducted using an inverted triangular lateral load pattern. The sequences of cracking, yielding and failure in structural components are established in addition to the lateral strength and ductility capacity and these are mapped on the corresponding pushover curves for the attainment of limit states in a detailed manner.

Nonlinear time–history analyses are conducted to obtain the response statistics for the MDOF analytical models considered in this study. In IDARC–2D, dynamic analysis is performed using a combination of the Newmark–Beta integration method and the pseudo–force method. Throughout the analysis, sufficiently small time increments are chosen in order to prevent convergence problems due to unbalanced forces. Unfortunately, for some of the time–history analysis, structural response results are not obtained due to numerical instabilities in the solution algorithm. Hence the fragility computations are conducted without considering these runs. Since the number of terminated runs is less than 5% of total runs, the effect of this computational weakness of IDARC–2D on generated fragility curves is assumed negligibly small.

CHAPTER 4

CLASSIFICATION OF LOW–RISE AND MID–RISE RC BUILDINGS

4.1 BUILDING SUBCLASS DEFINITIONS

In order to reflect the inherent characteristics of RC frame construction in Turkey, the building stock considered is classified in accordance with the structural deficiencies stated previously in Chapter 1. Previous studies and post–earthquake damage surveys of actual buildings are also considered. Three different condition states for the building type under consideration are studied that are designated as the "building subclasses". These are variants of the generic buildings, reflecting the characteristics of superior, typical and poor construction practice in Turkey and they can be described in general qualitative terms as follows:

Superior Subclass: The buildings in this subclass are designed according to the current codes and have adequate structural capacity in terms of strength and ductility in a severe earthquake. Good material quality, earthquake resistant design, and good supervision in the construction stage result in reliable performance levels. This is the desired level of construction practice.

Typical Subclass: It represents the majority of the building stock concerning the RC residential buildings in Turkey. They are generally engineered structures but may violate some fundamental requirements of earthquake resistant design and construction.

Poor Subclass: Unfortunately some of RC buildings in Turkey fall into this category. They are not designed to resist earthquake loads nor are they even engineered structures. Recent earthquakes in Turkey revealed that this type of structures is extremely vulnerable in seismic action. Consequently, they suffer heavy damage or even collapse when subjected to earthquake ground motions. Most of the RC construction, detailing and design deficiencies stated previously are frequently observed in this subclass of RC buildings.

The analytical models were classified previously in Chapter 3 according to number of stories and design spectrum used. At this stage, they are reclassified by also considering the construction quality state. Hence there exist 12 classes of structural models for which the fragility functions are to be developed. The abbreviations used for the current classification are listed in Table 4.1. In the current classification, number of stories and construction quality are explicit parameters whereas design level is an implicit parameter. For example, building class MRF3-T stands for 3–story RC moment resisting frame structures with typical construction quality and it includes subclasses 3SD1, 3SD2, and 3SD3 since the generated fragility curves should cover whole range of seismic hazard intensity.

Table 4.1 12 structural types used for fragility analysis

Story Number	**Subclass of Structure**		
	Superior	**Typical**	**Poor**
3	MRF3–S (3SD1, 3SD2, 3SD3)	MRF3–T (3SD1, 3SD2, 3SD3)	MRF3–P (3SD1, 3SD2, 3SD3)
5	MRF5–S (5SD1, 5SD2, 5SD3)	MRF5–T (5SD1, 5SD2, 5SD3)	MRF5–P (5SD1, 5SD2, 5SD3)
7	MRF7–S (7SD1, 7SD2, 7SD3)	MRF7–T (7SD1, 7SD2, 7SD3)	MRF7–P (7SD1, 7SD2, 7SD3)
9	MRF9–S (9SD1, 9SD2, 9SD3)	MRF9–T (9SD1, 9SD2, 9SD3)	MRF9–P (9SD1, 9SD2, 9SD3)

4.2 MATERIAL PARAMETERS FOR BUILDING SUBCLASSES

The variability in the material characteristics should be taken into account when constructing the fragility functions of different building subclasses. Since each subclass represents a predefined level of construction quality; the differences between levels of quality can be quantified by the statistical descriptors of the material characteristics.

This section includes the specification of material characteristics determined for each building subclass in terms of strength and stiffness. Variability in structural strength and stiffness has been of major interest by a number of probabilistic studies of RC members and systems (Dymiotis et al., 1999; Lee and Mosalam, 2004). As suggested by these studies, the random variables that represent the variability in material strength are considered as concrete strength (f_c) and steel yield strength (f_y) whereas the random variables that specify the variability in structural stiffness are considered as concrete modulus of elasticity (E_c) and steel modulus of elasticity (E_s).

4.2.1 CONCRETE STRENGTH (f_c)

The field observations concerning the damaged buildings after Kocaeli (1999) and Düzce (1999) earthquakes reveal the fact that the variation in concrete strength is very high and there is a significant difference between the design strength values and in–situ strength values (Booth et al., 2004; Aydoğan, 2003). Hence, concrete compressive strength is assumed as an important random variable affecting the vulnerability of building stock. Referring to the previous studies conducted by different researchers (Mirza et al., 1979; Dymiotis et al., 1999; Ellingwood, 1977; Julian, 1955; Ang and Cornell, 1974; Ghobarah et al., 1998) a normal distribution is employed to characterize the variability in concrete strength. The mean values, the dispersion represented by COV values, and the distributions employed for superior, typical and poor building subclasses are listed in Table 4.2.

Table 4.2 Concrete strength variability for each building subclass

Building Subclass	**Concrete Strength (f_c)**		
	Mean (MPa)	COV (%)	Distribution
SUPERIOR	20	16	Normal
TYPICAL	15	18	Normal
POOR	10	20	Normal

Probability density functions and mean values for each building subclass are shown in Figure 4.1.

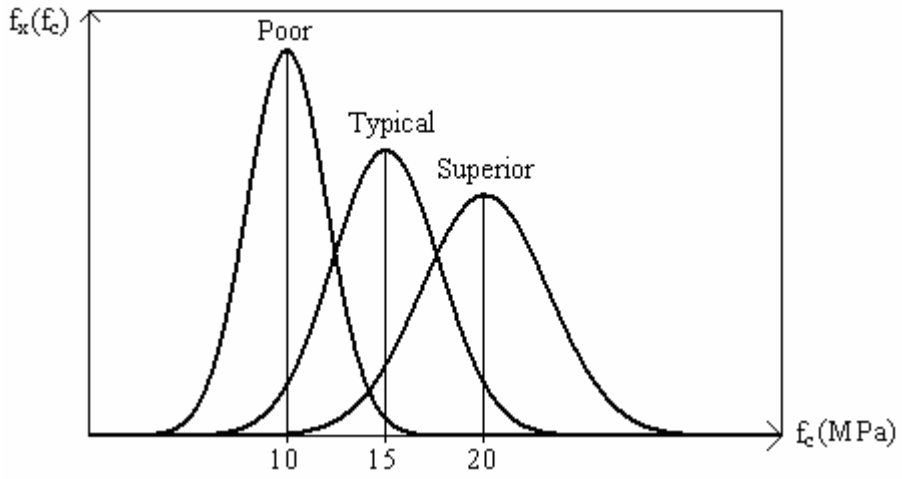

Figure 4.1 Probability density function of concrete strength for subclasses

The mean values are determined in accordance with the information obtained form Düzce building damage database (Aydoğan, 2003). Hence a mean concrete strength value of 20 MPa is appropriate to represent superior building subclass whereas a mean value of 10 MPa is assumed for poor building subclass. A mean value of 15 MPa is considered for the typical building subclass. As stated above, the variation in concrete strength is high, and it becomes even higher shifting from superior

subclass to poor subclass (Mirza et al., 1979; Ellingwood et al., 1980; Mosalam et al., 1997; Hwang and Huo, 1997). Considering the stated studies, the variation in concrete strength is determined accordingly by assuming a COV value of 16% for superior building subclass, 18% for typical building subclass, and 20% for poor subclass.

4.2.2 STEEL YIELD STRENGTH (f_y)

As a serious damage indicator of moment resisting frames, yield drift ratio of column members are affected by the yield strength of longitudinal reinforcement. Studies reveal that, the damage level of column members reduces with increasing steel yield strength whereas from beam damageability point of view, higher steel yield strength reduces damage level for a constant rotation and increases plastic rotation capacity of beams (Erduran, 2005). Therefore, steel yield strength is assumed as a random variable affecting structural fragility of RC frame structures. The mean steel yield strength values, the related COV values and employed distributions are listed in Table 4.3 for the building subclasses.

Table 4.3 Steel yield strength variability for each building subclass

Building Subclass	**Steel Yield Strength (f_y)**		
	Mean (MPa)	COV (%)	Distribution
SUPERIOR	480	10	Normal
TYPICAL	365	11	Normal
POOR	250	12	Normal

In determination of the steel yield–strength mean values, it is assumed that Reinforcing Steel Type III (St–III) is used in superior building subclass whereas Reinforcing Steel Type I (St–I) is used in poor building subclass. Hence the mean yield strengths of the subclasses are determined by Equation 4.1.

$$f_{y,mean} = 1.15 \times f_{yk} \quad (4.1)$$

In Equation 4.1, f_{yk} is the characteristic yield strength of steel (420 MPa for ST–III and 220 MPa for ST–I). The mean value for typical building subclass is determined by using the actual data based on the tested coupons (Erberik and Sucuoğlu, 2004). A normal distribution is assumed for steel yield strength and COV values are determined in accordance with previous studies (Mirza and MacGregor, 1979; Dymiotis et al., 1999; Ghobarah et al., 1998; Ellingwood, 1977).

Probability density functions of normal distribution and mean values of steel yield strength for superior, typical and poor building subclasses are given in Figure 4.2.

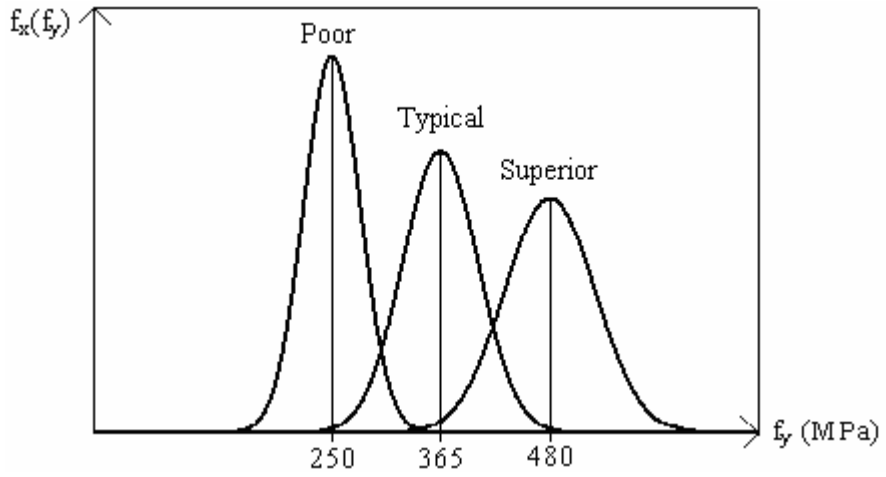

Figure 4.2 Probability density function of steel yield strength for subclasses

4.2.3 CONCRETE MODULUS OF ELASTICITY (E_c)

The initial concrete modulus of elasticity, E_c, affects the stiffness of the RC moment resisting frame structures. To acknowledge the uncertainty in stiffness independently, E_c is taken as a random variable related to the structural stiffness in

this study. The resulting mean, COV values and the distribution employed are listed in Table 4.4.

Table 4.4 Concrete modulus of elasticity variability for each building subclass

Building Subclass	Concrete Modulus of Elasticity (E_c)		
	Mean (MPa)	COV (%)	Distribution
SUPERIOR	21150	8	Normal
TYPICAL	18950	9	Normal
POOR	16400	10	Normal

The concrete modulus of elasticity is assumed to be normally distributed. Since there is a strong correlation between the concrete compressive strength and E_c, the mean values for concrete elasticity modulus, $E_{c,mean}$, are determined by using the Equation 4.2 proposed by IDARC–2D Manual (Valles et al., 1996).

$$E_{c,mean} = 57\sqrt{1000 \times f_{c,mean}} \qquad \text{(in ksi)} \qquad (4.2)$$

In Equation 4.2, $f_{c,mean}$ denotes the mean concrete strength value for each subclass (Table 4.2). The COV values are determined in accordance with Lee and Mosalam (2003).

4.2.4 STEEL MODULUS OF ELASTICITY (E_s)

Steel modulus of elasticity, E_s, also affects the stiffness of RC structural systems. Accordingly, E_s is taken as another random variable to consider the uncertainty in the structural stiffness. The mean modulus of elasticity of steel, E_s, is assumed to be a constant parameter with a value of 200000 MPa. The statistical values of steel modulus of elasticity, E_s, for each building subclass are given in Table 4.5.

Table 4.5 Steel modulus of elasticity variability for each building subclass

Building Subclass	Steel Modulus of Elasticity (E_s)		
	Mean (MPa)	COV (%)	Distribution
SUPERIOR	200000	3	Normal
TYPICAL	200000	4	Normal
POOR	200000	5	Normal

The COV values are determined in accordance with previous studies (Mosalam et al., 1997; Mirza and MacGregor, 1979).

4.3 STORY MASS AND DAMPING

Uncertainty in mass and damping is also considered while generating the fragility functions. Random nature of material properties, geometrical variations in structural components, imperfectly known live loads and loads due to nonstructural components are the main sources of uncertainty in mass. As Ellingwood et al. (1980) stated; it is commonly accepted that a normal distribution is appropriate in order to quantify the mass uncertainty, with a mean value equal to the nominal (calculated) dead load and a typical COV value of 0.10. Accordingly, mass is considered as a random variable. The mean and the COV values for all building subclasses are given in Table 4.6. For mean story mass, the values obtained from the story mass calculation of the prototype buildings under concern are directly used and mean values are assumed to be constant regardless of the building subclass. Furthermore, all lumped masses are increased or decreased together with the appropriate ratio in order to provide a uniform variation within the structure.

Some experimental data on the variability in viscous damping are available (McVerry, 1979; Camelo et al., 2001). In light of these observations and as discussed by Porter et al. (2002), damping ratio is considered as a random variable.

The mean value for viscous damping ratio is taken as 5%, constant for all building subclasses, and the COV value is taken as 0.30 (Table 4.6).

Table 4.6 Variability in story mass and damping for each building subclass

Building Subclass	**Story Mass (MS)**		**Damping, ζ**	
	Mean (ton)	COV (%)	Mean (%)	COV (%)
SUPERIOR	45.5	10	5	30
TYPICAL	45.5	10	5	30
POOR	45.5	10	5	30

4.4 HYSTERESIS MODEL PARAMETERS FOR BUILDING SUBCLASSES

The accuracy of dynamic inelastic response analysis is primarily dependent on the validity of the model used to describe the hysteretic behavior of the structural components. For analysis of RC structures, the model should be sophisticated enough to simulate stiffness degradation, strength degradation, pinching behavior, and unsymmetric hysteresis. On the other hand, the model should be simple enough since every additional parameter increases the complexity of the model and the computational time of the analysis.

As a seismic response analysis platform, IDARC–2D includes many different types of hysteretic response curves. In this study, the piece–wise linear hysteretic model that incorporates stiffness degradation, strength deterioration, non–symmetric response and slip–lock is used to simulate the cyclic response of beams and columns. There exist four major parameters that characterize the hysteretic response in the model. These are stiffness degradation parameter (α), ductility based strength degradation parameter (β_1), hysteretic energy based strength degradation parameter (β_2), and slip parameter (γ). Schematic representation of the model parameters is shown in Figure 4.3 (Phan et al., 1993).

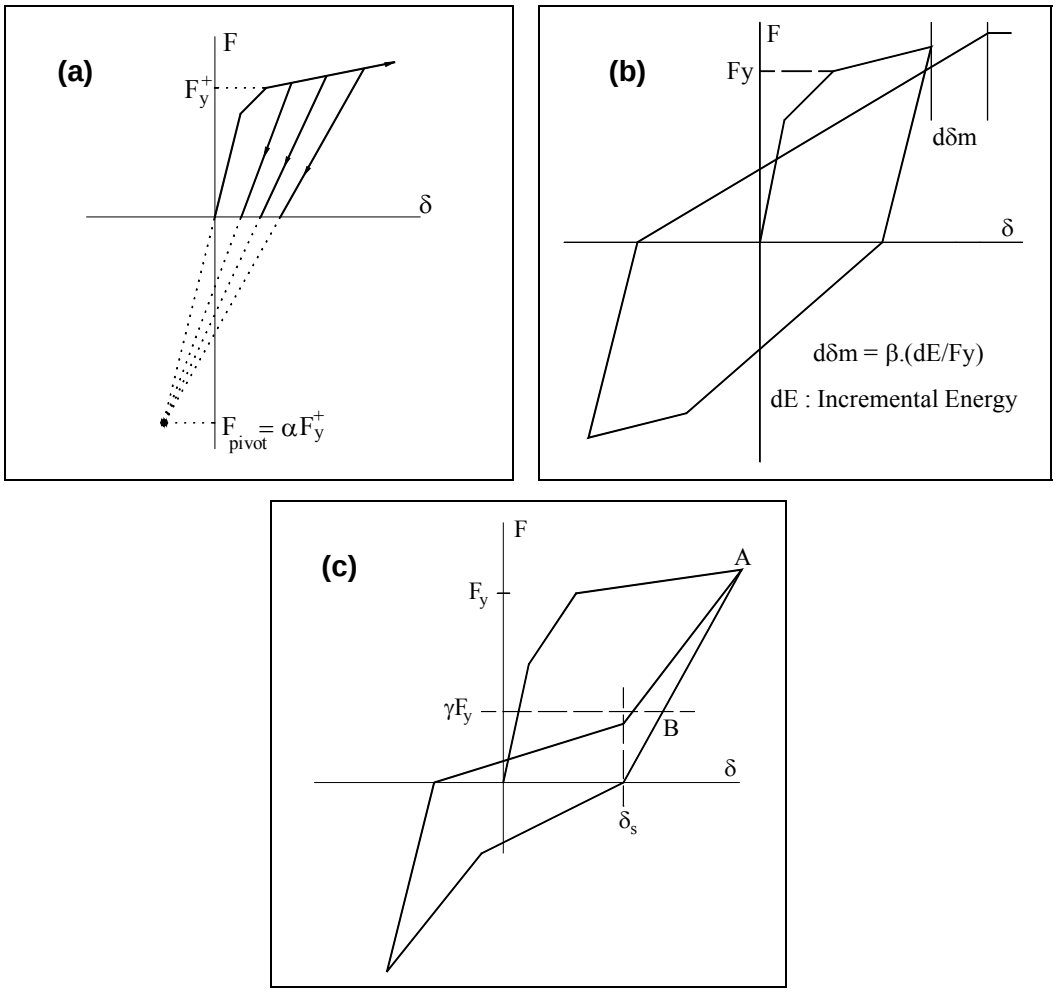

Figure 4.3 Schematic representations of the IDARC hysteresis model parameters a) unloading stiffness degradation, b) strength degradation, c) pinching or slip

Parameters proposed by IDARC–2D to be used for different levels of hysteretic performance are given in Table 4.7 (Valles et al., 1996).

Table 4.7 Recommended values for IDARC–2D hysteresis parameters

Parameter	Effect			
	No Degrading	**Mild Degrading**	**Moderate Degrading**	**Severe Degrading**
α	200	15	10	4
β_1	0.01	0.15	0.30	0.60
β_2	0.01	0.08	0.15	0.60
γ	1.00	0.40	0.25	0.05

Stiffness degradation generally occurs in RC members, basically caused by cracking of concrete under repeated cyclic loading. The elastic stiffness degrades with increasing ductility. This behavior is generally adapted to hysteresis models in the form of degradation in the initial elastic stiffness as a function of the maximum amplitude of cyclic deformation for the unloading branch. One specific way to model the unloading stiffness degradation is to employ the pivot approach. In this approach, the stiffness degradation is introduced by setting a common point on the extrapolated initial skeleton curve line, and assuming that the unloading lines aim to this point until they reach the x–axis (Figure 4.3.a). The parameter α specifies the degree of unloading stiffness degradation, and more importantly, the area enclosed by the hysteresis loops. The default value of the parameter for the non–degrading case is 200, and takes smaller values to simulate stiffness degradation characteristics.

Strength degradation determines the stability of response and the rate of approaching failure. It depends on many parameters such as the plastic deformation range and the dissipated energy per cycle. Since it is a history dependent phenomenon, it is also influenced by the number of inelastic excursions or low

cycle fatigue. In IDARC–2D, strength degradation is modeled by reducing the capacity in the backbone curve (Figure 4.3.b). The β_i parameters represent the rate of strength degradation in terms of ductility and hysteretic energy dissipation characteristics, respectively. The default value for both hysteresis parameters is 0.01 which represents no degradation, and the increase in the values indicates more strength degradation.

The pinching behavior is introduced by lowering the target maximum point (point A in Figure 4.3.c) to a straight level of γF_y (point B in Figure 4.3.c) along the previous unloading line. Reloading point aims this new target point B until it reaches the crack closure deformation, δ_s. The stiffness of the reloading path is changed at this point to aim the previous target maximum point A. The introduction of such a pinching behavior also leads to a reduction in hysteresis loop areas, and indirectly, in the amount of dissipated energy. The default value for parameter γ is 1.0, for no degradation, and as the value decreases, the pinching becomes more severe.

4.4.1 DETERMINATION OF HYSTERESIS MODEL PARAMETERS FROM OBSERVED BEHAVIOR

The seismic response characteristics of the RC structures in each subclass primarily depend on the values of the hysteretic model parameters because of deterioration in mechanical properties such as strength and stiffness. The selection of the values in this study are based on the recommended values by IDARC–2D itself and also on the experimentally observed behavior of the column specimens tested under cyclic loading, taken from the PEER Structural Performance Database (SPD, 2003). The web site provides results of over 400 cyclic, lateral–load tests of RC columns with rectangular and circular cross–sections. For each test in the database, a reference, digital top force–displacement history, key material properties and details of the test geometry are provided.

For superior building subclass, the structural members are assumed to exhibit no degradation. Hence the default values of the parameters for no degradation listed in Table 4.7 are employed to simulate the cyclic response of structural members in the superior building subclass. The schematic representation of the hysteresis model under constant amplitude cyclic loading with α=200, β_1=0.01, β_2=0.01 and γ=1.0 is presented in Figure 4.4. There is a stable behavior with high energy dissipation characteristics and members exhibit degradation neither in stiffness nor in strength although the structural system is subjected to numerous inelastic cyclic reversals as seen in the figure.

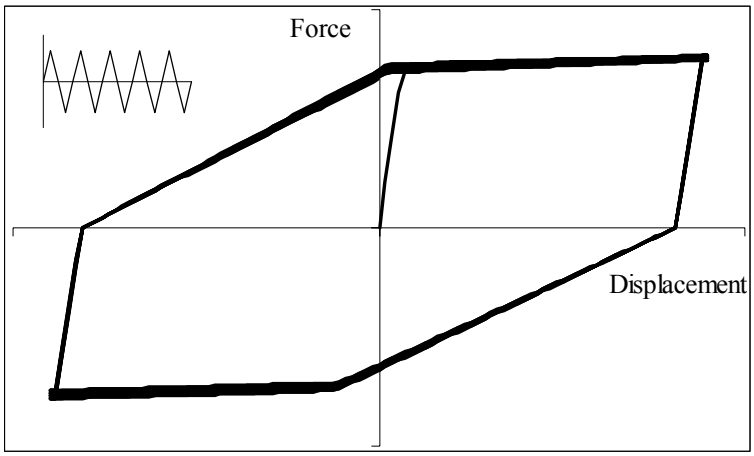

Figure 4.4 Representative hysteresis behavior with α=200, β_1=0.01, β_2=0.01 and γ=1.0

Such a stable behavior can also be compared with the experimental observations under variable amplitude cyclic loading. Figure 4.5 illustrates the comparison of the analytical model with the values α=200, β_1=0.01, β_2=0.01 and γ=1.0, by the observed cyclic response of the column specimen tested by Saatçioğlu and Özcebe (1989). The test specimen was a full size RC column having a square cross–section of 35 cm × 35 cm. Longitudinal reinforcement ratio was 3.2% whereas the

transverse reinforcement ratio was 2.0%. The specimen was subjected to both lateral cyclic loads and axial compressive loads, for which axial load ratio was 0.13. The specimen had a concrete strength of 37 MPa. As it can be observed from Figure 4.5b, the hysteresis loops were very stable and the specimen showed a ductile behavior with insignificant strength decay throughout the test. Figure 4.5a represents the analytical simulation of the same test program and the comparison of the energy dissipation characteristics of experimental and analytical results encourages the use of above parameter values for member behavior in superior building subclass.

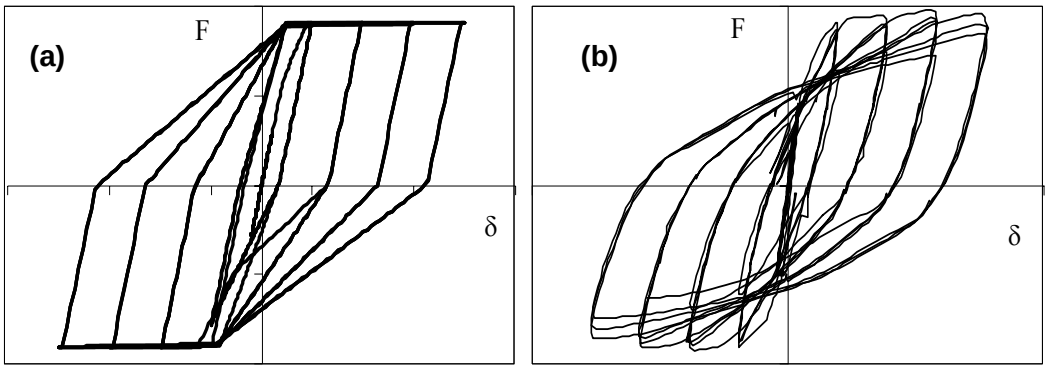

Figure 4.5 Comparison of analytical hysteretic model response and experimentally observed behavior for superior building subclass

In case of typical building subclass, the structural members are assumed to exhibit slight–to–moderate degradation. Hence the values that are employed to simulate the cyclic response of structural members in this building subclass are α=20, β_1=0.25, β_2=0.25 and γ=0.6. In Figure 4.6 the schematic representation of the hysteresis model under constant amplitude cyclic loading with the above values is shown. The strength at the maximum displacement slightly decreases with the number of cycles and the area enclosed by the hysteresis loops is not as large as the non–degrading case.

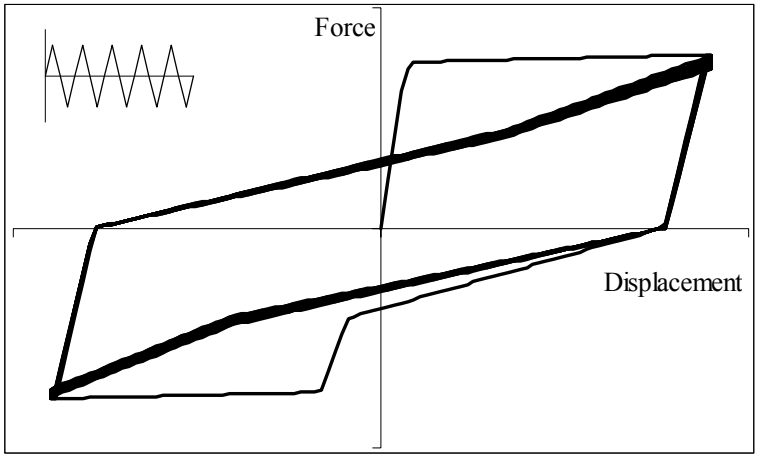

Figure 4.6 Representative hysteresis behavior with α=20, β_1=0.25, β_2=0.25 and γ=0.6

Comparison of the analytical behavior with the parameter values α=20, β_1=0.25, β_2=0.25 and γ=0.6 by the experimental cyclic behavior under variable amplitude loading is given in Figure 4.7. The specimen used in this comparison is taken from Atalay and Penzien (1975) and it is a double–ended specimen with pinned boundary conditions at both ends. The cyclic lateral displacement was applied to the central stub. The square specimen having 30.5 cm × 30.5 cm cross–sectional dimensions was also subjected to axial loading, for which the axial load ratio was 0.10. Longitudinal reinforcement ratio of the specimen was 1.7% whereas the transverse reinforcement ratio was 1.5%. The concrete strength of the specimen was determined as 29 MPa from cylinder specimens. The load–deformation curve of the specimen (Figure 4.7b) reflects the hysteretic behavior of a typical structural component with slight–to–moderate strength degradation. Furthermore the considerable effect of pinching becomes noticeable since the axial load level is relatively low. The experimental curve is comparable to the analytical curve (Figure 4.7) with the model parameters given above. The overall resemblance between the analytical and experimental hysteretic behavior encourages the use of the aforementioned parameter value set for the typical building subclass.

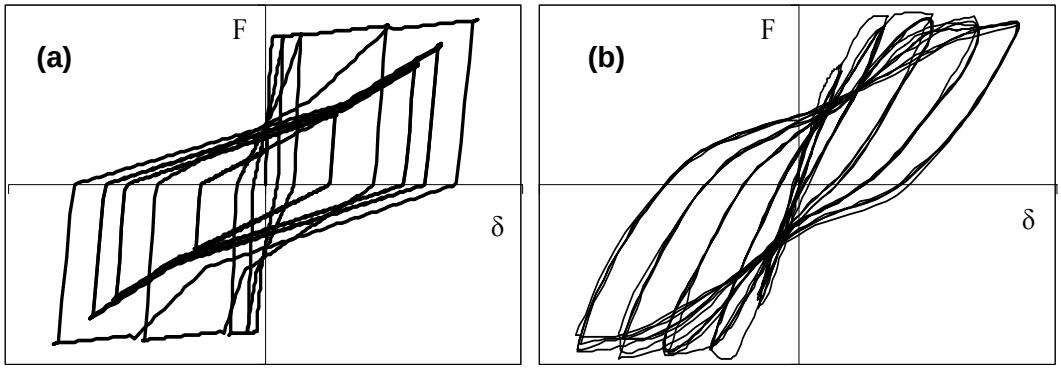

Figure 4.7 Comparison of analytical hysteretic model response and experimentally observed behavior for typical building subclass

For poor building subclass, the structural members are assumed to exhibit severe degradation and pinching. Referring to the recommended values and experimental observations, the values selected for the hysteretic response of the structural members in this subclass are α=5, β_1=0.5, β_2=0.5 and γ=0.3. The schematic representation of the hysteresis model under constant amplitude cyclic loading with the hysteresis model values given above is shown in Figure 4.8.

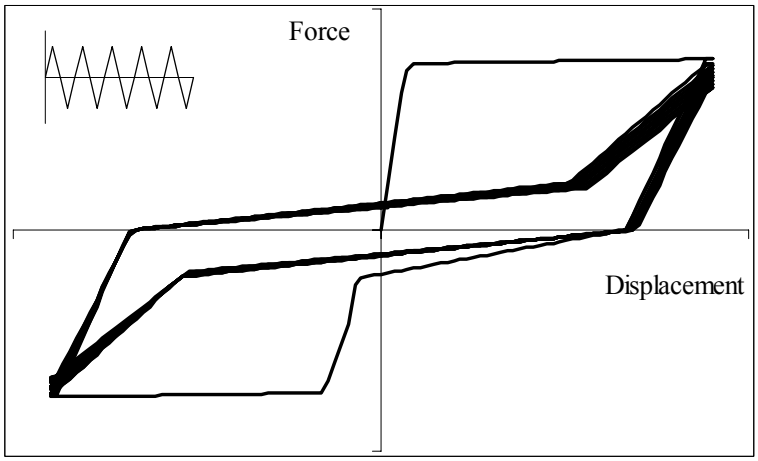

Figure 4.8 Representative hysteresis behavior with α=5, β_1=0.5, β_2=0.5 and γ=0.3

As seen from the Figure 4.8, in addition to strength degradation, there is a considerable amount of pinching in the analytical model, which narrows the area enclosed by the loops and reduces the dissipated energy significantly.

Analytical behavior with the parameter values α=5, β_1=0.5, β_2=0.5 and γ=0.3 is compared with the experimental cyclic behavior under variable amplitude loading in Figure 4.9.

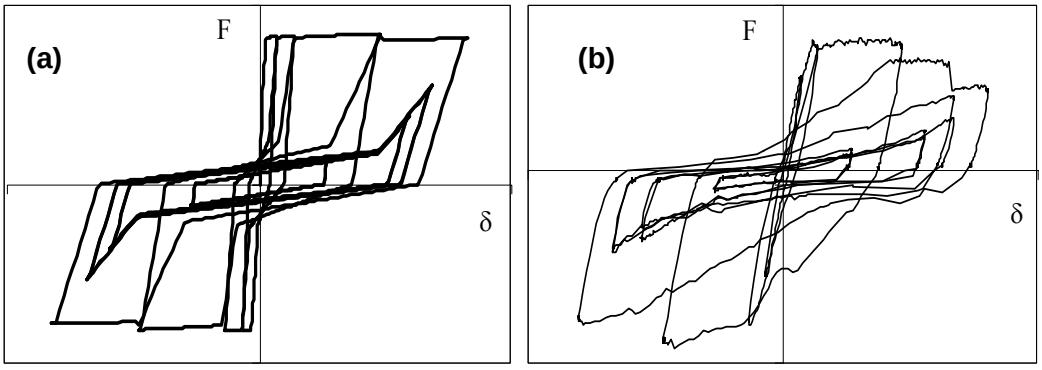

Figure 4.9 Comparison of analytical hysteretic model response and experimentally observed behavior for poor building subclass

The experimental data is taken from the test program conducted by Erberik and Sucuoğlu (2004). The selected specimen was a 1/3 scale cantilever model which was tested under cyclic lateral load only (no axial load). The specimen had a rectangular cross–section of 10 cm × 15 cm. The longitudinal reinforcement ratio was 1.3% whereas the transverse reinforcement ratio was 1.34%. The concrete strength was determined as 21 MPa. As seen in Figure 4.9b, the specimen exhibits significant deterioration in stiffness and strength accompanied by excessive pinching. The main reason of excessive pinching is the use of plain bars as longitudinal reinforcement. Furthermore low span–to–depth (a/d≈3) ratio of the specimen indicates significant interaction between shear and flexure effects. This

kind of interaction influences the stiffness degrading and energy dissipation characteristics to a great extent. However, the test specimen was intentionally designed to exhibit significant amount of stiffness and strength deterioration. The force–displacement curve of the analytical model with the same loading history seems to have a similar trend in general terms. Hence the use of model parameter values given above is validated for poor building class.

All the hysteretic parameters that have been employed in the analytical modeling of structures in three different subclasses are listed in Table 4.8.

Table 4.8 Hysteretic model parameters employed

Hysteretic Model Parameter	**Superior Building Subclass**	**Typical Building Subclass**	**Poor Building Subclass**
α	200	20	5
β_1	0.01	0.25	0.5
β_2	0.01	0.25	0.5
γ	1	0.6	0.3

By employing hysteresis model parameters according to the structural subclasses, deterioration in mechanical properties and increase in damage of RC moment resisting frames are included into fragility analysis of Turkish building stock. Hence in addition to strength, stiffness, mass and damping uncertainty, response variability under cyclic loading is also taken into account for superior, typical and poor subclasses.

CHAPTER 5

FRAGILITY CURVE GENERATION

5.1 SELECTION OF GROUND MOTION INTENSITY PARAMETER

Ground motion intensity expresses the ability of the earthquake to cause damage on structures. Hence selecting the ground motion intensity is a debate of earthquake engineering for a long period of time. Besides, some difficulties in explaining unexpected damage due to large earthquakes with conventional intensity measures have made this subject attractive for many researchers. Especially in fragility-based assessment studies, the correlation between the selected ground motion intensity parameter and the structural deformation demand requires elaborate consideration.

In Chapter 2, some quantitative and qualitative ground motion parameters are described in detail. Among these, PGA and S_a play an important role in traditional seismic design approach because of the ground motion prediction equations and probabilistic seismic hazard curves that are derived for PGA and S_a (Akkar and Özen, 2005). Especially for earthquake resistant design of conventional structures, PGA is commonly accepted since design ground motions and spectrum shapes are expressed in terms of this parameter. On the other hand, recent studies on near-fault earthquakes and their impact on seismic response of structures have revealed the importance of other ground motion parameters. A popular one among these parameters is PGV that expresses the acceleration cycle with maximum energy (Sucuoğlu et al., 1999). Conveniently, Akkar and Özen (2005) emphasized that PGV correlates well not only with particular ground motion parameters such as

earthquake magnitude, ground motion duration and frequency content but also the SDOF deformation demand. Besides the stable correlation between PGV and deformation demands as compared to S_a, the limitations of PGA and the ratio of PGV to PGA measures in deformation demand expression is salient. Although the study of Akkar and Özen (2005) is conducted for SDOF systems; it is worth considering the fairly good correlation between PGV and spectral displacement. Furthermore, PGV primarily influences the seismic spectral response of medium period systems, approximately in the period range $0.5<T<2.0$ seconds (Sucuoğlu et al., 1999). Predominant periods of most of the analytical models considered in this study reside in this period range. Based on the above discussions, this study employs PGV in the selection and grouping of ground motion records as well as the hazard intensity parameter in fragility curves.

5.2 STRUCTURAL SIMULATION AND RESPONSE STATISTICS

In Chapter 4, the material properties, story mass and damping values for building subclasses are given in a probabilistic manner. Besides, building subclass definitions are stated in detail. To reflect these properties into building subclass characteristics quantitatively, this study employs LHS method stated in Chapter 2.

A fundamental step of LHS method is the selection of sample size. This decision mainly depends on the sensitivity of results compared with computational expense. Considering the past experience from previous studies (Elnashai and Borzi, 2000; Erberik and Elnashai, 2003), the sample size is chosen as 20.

In Table 5.1, the detailed process of LHS method application for random variable "f_c" is given. Corresponding mean and COV values are taken for superior building subclass whereas, m, U_m and P_m are the parameters stated in Chapter 2. "ICDF" is the value obtained from the inverse cumulative distribution using Equation 2.8. "RNP" is the random permutation of these values whereas "REP" is the order of sampling value. Finally, "SV" is the sampling value obtained by LHS method.

Table 5.1 LHS application for random variable "f_c" of superior structural subclass

Concrete Compressive Strength, f_c						
m	Um	Pm	ICDF	RNP	REP	SV (MPa)
1	0.206	0.010	12.56	5	1	22.30
2	0.988	0.099	15.88	4	2	18.73
3	0.007	0.100	15.90	14	3	19.67
4	0.219	0.161	16.83	20	4	15.88
5	0.375	0.219	17.52	8	5	12.56
6	0.056	0.253	17.87	17	6	20.20
7	0.921	0.346	18.73	2	7	19.37
8	0.177	0.359	18.84	12	8	17.52
9	0.438	0.422	19.37	7	9	23.49
10	0.190	0.459	19.67	3	10	25.68
11	0.508	0.525	20.20	6	11	20.93
12	0.631	0.582	20.66	13	12	18.84
13	0.273	0.614	20.93	11	13	20.66
14	0.080	0.654	21.27	19	14	15.90
15	0.933	0.747	22.13	18	15	22.98
16	0.290	0.764	22.30	1	16	24.82
17	0.487	0.824	22.98	15	17	17.87
18	0.245	0.862	23.49	9	18	22.13
19	0.686	0.934	24.82	16	19	21.27
20	0.241	0.962	25.68	10	20	16.83

Besides the concrete strength, the LHS method is applied to other material properties, damping and story mass which are taken as random variables in this study. Moreover, appropriate hysteretic behavior parameters covered in Chapter 4.4 as stiffness degradation parameter, α; ductility based strength degradation parameter, β_1; hysteretic energy based strength degradation parameter, β_2; and slip parameter, γ are incorporated to imply the hysteretic behavior into the simulations.

Lateral reinforcement in RC columns improves capacity by providing ductility and confinement, preventing the buckling of longitudinal bars and holding the longitudinal bars in place. Hence in detailing, column longitudinal bars should be braced properly by closely spaced lateral reinforcement bars. In case of tied columns, every longitudinal bar in columns should be braced by the corner of a hoop or cross–ties. In particular, for seismic prone regions, to achieve ductility together with resistance against bar buckling, the closed ties and cross–ties should be spaced closely (Ersoy and Özcebe, 2001). Studies and investigations after major earthquakes in Turkey reveal that there are many detailing deficiencies and wrong applications in construction practice. Consequently, lateral reinforcement confinement efficiency in columns is taken into consideration in this study. C_{eff} is the confinement effectiveness parameter defining the effectiveness of hoop arrangements. Some typical hoop arrangements and corresponding IDARC–2D values used in this study are given in Figure 5.1.

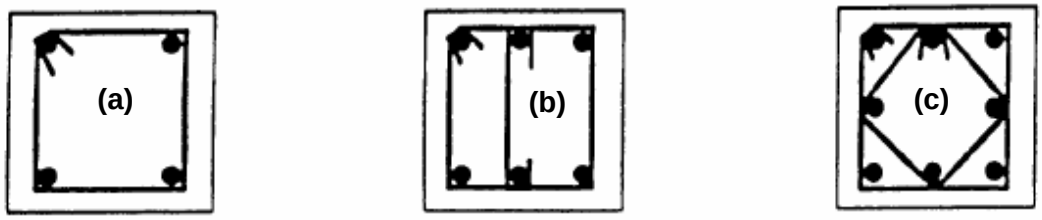

$C_{eff} = 0.50$ $C_{eff} = 0.66$ $C_{eff} = 1.00$

Figure 5.1 Lateral reinforcement effectiveness coefficient for a) poor, b) typical, and, c) superior building subclass

The results computed from LHS Method are given in Table 5.2 for the superior building subclass whereas Tables 5.3 and 5.4 present the similar results for typical and poor building subclasses respectively. In these tables, f_c, f_y, E_c and E_s are the material property values, whereas ζ is damping, and MS is story mass value. The abbreviation used for stiffness degradation parameter is α; ductility based strength degradation parameter is β_1; hysteretic energy based strength degradation parameter is β_2; and slip parameter is γ. The confinement effectiveness parameter is designated as C_{eff}.

Table 5.2 Material and behavior properties obtained for superior building subclass

SUPERIOR										
f_c(MPa)	**f_y(MPa)**	**E_c(MPa)**	**E_s(MPa)**	**ζ**	**α**	**β_1**	**β_2**	**γ**	**C_{eff}**	**MS(ton)**
22.30	467.72	19047	194322	7.10	200	0.01	0.01	1.00	1.00	52.974
18.73	478.07	19633	209379	4.69	200	0.01	0.01	1.00	1.00	48.777
19.67	559.90	23516	189952	5.59	200	0.01	0.01	1.00	1.00	44.361
15.88	398.11	22550	203623	5.05	200	0.01	0.01	1.00	1.00	46.409
12.56	537.13	21797	205071	6.23	200	0.01	0.01	1.00	1.00	48.048
20.20	500.85	21290	201089	3.76	200	0.01	0.01	1.00	1.00	40.946
19.37	522.32	23056	192311	4.57	200	0.01	0.01	1.00	1.00	55.76
17.52	486.40	21922	197294	5.86	200	0.01	0.01	1.00	1.00	47.759
23.49	438.21	20447	201991	1.02	200	0.01	0.01	1.00	1.00	45.216
25.68	427.49	22121	195407	5.40	200	0.01	0.01	1.00	1.00	41.789
20.93	407.32	23984	198896	6.87	200	0.01	0.01	1.00	1.00	49.707
18.84	440.62	20638	218541	7.54	200	0.01	0.01	1.00	1.00	47.158
20.66	457.95	20219	199337	3.63	200	0.01	0.01	1.00	1.00	38.528
15.90	485.43	17639	204797	4.89	200	0.01	0.01	1.00	1.00	45.752
22.98	496.06	22758	206787	4.26	200	0.01	0.01	1.00	1.00	37.678
24.82	549.78	21371	202958	2.96	200	0.01	0.01	1.00	1.00	42.729
17.87	510.88	20847	197945	5.30	200	0.01	0.01	1.00	1.00	50.791
22.13	520.23	19905	200376	6.54	200	0.01	0.01	1.00	1.00	39.933
21.27	471.90	21129	190671	3.22	200	0.01	0.01	1.00	1.00	43.156
16.83	453.16	18714	196521	4.02	200	0.01	0.01	1.00	1.00	44.148

Table 5.3 Material and behavior properties obtained for typical building subclass

TYPICAL										
f_c(MPa)	**f_y(MPa)**	**E_c(MPa)**	**E_s(MPa)**	**ζ**	**α**	**β_1**	**β_2**	**γ**	**C_{eff}**	**MS(ton)**
12.61	331.92	18677	202513	4.51	20	0.25	0.25	0.60	0.66	40.68
14.23	350.05	17644	208977	2.20	20	0.25	0.25	0.60	0.66	43.81
19.25	280.32	20062	206578	5.92	20	0.25	0.25	0.60	0.66	51.64
13.00	394.75	17011	189758	5.27	20	0.25	0.25	0.60	0.66	49.73
8.02	414.28	19242	204224	2.93	20	0.25	0.25	0.60	0.66	46.50
14.74	324.22	19584	201851	5.58	20	0.25	0.25	0.60	0.66	42.90
22.19	317.15	18944	199804	6.53	20	0.25	0.25	0.60	0.66	44.86
15.17	357.20	16296	194999	6.96	20	0.25	0.25	0.60	0.66	49.07
18.02	369.63	20262	197059	5.00	20	0.25	0.25	0.60	0.66	50.57
15.84	338.70	20520	193697	4.12	20	0.25	0.25	0.60	0.66	45.12
15.67	428.92	15415	187851	6.72	20	0.25	0.25	0.60	0.66	45.98
13.44	304.71	17416	200164	6.05	20	0.25	0.25	0.60	0.66	38.78
17.26	347.81	17984	207128	3.38	20	0.25	0.25	0.60	0.66	42.42
11.24	402.13	18478	198641	3.87	20	0.25	0.25	0.60	0.66	47.86
17.44	385.51	21974	195926	4.22	20	0.25	0.25	0.60	0.66	47.09
12.19	372.77	20766	203993	4.73	20	0.25	0.25	0.60	0.66	43.53
16.64	389.00	19026	182278	5.04	20	0.25	0.25	0.60	0.66	55.36
13.84	380.06	19743	212962	5.44	20	0.25	0.25	0.60	0.66	41.20
16.31	439.92	18208	191806	3.52	20	0.25	0.25	0.60	0.66	47.99
14.64	361.83	21310	214129	7.67	20	0.25	0.25	0.60	0.66	37.92

Table 5.4 Material and behavior properties obtained for poor building subclass

POOR										
f_c(MPa)	**f_y(MPa)**	**E_c(MPa)**	**E_s(MPa)**	**ζ**	**α**	**β_1**	**β_2**	**γ**	**C_{eff}**	**MS(ton)**
11.26	281.86	17804	184052	4.32	5	0.50	0.50	0.30	0.50	47.50
10.47	240.38	17099	182427	3.75	5	0.50	0.50	0.30	0.50	39.91
9.57	306.91	18525	198751	5.97	5	0.50	0.50	0.30	0.50	40.96
10.69	224.16	16066	202957	5.60	5	0.50	0.50	0.30	0.50	42.56
11.58	280.88	17598	210277	3.61	5	0.50	0.50	0.30	0.50	49.96
7.63	226.02	19212	198316	5.47	5	0.50	0.50	0.30	0.50	43.49
13.45	235.75	14390	187187	2.23	5	0.50	0.50	0.30	0.50	47.00
9.43	216.45	15623	207731	4.10	5	0.50	0.50	0.30	0.50	38.84
12.23	297.75	13223	196174	3.17	5	0.50	0.50	0.30	0.50	48.70
7.07	247.45	16567	191378	5.03	5	0.50	0.50	0.30	0.50	42.19
10.19	206.60	17003	200496	5.35	5	0.50	0.50	0.30	0.50	36.06
12.62	231.58	14916	192772	7.76	5	0.50	0.50	0.30	0.50	45.17
8.03	274.79	16369	214635	6.61	5	0.50	0.50	0.30	0.50	46.50
11.71	262.94	15026	203884	4.87	5	0.50	0.50	0.30	0.50	45.50
10.95	195.24	17351	202452	2.73	5	0.50	0.50	0.30	0.50	50.21
8.74	252.75	15481	212100	4.57	5	0.50	0.50	0.30	0.50	51.61
9.16	256.88	15769	205900	4.76	5	0.50	0.50	0.30	0.50	54.03
9.86	244.68	18210	195689	6.35	5	0.50	0.50	0.30	0.50	44.19
6.96	257.96	16755	193260	6.14	5	0.50	0.50	0.30	0.50	48.11
8.43	268.17	13744	217913	7.11	5	0.50	0.50	0.30	0.50	44.41

5.3 ATTAINMENT OF LIMIT STATES

In this study, the limit states for the RC frame structures considered are specified in terms of drift. A set of performance objectives based on this structural response parameter has already been declared by several publications. It is appropriate to refer to these studies before explaining in detail the procedure that is employed in this study for the attainment of limit states.

The relationship between the desired seismic performance and the maximum transient interstory drift ratio for the framed structures recommended by the Structural Engineers Association of California (SEAOC, 1995) is shown in Table 5.5. The transient and permanent interstory drift values for RC frames suggested by FEMA 273 (ASCE, 1996) are given in Table 5.6.

Table 5.5 Performance levels in terms of interstory drift as suggested by SEAOC (1995)

Performance Level	Building Damage	Transient Drift
Fully Operational	Negligible	Interstory Drift < 0.2 %
Operational	Light	0.2 % < Interstory Drift < 0.5 %
Life Safe	Moderate	0.5 % < Interstory Drift < 1.5 %
Near Collapse	Severe	1.5 % < Interstory Drift < 2.5 %
Collapse	Complete	2.5 % < Interstory Drift

Table 5.6 Structural performance levels recommended by FEMA 273 (ASCE,1996)

Performance Level	Concrete Frames	
	Transient Drift	Permanent Drift
Immediate Occupancy	1 %	Negligible
Life Safety	2 %	1 %
Collapse Prevention	4 %	4 %

Other than these commonly referred publications, several researchers defined drift–based limit state criteria according to the RC structural frame systems that they considered in their own studies. Sözen (1981) suggested that an interstory drift of 2% may be set as the collapse limit for three–quarters of reinforced concrete buildings. At values in excess of this limit, P–delta effects are significant and lead to reduced lateral load resistance causing failure. Ghobarah et al. (1997) suggested five damage states for performance evaluation of a ductile RC moment resisting frame (MRF). Based on the results of a series of dynamic analyses, the drift values assigned to each limit state are as follows: 0.7 % for the elastic limit, 2 % for the minor damage limit, 4.6 % for the repair limit and 5.6 % for the collapse limit. Dymiotis et al. (1999) derived a statistical distribution for the critical interstory drift using experimental results obtained from the literature. The study utilized data from tests conducted using shaking table, pseudo–dynamic, monotonic, and cyclic loading. It was concluded that the ultimate drift of 3 % lies in the lower tail of the statistical distribution. The mean interstory drift values obtained from the distribution were 4.0 % and 6.6 % for near failure and failure, respectively. These values were then used for the seismic reliability assessment of a 10–story RC frame. Limniatis (2001) stated that interstory drift ratios of 1 % and 3 % are commonly suggested for RC buildings, corresponding to serviceability and ultimate limit states, respectively. Rossetto and Elnashai (2003) derived empirical fragility curves for RC building structures based on a database of 99 post–earthquake damage distributions observed in 19 earthquakes and concerning a total of 340000 RC structures. They proposed interstory drift limits for nonductile moment resisting frames by using a new damage scale named the homogenized RC damage scale (HRC scale) as listed in Table 5.7. Ghobarah (2004) assigned drift ratio limits for the five limit states that he used before in his research. The drift values are specified for ductile and nonductile moment resisting frames separately and they are listed in Table 5.8. Booth et al. (2004) studied on the vulnerability assessment of building structures. The study was conducted for 4–7 story RC buildings in Turkey. Based on the building data, they specified approximate ranges of drift values for five different limit states (Table 5.9).

Table 5.7 Limit values of interstory drift defining the HRC–damage scale (Rossetto and Elnashai, 2003)

HRC Limit State	Interstory Drift
No damage	0.00 %
Slight	0.32 %
Light	0.43 %
Moderate	1.02 %
Extensive	2.41 %
Partial collapse	4.27 %
Collapse	> 5.68 %

Table 5.8 Drift limits associated with different damage states (Ghobarah, 2004)

Limit State	Ductile MRF	Nonductile MRF
No damage	< 0.2 %	< 0.1 %
Repairable damage a) Light b) Moderate	 0.40 % < 1.0 %	 0.20 % < 0.5 %
Irreparable	> 1.0 %	> 0.5 %
Severe – Partial Collapse	1.80 %	0.80 %
Collapse	> 3.0 %	> 1.0 %

Table 5.9 Drift ranges for different damage states (Booth et al., 2004)

Damage State	Drift Value
None	0 – 0.5 %
Low	0.5 % – 0.9 %
Moderate	0.9 % – 1.7 %
Extensive	1.7 % – 4.5 %
Complete	> 4.5 %

The proceeding discussions reveal the fact that the drift values suggested for limit states show a large scatter, especially for ultimate or collapse limit state. Therefore it is more appropriate to consider each limit state as a random variable rather than a single–valued parameter. This also enables the reflection of uncertainty in structural capacity to the final fragility curves.

In this study, three limit states are defined as Immediate Occupancy (IO), Life Safety (LS), and Collapse Prevention (CP) (Figure 5.2). Structures at IO limit state should have slight or no damage. Structures at LS limit state may sustain significant damage, but they should still provide an adequate margin against collapse. Structures at CP limit state are expected to remain standing, but with little margin against collapse. Accordingly, four damage states are introduced as slight or no damage (DS1), significant damage (DS2), severe damage (DS3) and collapse (DS4).

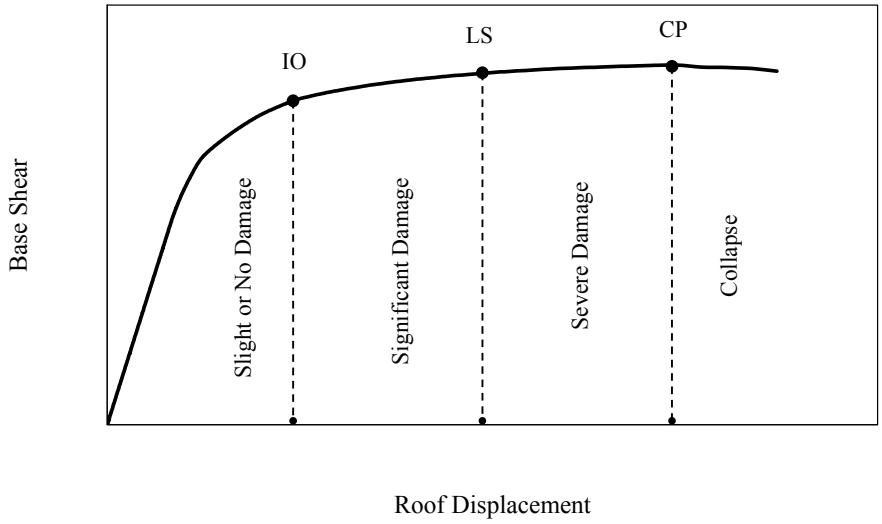

Figure 5.2 Performance levels and corresponding damage states used

Pushover curves obtained from the building models are employed for the decision on limit states. Roof displacement and base shear force are the axes of the curve as

seen in Figure 5.3. Earthquake load is idealized as an inverted triangular distribution and pushover analysis is carried out by applying the load incrementally. Hence propagation of damage can be observed from the initial stage of loading till collapse state.

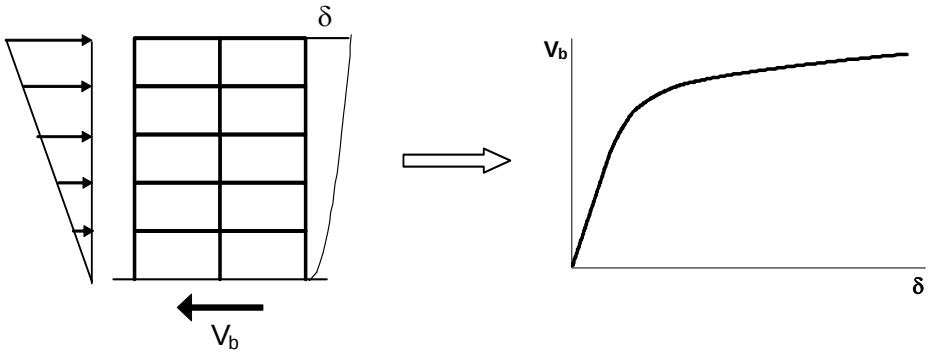

Figure 5.3 Pushover analysis and corresponding pushover curve

Different criteria are employed in the specification of interstory drift values for each limit state. The first criterion is to examine the progressive damage accumulation in the structure by monitoring the local performance stages such as yielding of beams and columns, failure of beams and columns, and strength degradation. The pushover curves were obtained by using the structural analysis software IDARC–2D and this study refers to the yield and ultimate state formulations for structural elements given in the documentation of the software (Valles et. al, 1996). The local response stages (cracking, yielding, failure, strength degradation) in the first two stories of model buildings 3SD2, 5SD2, 7SD2 and 9SD2 for each subclass (poor, typical and superior) are mapped on the corresponding pushover curves (see Figures A.1–A.12). From the curves it is observed that the consecutive yielding in beams of the first and second story induces significant reduction in the overall stiffness of the structure. Hence this abrupt change may be regarded as the onset of significant damage or in other

words, Immediate Occupancy Limit State. Thereafter, yielding in columns, which is an indicator of a reduction in the lateral strength capacity of the structure, is observed. Hence this may be regarded as the transition from significant to severe damage, or in other words, Life Safety Limit State. As damage propagates with the increased lateral load during the pushover analysis, yielding occurs in many of the structural members and even failure in some members can be observed. This is the stage where the collapse mechanism initiates and the stability of the structure under lateral load is no longer ensured. This transition from severe damage to collapse can be identified as Collapse Prevention Limit State.

The second criterion employed for the determination of limit states in this study is the softening index SI which was originally proposed by DiPasquale and Çakmak (1987). It is a function of the change in the stiffness of the structure with increasing damage caused by an external disturbance to the structure. The index can be defined as:

$$SI = 1 - \frac{K_{eff}}{K_0} \tag{5.1}$$

In Equation 5.1, K_0 is the initial stiffness of the pushover curve and K_{eff} is the effective secant stiffness at some intermediate roof displacement (Figure 5.4). The index is equal to zero when $K_0 = K_{eff}$ and takes values between 0 and 1 regarding the amount of stiffness change due to inelastic action. The upper bound of unity is a theoretical value with the condition that K_{eff} approaches to zero and physically this value defines the failure state of the structure. A similar index was used by Ghobarah (2004) to specify the drift ratio limits associated with various damage levels for ductile and nonductile moment resisting frames. Relationship between the maximum interstory drift ratio (MIDR) and the softening damage index was established by using the actual building data from 3, 6, 9 and 12–story frame buildings in the case of ductile moment resisting frames, 3 and 9–story frame buildings in the case of nonductile moment resisting frames. Then a smooth curve

was fitted for each case. The curve stabilizes at a damage index value of 0.70, corresponding to an interstory drift ratio of approximately 3 % for ductile moment resisting frame and at a damage index value of 0.80, corresponding to an interstory drift ratio of approximately 1 % for nonductile moment resisting frame.

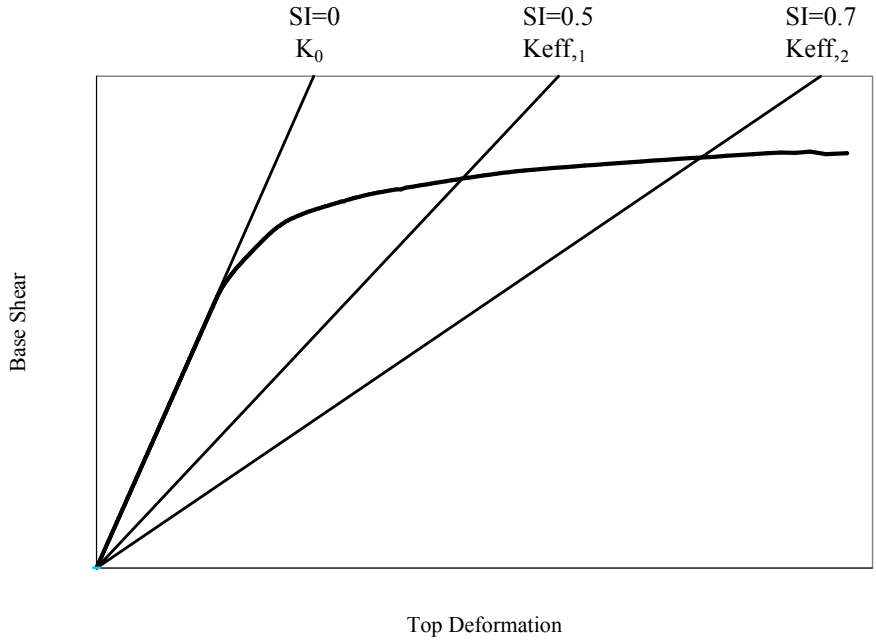

Figure 5.4 Pushover curve and change in softening index

The pushover curves for each building subclass together with the secant lines that represent SI values for different stages of structural response are presented in Appendix A. As observed in the Figures A.1–A.12, in the vicinity of consecutive yielding in beams, where there is an abrupt change of overall stiffness, the index generally takes values between 0.10 and 0.20. As the displacement increases, the secant stiffness decreases with an increase in the overall damage of the structure. Hence in the vicinity of life safety performance level, the SI index takes values between 0.45 and 0.55 depending on the structural model type (poor, typical or superior). In the vicinity of collapse, the SI index takes between 0.70 and 0.85.

The third and the last criterion is the equivalent ductility capacity of the structure, which is obtained by the bilinearization of the pushover curve in accordance with FEMA 356 (ASCE, 2000) approach. According to the iterative procedure, first a straight line is drawn from the origin having the same slope (stiffness) with the initial portion of the curve. Another line is drawn from the last point of the curve in the direction of the initial line. Taking the last point as the pivot, the slope of the second line is changed until the areas under the original pushover curve and the corresponding bilinear idealization are very close to each other. The point at the intersection of initial and second line is defined as "yield point". Then the slope of the initial line is changed in the direction of a point located on the capacity curve with a base shear force equal to 60 % of yield strength. From this point on, the equal area and 0.6 V_y requirements are provided one by one iteratively to obtain the "yield deformation" at the intersection of effective lateral stiffness and post yield stiffness. Accordingly, the equivalent ductility capacity is found by Equation 5.2 where, δ is the current deformation and δ_y is the yield deformation.

$$\mu = \delta/\delta_y \tag{5.2}$$

There are several studies in which the limit states are defined in terms of ductility capacity. A related study was conducted by Calvi (1999) for the specification of ductility values for Immediate Occupancy and Life Safety Limit States. Calvi proposed the following ductility limits in transition from slight–to–moderate damage for existing structures.

$$\mu_{min} = 1 + 1.05/n \tag{5.3}$$

$$\mu_{max} = 1 + 2.24/n \tag{5.4}$$

In these equations n is the number of stories. Hence, for buildings with 3, 5, 7 and 9 stories, the ductility values range between 1.1 and 1.8. In the case of well designed buildings where the damage is evenly distributed within the structure, the following values are proposed for the same limit state.

$$\mu_{min} = 1.35 \tag{5.5}$$

$$\mu_{max} = 1.91 \tag{5.6}$$

Calvi also proposed displacement ductility limits in transition from moderate–to–severe damage for both existing structures with structural deficiencies and well designed structures. In the former case, a single value for ductility capacity is given in terms of number of stories.

$$\mu_{min} = \mu_{max} = 1 + 2.99/n \tag{5.7}$$

For frame structures with 3, 5, 7, and 9 stories, the ductility value range between 1.3 and 2.0. For the latter case, Calvi stated that a ductility value of 3 to 4 is attainable for well engineered structures.

Regarding limit state discussions in terms of ductility, it is worth considering the study conducted by Booth et al. (2004) since the authors studied a building database composed of Turkish low–rise and mid–rise RC frame structures. They employed building surveys from 6 different sites in Marmara region, close to North Anatolian fault. According to their observations, immediate occupancy and life safety limit states are close to each other for Turkish frame buildings. In other words, the building may experience little damage up to the effective yield state. However even small demands beyond this state may lead to a rapid increase in deflections and damage, due to loss of stiffness and strength. Their observation is especially valid for non–ductile concrete frames, which are generally brittle and vulnerable to seismic action due to inherent deficiencies encountered in Turkish RC frame construction. For Life Safety and Collapse Prevention limit states, the authors proposed an idealized capacity spectrum with two ductility parameters μ_1 and μ_2, which represent the first loss of strength capacity and collapse, respectively. By definition, μ_1 and μ_2 correspond to ductility values for Life Safety and Collapse Prevention limit states. In the study, the values specified for μ_1 range between 1.5

and 3.0 whereas the values specified for μ_2 range between 3.0 and 6.0. The values are mainly based on the aforementioned Turkish building database, especially extracted from building inventory in Kocaeli and Sakarya districts.

Local response stages, specific values of softening index and displacement ductility are mapped on the pushover curves as shown in Appendix A for all building subclasses (Figures A.1–A.12). Based on these criteria, ranges of values in terms of top deformation are specified. The values are then converted to interstory drift that is the common parameter used in the other studies. The interstory drift values are listed in Table 5.10.

Table 5.10 Interstory drift values (%) associated with limit states

Building Class	**Maximum Interstory Drift Ratio (%)**					
	Immediate Occupancy		Life Safety		Collapse Prevention	
	Lower Limit	Upper Limit	Lower Limit	Upper Limit	Lower Limit	Upper Limit
MRF3–P	0.26	0.34	0.52	0.80	1.19	1.64
MRF3–T	0.35	0.47	1.17	1.75	2.41	3.22
MRF3–S	0.43	0.58	1.07	1.54	2.93	3.89
MRF5–P	0.20	0.26	0.38	0.49	0.85	1.43
MRF5–T	0.26	0.36	0.58	0.95	1.84	2.50
MRF5–S	0.36	0.46	0.86	1.28	2.70	3.47
MRF7–P	0.17	0.22	0.38	0.50	0.61	0.89
MRF7–T	0.18	0.25	0.54	0.72	1.03	1.62
MRF7–S	0.22	0.29	0.51	0.73	1.93	2.76
MRF9–P	0.16	0.21	0.32	0.40	0.54	0.69
MRF9–T	0.16	0.21	0.45	0.57	0.90	1.49
MRF9–S	0.18	0.25	0.48	0.62	1.78	2.68

As discussed above, intervals are selected for each limit state rather than a single value, and each limit state is regarded as a random variable rather than a deterministic parameter. This is deemed to be a more appropriate way of specifying

the limit states since there is not an exact definition for any limit state and it is neither easy nor proper to assign a single value to any limit state that is uncertain in nature. Since the value of a random variable represents an event, it can attain a numerical value only with an associated probability or probability measure. Hence the most suitable probability measure for the limit state variable in this study is regarded as uniform distribution, in which every limit state value within the range has the same probability of occurrence. The distribution of uniform probability density functions for the limit states of building subclasses are illustrated in Figures 5.5–5.8. In the figures, the horizontal axis that is abbreviated by "MIDR (%)" stands for maximum interstory drift in terms of percentage and the vertical axis denotes probability density function of maximum interstory drift, f_X(MIDR). From the figures it can be concluded that, the variation in limit state increases from Immediate Occupancy–to–Collapse Prevention, since there are more sources of uncertainty involved in later stages of complex inelastic behavior.

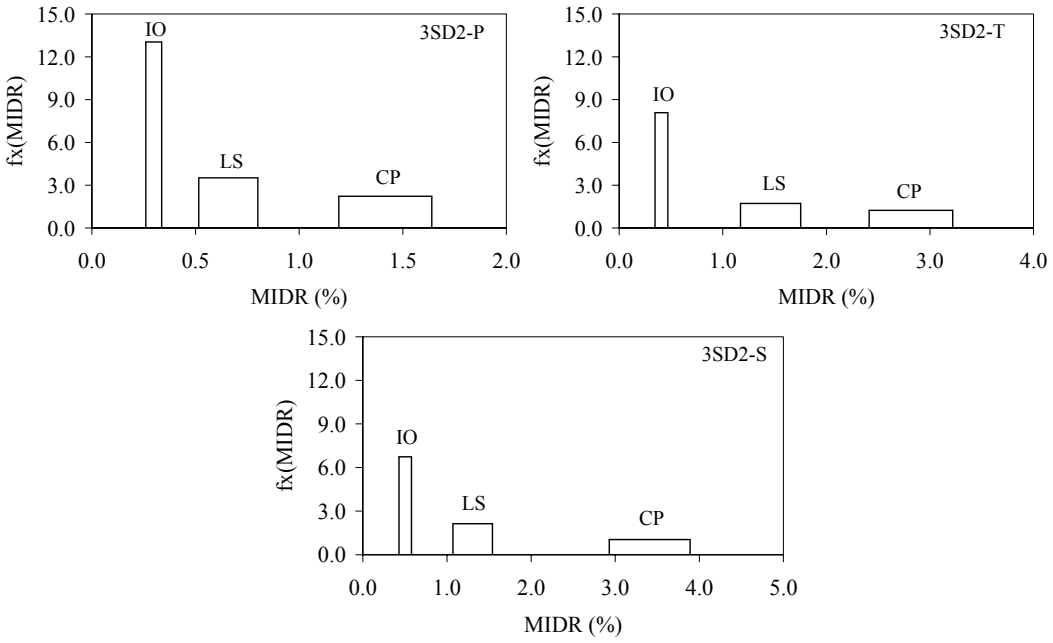

Figure 5.5 Uniform probability density functions for the limit states of 3–story models

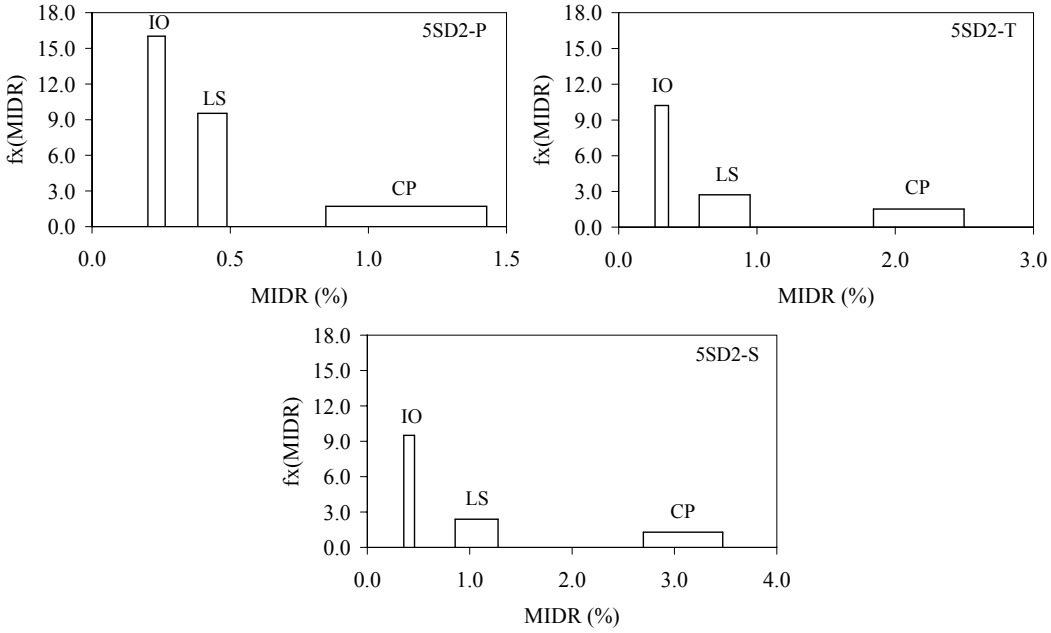

Figure 5.6 Uniform probability density functions for the limit states of 5–story models

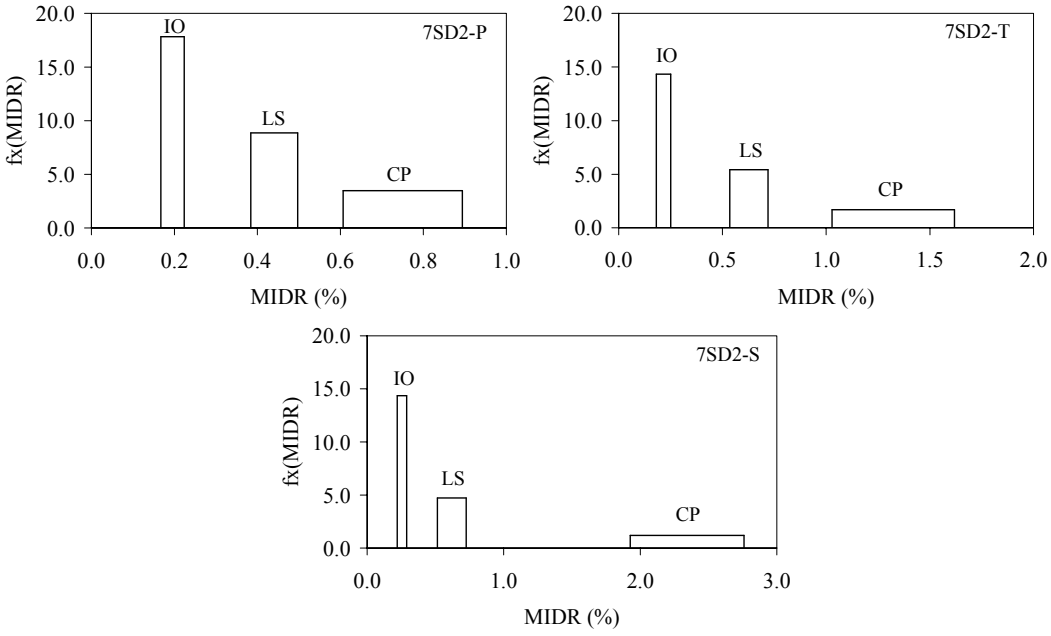

Figure 5.7 Uniform probability density functions for the limit states of 7–story models

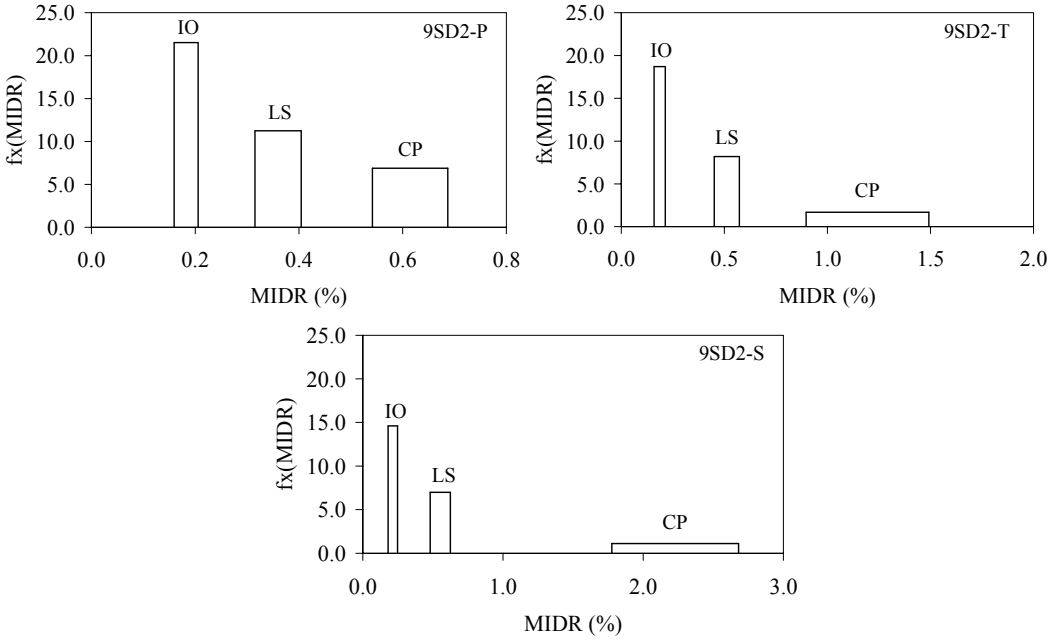

Figure 5.8 Uniform probability density functions for the limit states of 9–story models

5.4 DEVELOPMENT OF FRAGILITY CURVES FOR EACH SUBCLASS

The fragility of buildings is a performance measure in most basic terms. Previously in Chapter 2, fragility was described as the probability that the estimated structural response in engineering terms will exceed a damage level due to a given hazard intensity. The mathematical description of the fragility function is given in Equation 2.1. Using this equation with the choosen ground motion intensity parameter and limit states defined in this chapter yield the mathematical expression that is implemented during the fragility computations.

$$PE_{i,j} = P(DM \geq DL_i \left| PGV_j \right.) \tag{5.8}$$

In Equation 5.8, $PE_{i,j}$ expresses the probability of exceedance computed whereas DM and DL stand for demand measure and limit state value respectively. Hence

$PE_{i,j}$ is obtained as the structural demand measure exceeds a limit state i at a specific PGV value j. To obtain the demand measures, analytical models for superior, typical and poor structural subclasses with story number of 3, 5, 7, and 9 are subjected to time–history analyses and the results are obtained in terms of MIDR. More than 14000 time–history analyses were conducted to express the statistics of structural response. Hence at each of the PGV values corresponding to a record, 20 MIDR values of structural simulations are obtained using IDARC–2D. Scatter plot of time–history analysis results in terms of MIDR for different PGV values are given in Appendix B. MIDR values given as vertical scattered data for each PGV value reflect the material and response variability of structures. It is obvious that, the increase in ground motion intensity results in an increase of structural response in terms of MIDR values. To separate the performances of structures that are designed for different design spectrum levels, three vertical separation lines are included in the charts.

Schematic representation of calculating the probability of exceedance and methodology used in the derivation of fragility curves is given in Figure 5.9. Accordingly, the exceeding probability of a certain limit state is calculated as the area over the horizontal line of a limit state. Consequently, for every PGV value the exceeding probabilities are obtained and fragility curve is constructed by plotting this data against PGV (Figure 5.9). Finally, to visualize plotted data graphically a best line is fitted to these data points. In this study, lognormal cumulative distribution function is used to obtain fragility curves.

Fragility curves obtained for 12 building subclasses are given in Figures 5.10–5.21. As observed in fragility curves obtained for superior subclass, collapse prevention limit state does not exist. Since these structures are well designed and code requirements are fully satisfied, the probability of collapse damage state is found negligibly small within the PGV range considered. In most of the cases, seismic demand cannot exceed the ultimate limit state (capacity) even for high values of hazard intensity. Observation of poor subclass structures show that, as the number

of stories increase, first and second damage limits get closer because the tolerance of structural resistance between no damage state and severe damage state is low and the structure reaches the collapse state rapidly. This trend is consistent when compared to the observations by Booth et al. (2004) who stated that there is a little margin between low damage and high damage for Turkish RC frame structures with typical structural deficiencies.

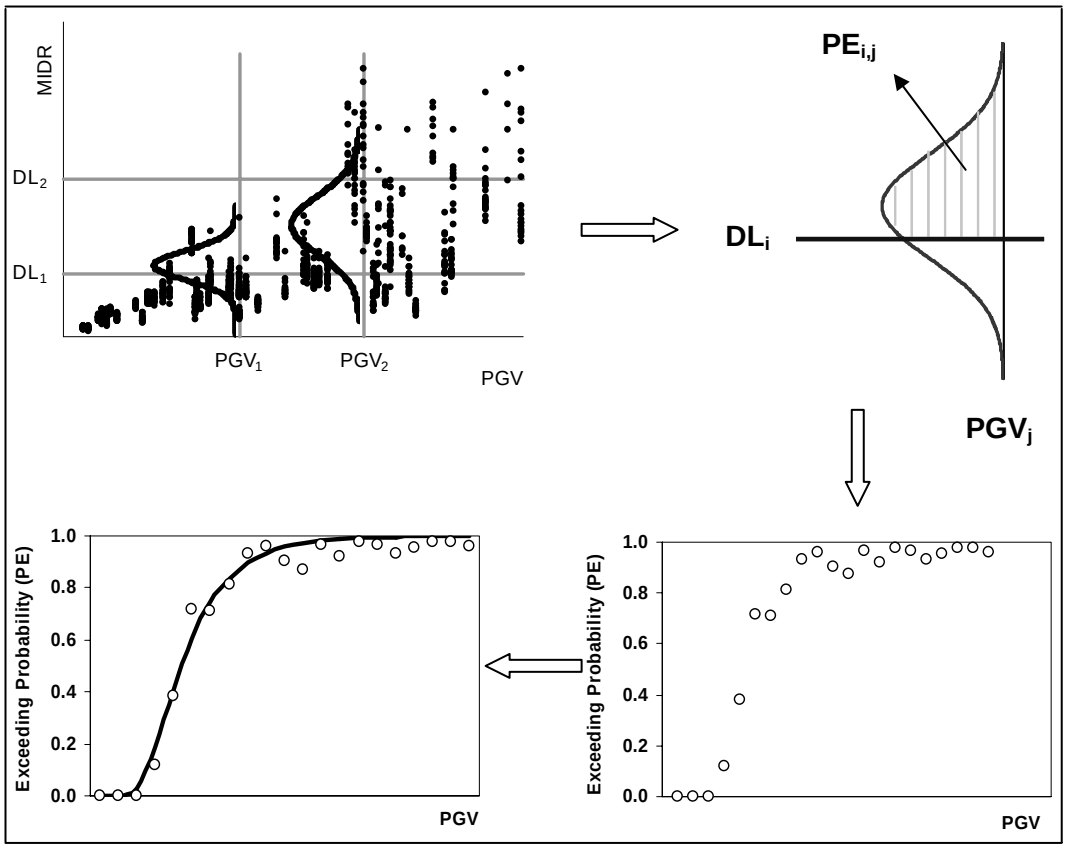

Figure 5.9 Schematic representation of obtaining fragility curve

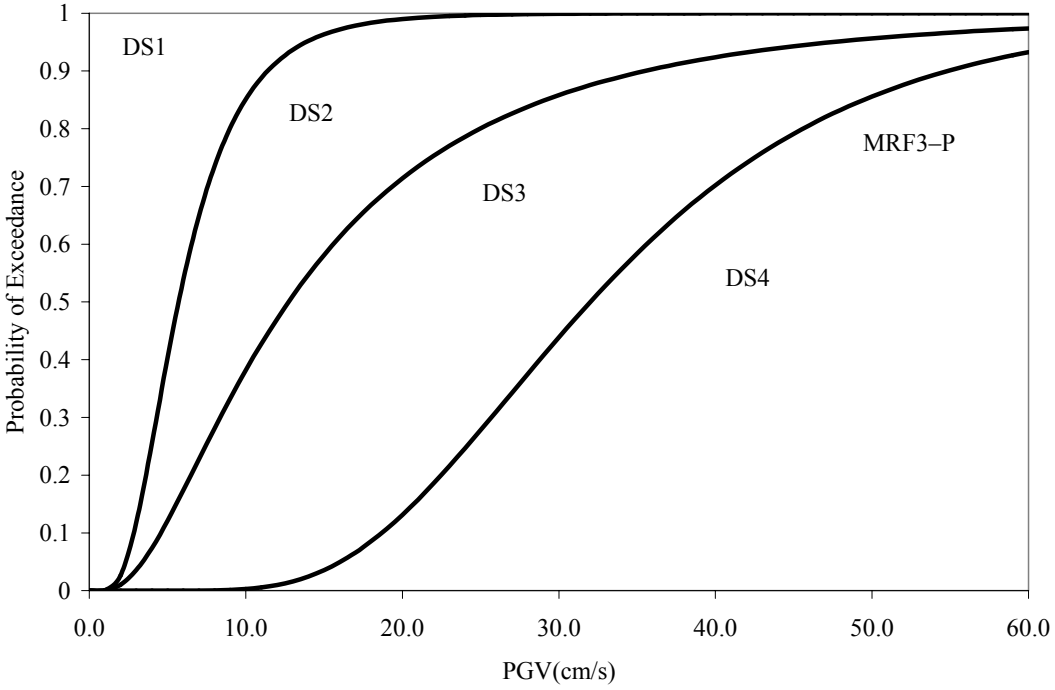

Figure 5.10 Fragility curves of building subclass MRF3–P

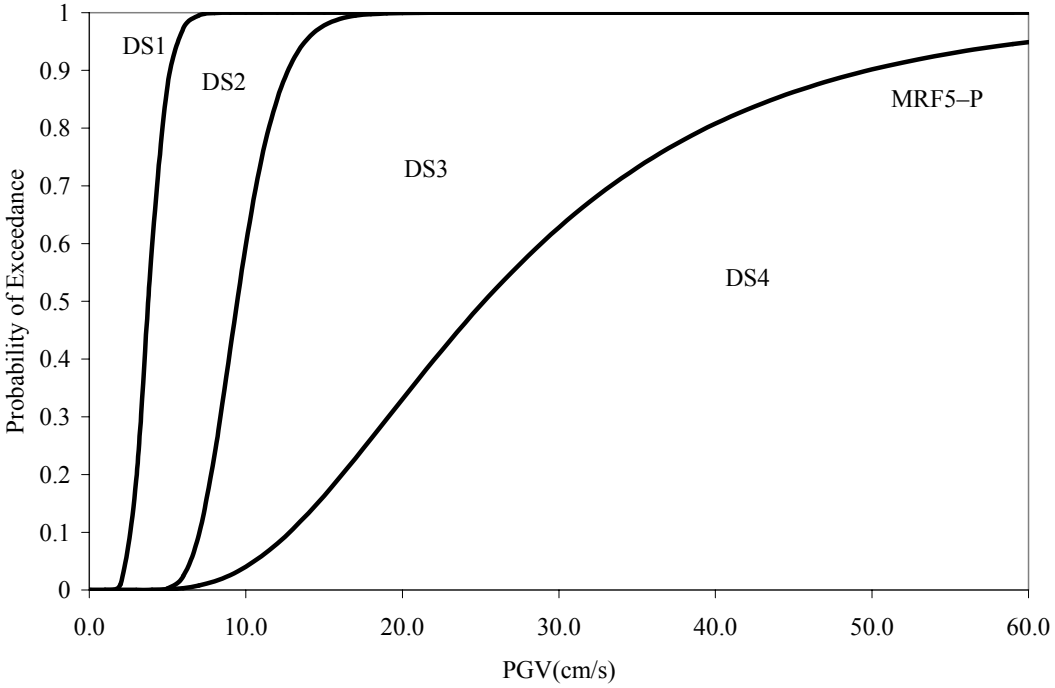

Figure 5.11 Fragility curves of building subclass MRF5–P

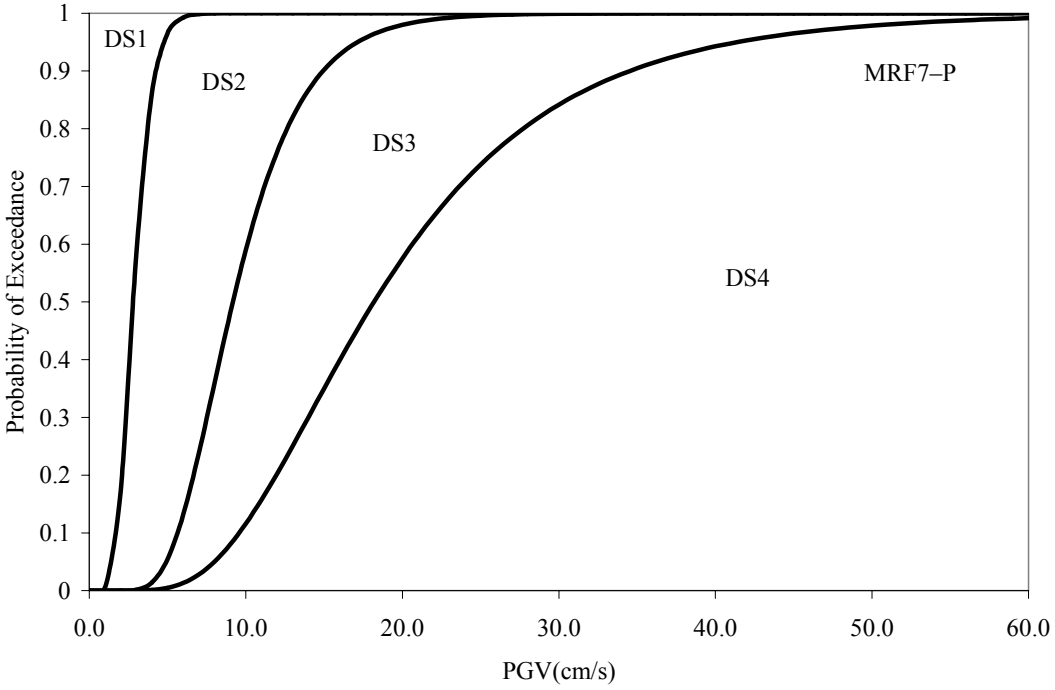

Figure 5.12 Fragility curves of building subclass MRF7–P

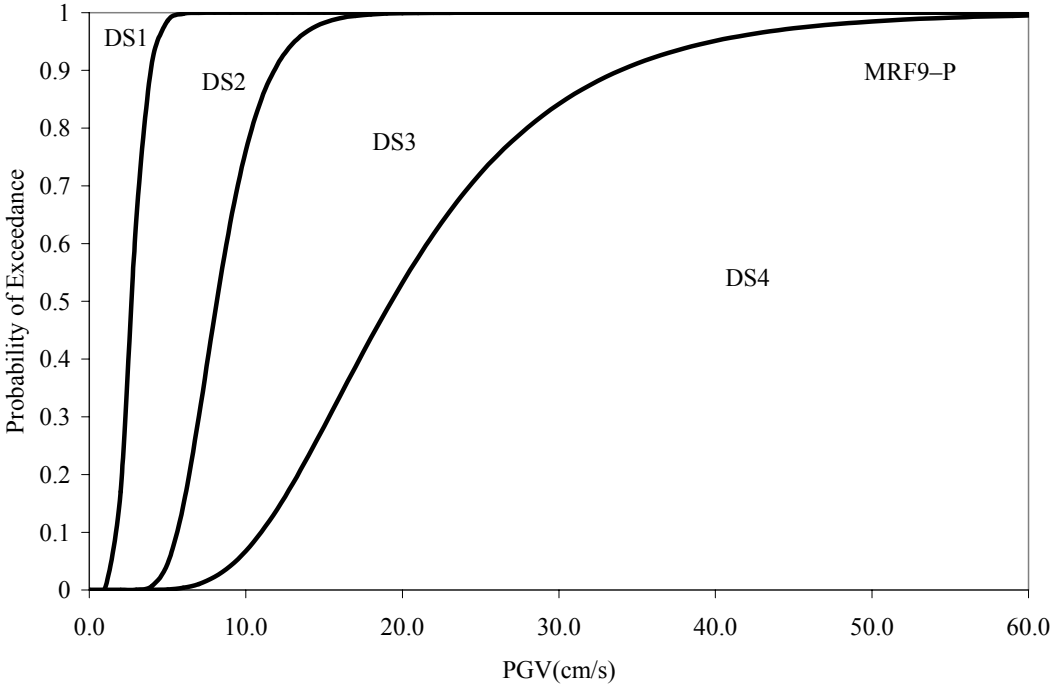

Figure 5.13 Fragility curves of building subclass MRF9–P

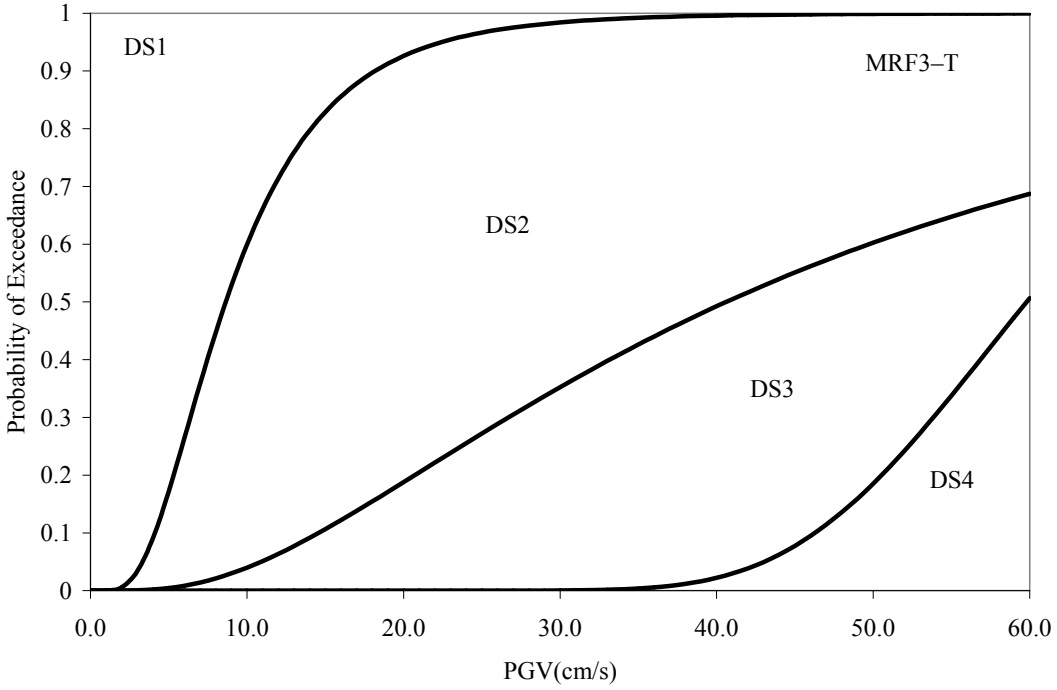

Figure 5.14 Fragility curves of building subclass MRF3–T

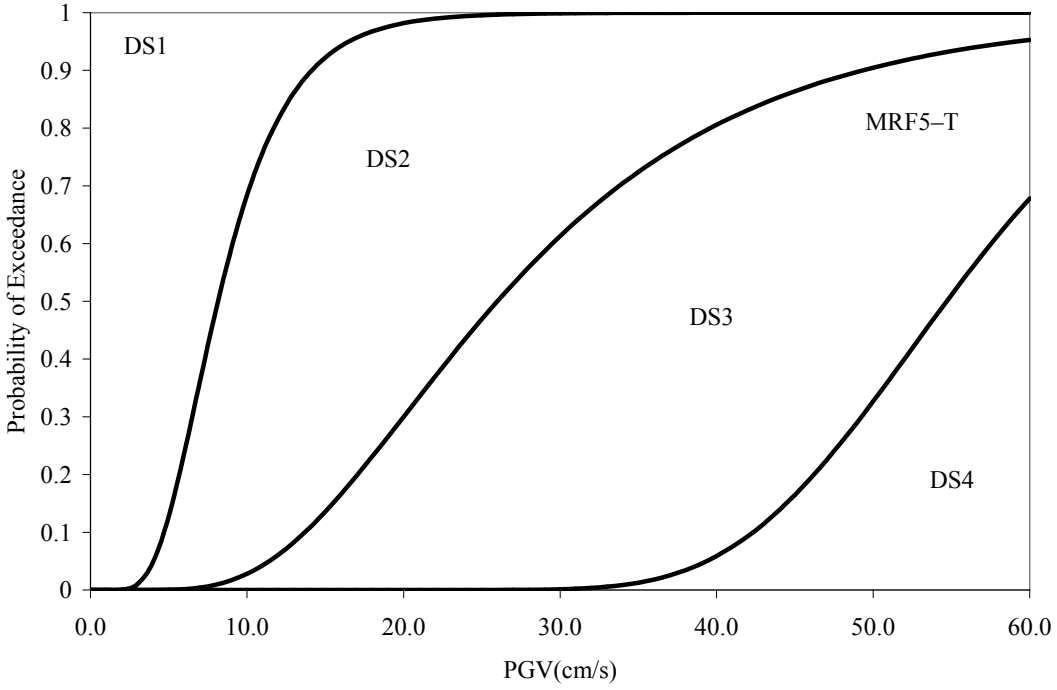

Figure 5.15 Fragility curves of building subclass MRF5–T

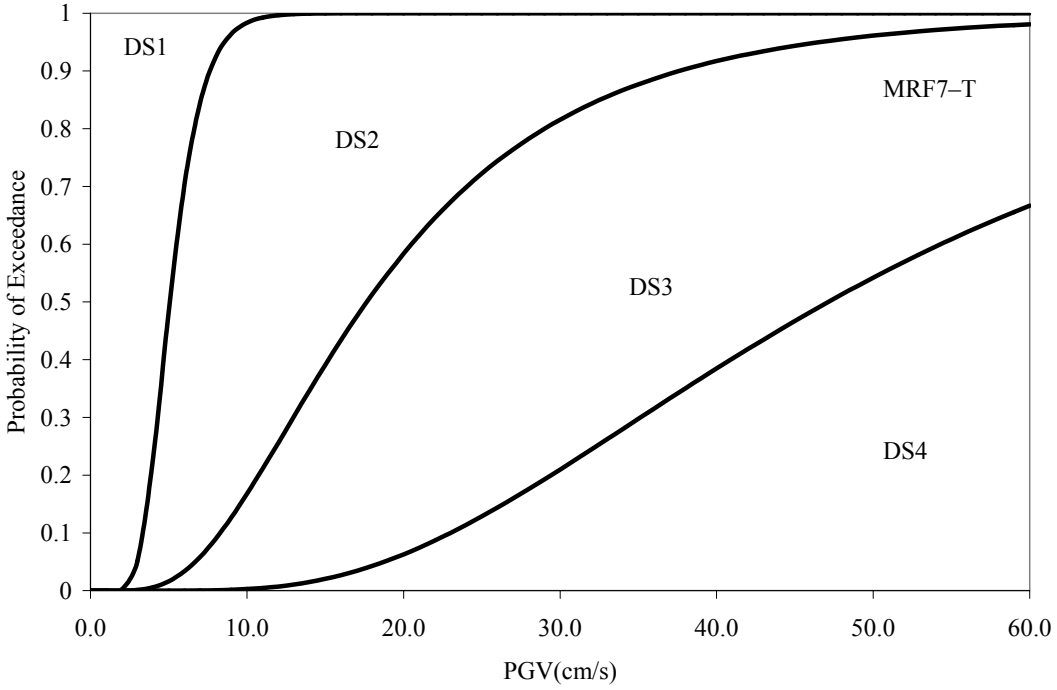

Figure 5.16 Fragility curves of building subclass MRF7–T

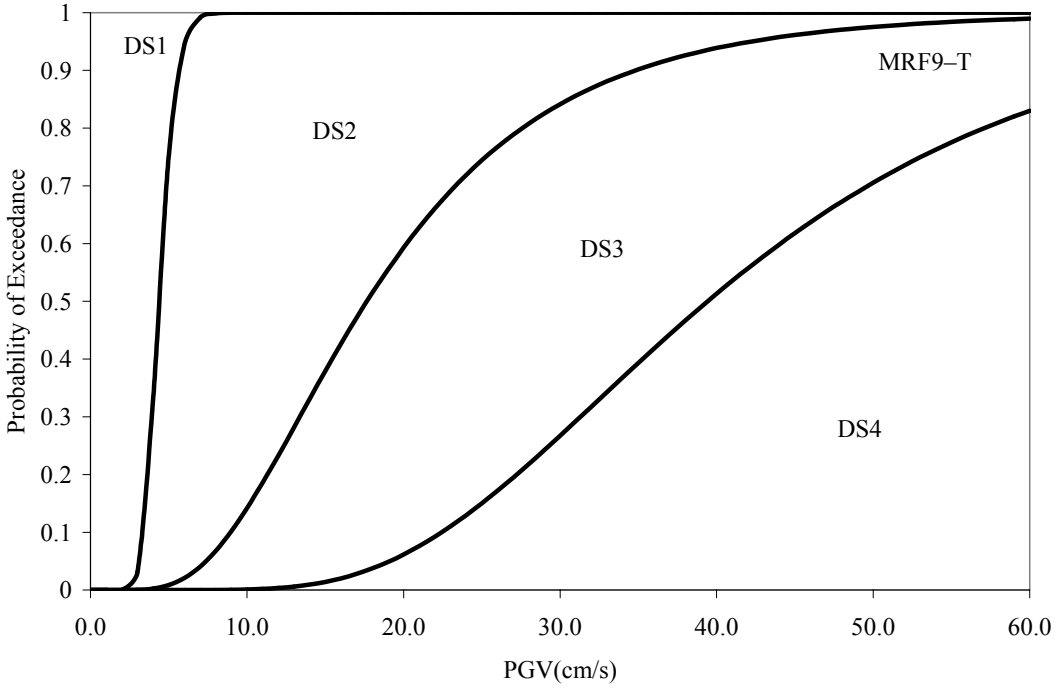

Figure 5.17 Fragility curves of building subclass MRF9–T

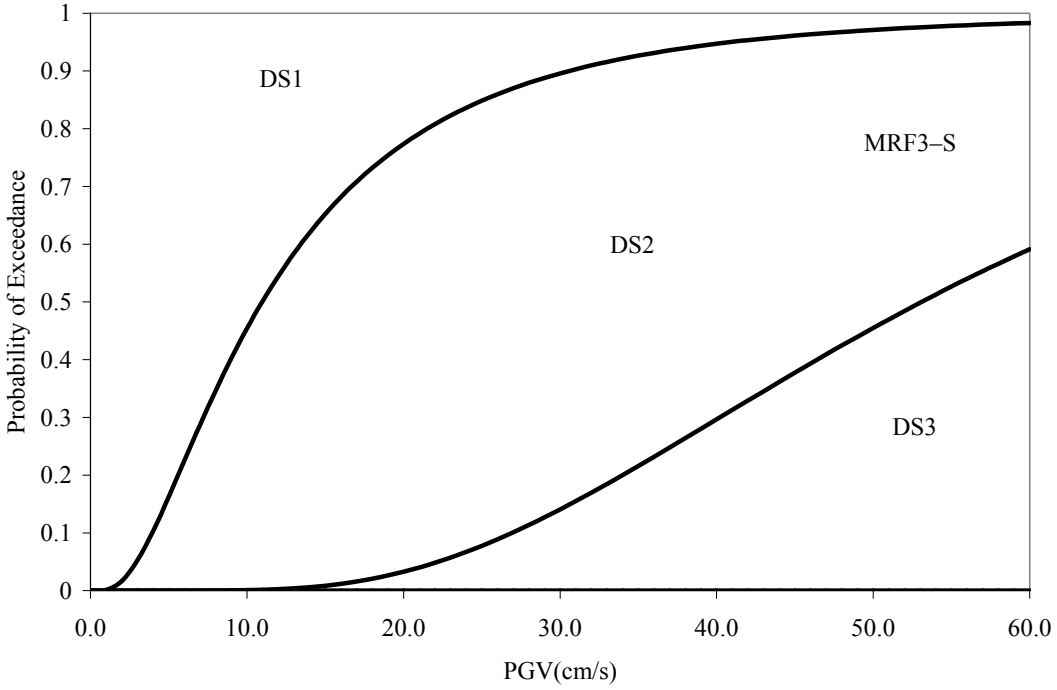

Figure 5.18 Fragility curves of building subclass MRF3–S

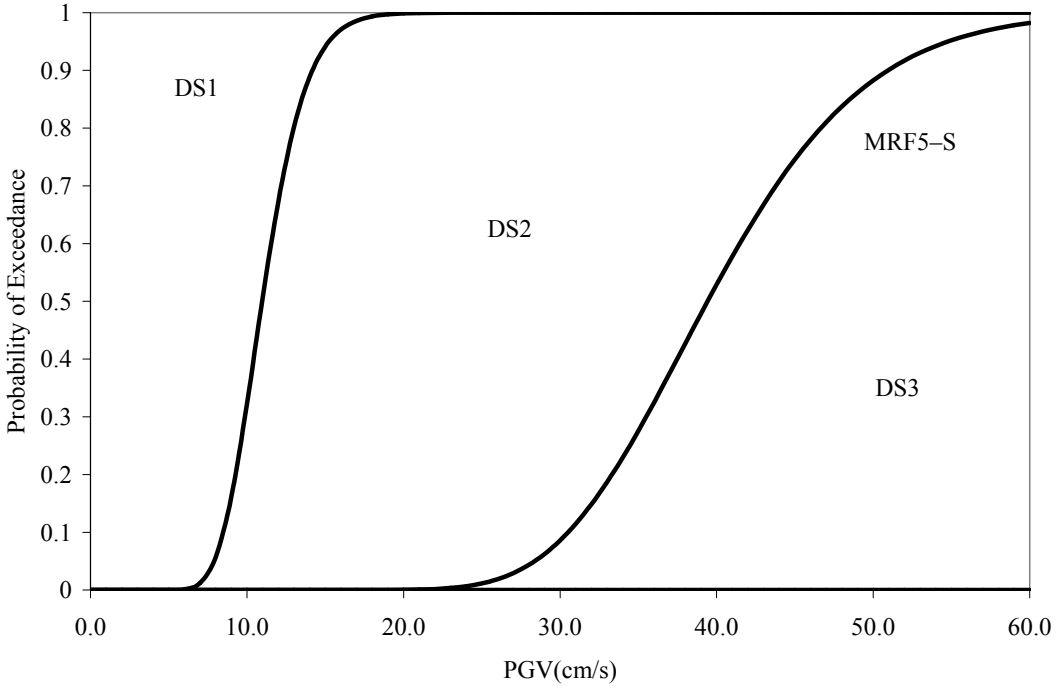

Figure 5.19 Fragility curves of building subclass MRF5–S

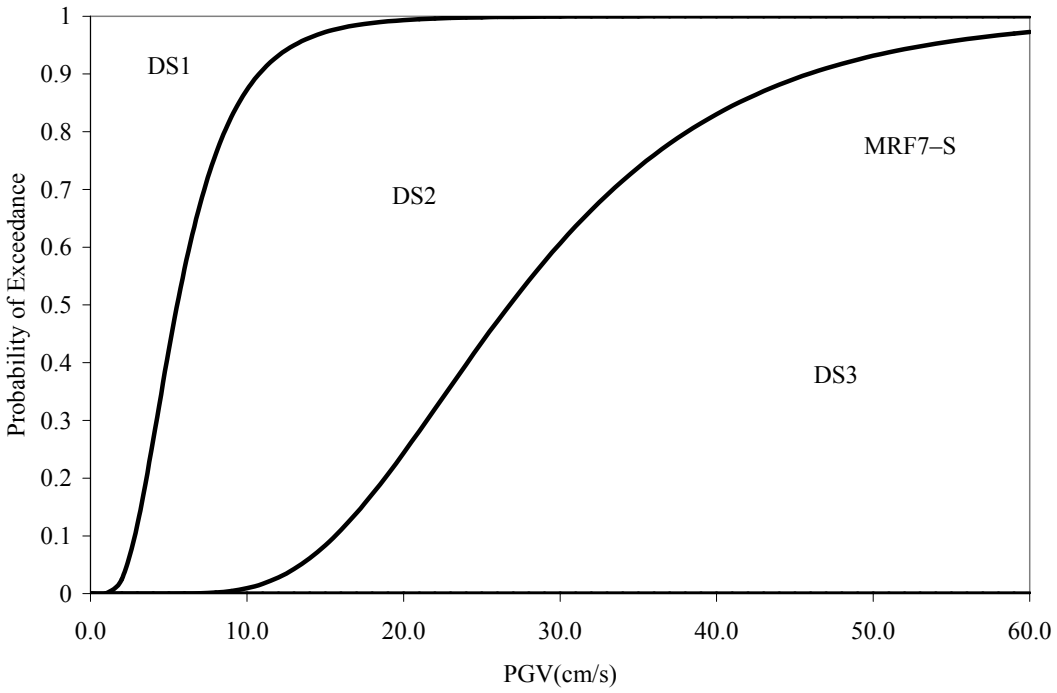

Figure 5.20 Fragility curves of building subclass MRF7–S

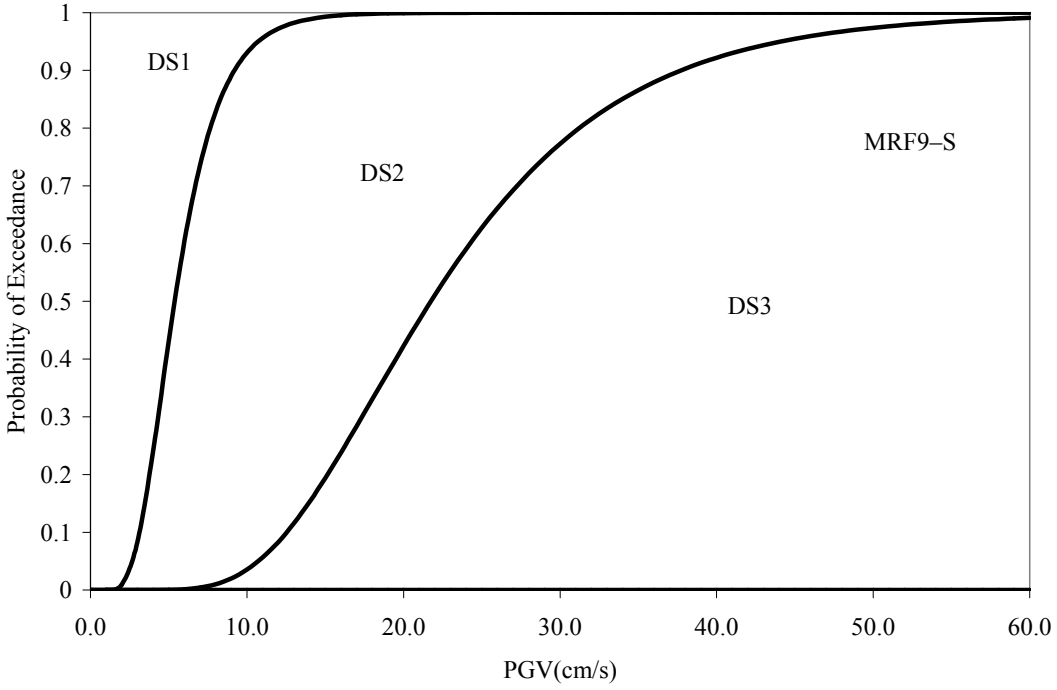

Figure 5.21 Fragility curves of building subclass MRF9–S

5.5 COMPARISON OF FRAGILITY CURVES

For the comparison of damage state probabilities of the RC frame structures for specific levels of hazard intensity, the fragility information obtained is used with an emphasis on the subclass definitions and number of stories. The PGV values that represent the hazard intensity are selected as 40 cm/s and 60 cm/s.

Figure 5.22 and 5.23 show the damage state probabilities of 3, 5, 7, and 9–story structures comparing superior, typical and poor subclasses for PGV values of 40 cm/s and 60 cm/s, respectively.

Figure 5.24 and 5.25 show the damage state probabilities of superior, typical and poor subclasses comparing 3, 5, 7, and 9–story structures for PGV values of 40 cm/s and 60 cm/s, respectively.

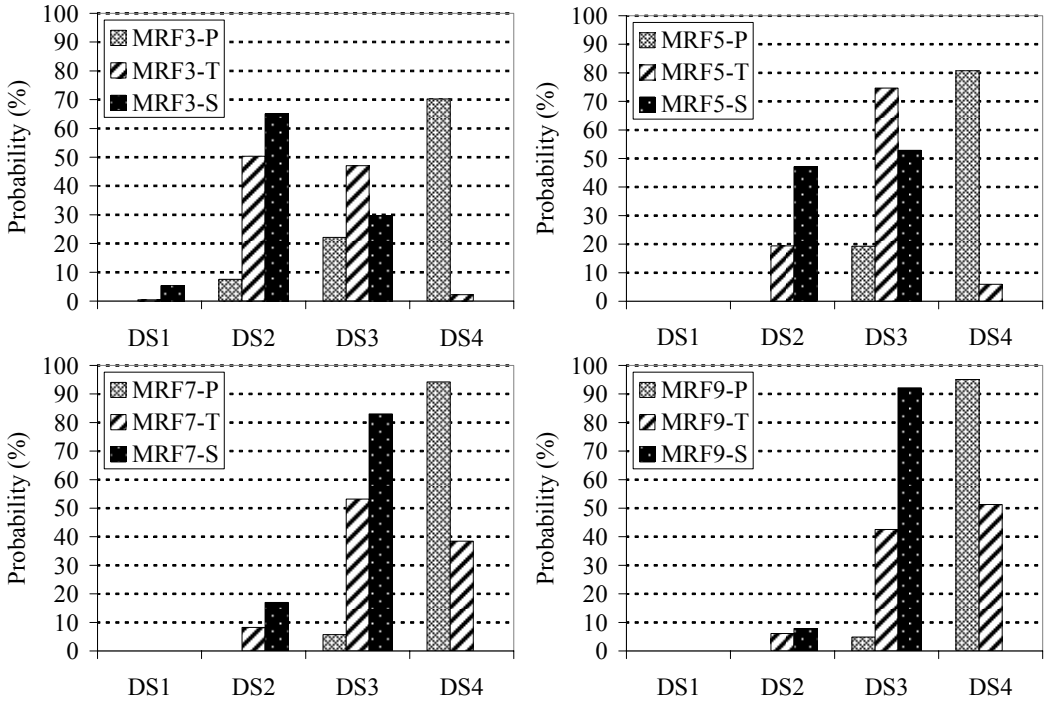

Figure 5.22 Damage state probability of building subclasses for PGV = 40 cm/s

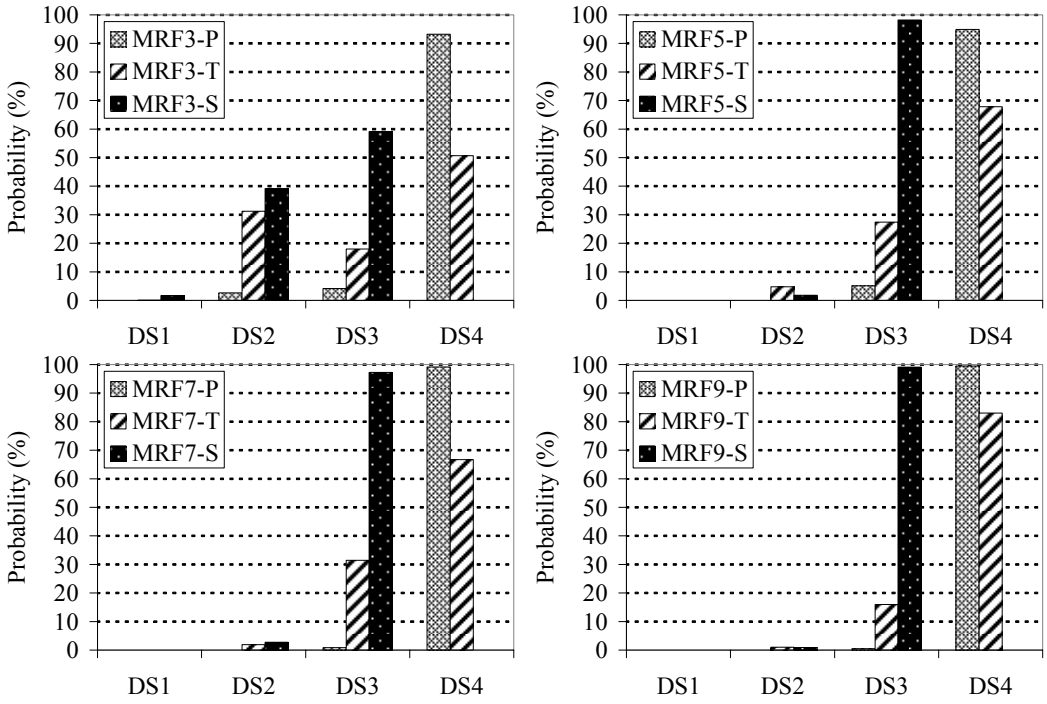

Figure 5.23 Damage state probability of building subclasses for PGV = 60 cm/s

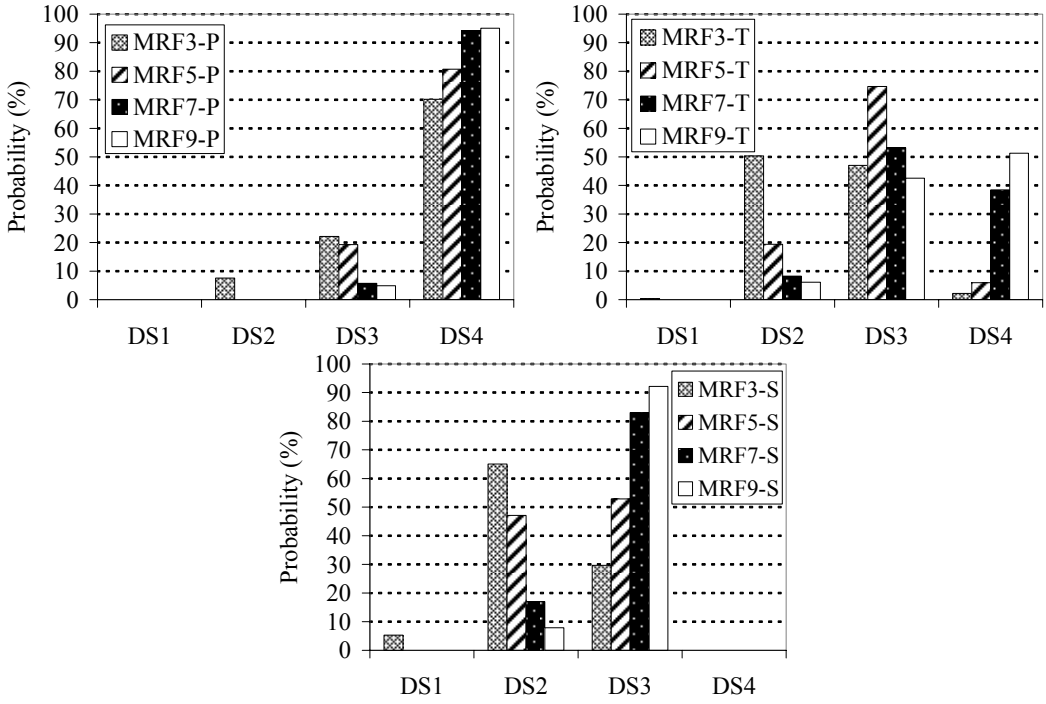

Figure 5.24 Story based damage state probability for PGV = 40 cm/s

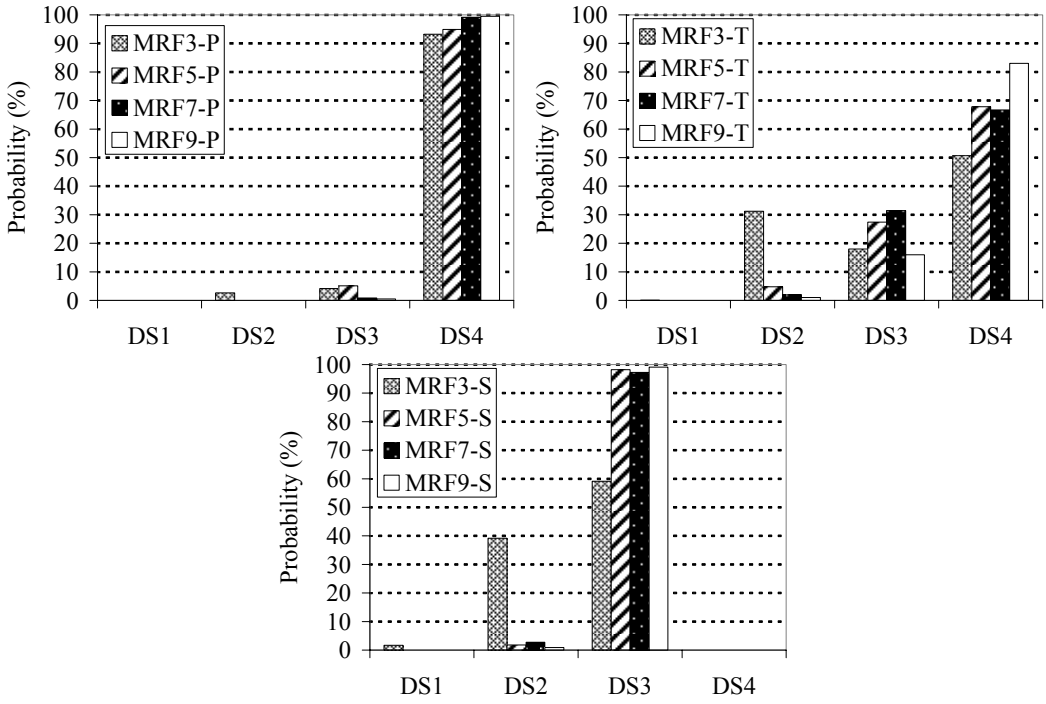

Figure 5.25 Story based damage state probability for PGV = 60 cm/s

As observed in the Figure 5.22–5.25, the damage state probabilities shift from low to high levels with decreasing structural subclass quality. Especially for high PGV values, this difference is much more pronounced. Overall, the inherent characteristics of RC considered structures that were reflected in fragility curves (degrading behavior, rapid evolution of damage after initiation, etc.) can also be observed through the damage state probabilities. Besides, the damage state probability increases with the story number especially for typical and poor structural subclasses. So, structures with more number of stories but of same subclass seem to be more vulnerable to seismic action. Such kind of a trend has also been observed before by other researchers (Aydoğan, 2003; Akkar et al., 2005).

CHAPTER 6

SEISMIC DAMAGE ESTIMATION OF LOW–RISE AND MID–RISE RC BUILDINGS IN TURKEY: A CASE STUDY

6.1 INTRODUCTION

In order to be successful in mitigation efforts and post–disaster decision making processes, the expected damage and the associated loss in urban areas caused by severe earthquakes should be properly estimated. It is appropriate to consider the expected damage as a measure of seismic vulnerability. The determination of such a vulnerability measure requires the assessment of seismic performances of different types of building structures typically constructed in an urban region when subjected to a potential scenario earthquake.

In this study, the seismic performance of low–rise and mid–rise RC residential buildings in Turkey is reflected in the form of fragility curves. Final phase of the study is devoted to efforts for the embedment of the generated fragility information into regional damage estimation studies. For this purpose, the study region is selected as Fatih, a highly populated earthquake–prone district in Istanbul.

The building database in Fatih district has been gathered for another project regarding the evaluation of seismic safety of existing building stock in Istanbul Metropolitan Area. In the project, a multi–level seismic evaluation method is employed for the existing buildings that have been developed within the scope of

NATO Science for Peace project SfP977231 (Özcebe et al., 2003; Yakut et al., 2003). Accordingly, there are three phases of evaluation:

1) Rapid screening based on simple tools (walkdown survey)
2) A more refined evaluation process (preliminary evaluation)
3) A very detailed evaluation process (final evaluation)

In the initial screening phase, the Walkdown Evaluation Procedure that was developed by Sucuoğlu and Yazgan (2003) has been used. For the RC buildings in Fatih, this stage of evaluation has been completed and the obtained results have been transferred to the second stage, preliminary evaluation stage.

The fragility information for low–rise and mid–rise RC buildings that has been generated in this study is proposed to be used as an alternative in the preliminary evaluation (second) stage of such a seismic safety evaluation process. This chapter is devoted to demonstrate the fragility–based evaluation procedure by employing the building stock in Fatih district.

6.2 BUILDING INVENTORY

The building inventory in Fatih provides information about 17108 RC frame structures. Since the generated set of fragility curves is limited to RC moment resisting frames with 3, 5, 7, and 9 stories, the corresponding building data is extracted from the inventory and used in damage estimation analysis. Therefore, there exist 8516 buildings in the scope of this case study, for which the distribution is presented in Figure 6.1. It is worth to mention that there is no 9–story building within the building inventory.

The building database contains information about geological position, site condition, seismic parameter value on site and other important structural

parameters of each building. Some of these parameters that are involved in Walkdown Evaluation Procedure are explained in the next section.

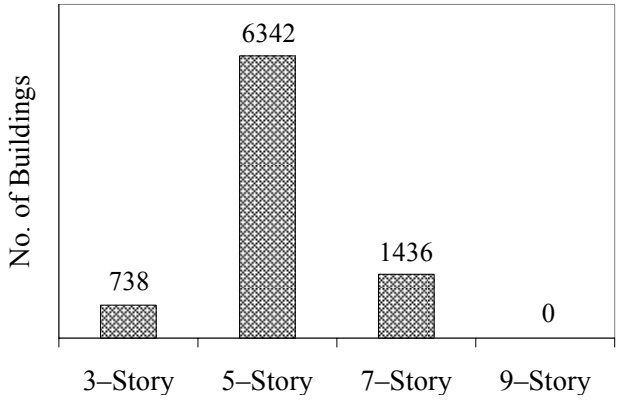

Figure 6.1 Number of RC buildings with 3, 5, 7, and 9 stories in Fatih district

6.3 WALKDOWN EVALUATION METHOD

Walkdown evaluation method is the first and the simplest level in seismic vulnerability analysis. The method does not require any analysis and its goal is to determine the priority levels of buildings that require immediate intervention (Sucuoğlu and Yazgan, 2003). The parameters in the walkdown survey can be listed as follows:

Number of stories: Previous studies on earthquake performance of buildings in Turkey revealed that the vulnerability increases with the increase in number of stories (Aydoğan, 2003; Akkar et al., 2005). Hence, number of stories above ground level is taken as a basic performance indicator.

Soft Story: The sudden changes in the stiffness and rigidity of consecutive stories result in soft story issue. In Turkish construction practice, especially ground floors with more story height and without infill wall may lead to soft–story behavior.

Such a deficiency is given as a score penalty in the walkdown survey method. In soft–story case, the vulnerability score multiplier is taken as one, otherwise zero.

Heavy Overhangs: One of the most frequent applications in Turkish building stock is heavy overhangs. Such an arrangement results in higher lateral loads affecting to the structure. In accordance with the previous observations after major earthquakes, the existence of heavy overhangs affects the building performance in a negative manner. In the case of heavy overhangs, the vulnerability score multiplier is taken as one, otherwise zero.

Estimated Construction Quality: The apparent quality of building is scored in terms of three levels. Assuming a good quality is required in case of adequate seismic performance, the vulnerability score multiplier for ordinary (moderate) construction quality is taken as one whereas for the poor quality is taken as two.

Short Column: Intermediate beams, continuous windows or semi infill walls result in accumulation of shear forces in columns. Such a condition decreases the performance score of the building. If short columns exist in a building, the vulnerability score multiplier is taken as one, otherwise zero.

Pounding: Insufficient distances between adjacent buildings with different story height and/or overall height result in pounding effect which requires a penalty in performance score. In this case, the vulnerability score multiplier is taken as one, otherwise zero.

Geographical Effects: The slope on which the building resides affects the seismic performance of structures especially if it is steeper than 30 degrees. Then the vulnerability score multiplier is taken as one, otherwise zero.

Site conditions and Earthquake Intensity: The intensity of ground motion mainly depends on the distance to the fault and site conditions. The microzonation maps

are evaluated in terms of earthquake hazard parameters considering these variables. In walkdown survey method, PGV is categorized in three intensity regions. The region with a PGV value lower than 40 cm/s is described as Zone I, the region with a PGV value between 40 cm/s and 60 cm/s is described as Zone II, whereas the region with a PGV value greater than 60 cm/s is described as Zone III.

According to the walkdown evaluation method, each structure is assigned with a score based on the corresponding intensity zone and then the penalty scores described above are subtracted from the base score. The base scores and the penalty scores are given in Table 6.1 and Table 6.2, respectively.

Table 6.1 Building base scores

Story	**Base Score**		
	ZONE I	ZONE II	ZONE III
3	90	120	140
5	65	85	100
7	60	80	90

Table 6.2 Vulnerability penalties

Story	**Penalties**					
	Soft Story	Heavy Overhangs	Construction Quality	Short Column	Pounding	Geographical Conditions
3	-15	-10	-10	-5	-2	0
5	-25	-15	-15	-5	-3	-2
7	-30	-15	-15	-5	-3	-2

The building scores are evaluated using Equation 6.1 where BS stands for building base score taken from Table 6.1, PP is penalty multiplication factor as given above,

PS for penalty scores taken from Table 6.2 and PAS is the performance assessment score found.

$$PAS = BS - \sum PS \times PP \tag{6.1}$$

The statistics regarding the performance assessment scores obtained by initial screening procedure are given in Table 6.3. These building scores are employed to assign a building subclass for each one of the existing buildings. This enables the characterization of each building by a set of fragility curves, which is required for the application of fragility–based preliminary evaluation procedure. Accordingly, the categorization of buildings in terms of performance assessment scores is carried out as follows:

Table 6.3 Number of buildings in terms of performance assessment scores

SCORE	**SUBCLASS**	**3–Story**	**5–Story**	**7–Story**
100≤PAS	SUPERIOR	353	56	0
90≤PAS<100	TYPICAL	156	67	7
80≤PAS<90		67	1454	15
70≤PAS<80		94	808	193
60≤PAS<70		17	1106	153
50<PAS<60		14	1120	189
40<PAS≤50	POOR	16	429	293
30<PAS≤40		3	996	154
20<PAS≤30		16	187	312
10<PAS≤20		2	77	77
0<PAS≤10		0	42	43

Buildings with PAS≥100 are assumed to be superior, buildings with 50<PAS<100 are assumed to be typical, and buildings with PAS≤50 are assumed to be poor. This means there are 409 superior, 5460 typical and 2647 poor buildings under consideration. The intervals for subclasses are determined by matching the

structural deficiencies observed during walkdown survey with the qualitative subclass definitions given in Chapter 4. It is worth to mention that story number is the major parameter that influences the classification of buildings.

6.4 DAMAGE ESTIMATION ANALYSIS

There exist three ingredients in damage estimation analysis, which is used as an alternative preliminary evaluation method for RC frame structures in this study: seismic hazard identification, building inventory, and the associated fragility information. For seismic hazard identification, other studies regarding seismic risk evaluation in Istanbul Metropolitan Area (Japan International Co–operation Agency and Istanbul Metropolitan Municipality, 2002) are referred. PGV is employed as the hazard parameter and a scenario earthquake with a return period of 72 years (50% probability of exceedance in 50 years) is selected. The characteristics of building inventory and the employment of the fragility have already been discussed in the previous part of the thesis. The method is simple and the steps are introduced as follows:

1) Obtain the performance assessment scores (PAS) of building with 3, 5, 7, and 9 stories from walkdown evaluation method.

2) Categorize the buildings in terms of performance scores as superior, typical and poor. The criteria are as follows:

Superior Subclass:	$PAS \geq 100$
Typical Subclass:	$50 < PAS < 100$
Poor Subclass:	$PAS \leq 50$

3) For each building, find the probability of being in damage states DS1, DS2, DS3, and DS4 using the on–site PGV value of an earthquake with a return period of 72 years. This is illustrated in Figure 6.2. For a 5–story building in typical building subclass that experiences an on–site PGV value of 40 cm/s,

the probability of being in DS1 is 0%, DS2 is 19%, DS3 is 75%, and DS4 is 6%. Hence the seismic damage of each building is obtained in a probabilistic manner.

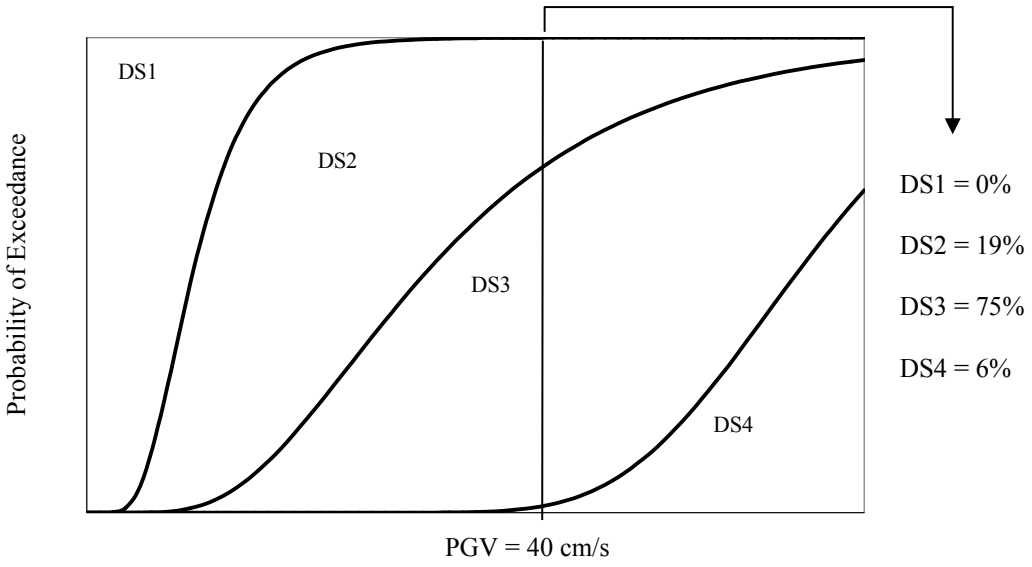

Figure 6.2 Damage states of MRF5–T on PGV value of 40 cm/s

6.5 EVALUATION OF RESULTS

The output of the fragility–based preliminary evaluation procedure is a set of damage state probabilities for each individual building. This valuable information can be examined in different ways:

1) Probability–based criteria can be introduced in order to interpret the estimated damage statistics obtained and to distinguish the buildings according to their relative seismic performance. For instance, if the buildings for which the probability of experiencing collapse damage state with a certain value is searched, the statistics in Table 6.4 and 6.5 can be obtained.

Table 6.4 Collapse prevention limit state statistics in terms of building subclass

	POOR	TYPICAL	SUPERIOR
P (CP≥0.5)	2627	25	0
P (CP≥0.6)	2567	7	0
P (CP≥0.7)	2464	0	0
P (CP≥0.8)	1577	0	0
P (CP≥0.9)	913	0	0

Table 6.5 Collapse prevention limit state statistics in terms of story number

	3–Story	5–Story	7–Story
P (CP≥0.5)	45	1726	881
P (CP≥0.6)	37	1656	881
P (CP≥0.7)	37	1548	879
P (CP≥0.8)	37	661	879
P (CP≥0.9)	37	73	803

As observed in Table 6.4, the number of buildings for which the probability of experiencing collapse damage state more than fifty percent increases drastically with the decreasing building subclass quality. Most of the buildings in poor subclass seem to have high probability of collapse whereas collapse is even not an issue for buildings in superior subclass. Besides as observed in Table 6.5, structures with more number of stories are more vulnerable at high levels of seismic intensity. Such kind of a trend has been stated previously within this study. Then these refined statistics can be used to eliminate some of the buildings in the database and transfer the rest of them to the third (final) stage of evaluation.

2) Also a single–valued vulnerability score can be obtained by multiplying the damage state probabilities by the corresponding damage state multipliers for a specific hazard intensity level. For the sake of demonstration the fragility curve that is given in Figure 6.2 is used and the multipliers are assumed as listed in Table 6.6.

Table 6.6 Damage state multipliers

Damage State	Multiplier
DS1	0
DS2	0.33
DS3	0.67
DS4	1.0

The vulnerability score can take values between the limits 0 and 1. Accordingly, higher vulnerability score means the building is more vulnerable to seismic action under the given intensity of shaking. The vulnerability score of the building whose fragility curve set is given in Figure 6.2 and which is subjected to a PGV level of 40 cm/s can be calculated as:

$$VS = 0 \times 0 + 0.33 \times 0.19 + 0.67 \times 0.75 + 1.0 \times 0.06 = 0.63 \qquad (6.2)$$

Hence the vulnerability scores of all the buildings in the Fatih inventory are calculated and the statistics are given in Table 6.7.

Table 6.7 Number of buildings based on vulnerability scores

VS	**3P**	**3T**	**3S**	**5P**	**5T**	**5S**	**7P**	**7T**	**7S**
0.9<VS≤1.0	37	0	0	1548	0	0	879	0	0
0.8<VS≤0.9	0	0	0	163	15	0	0	2	0
0.7<VS≤0.8	0	31	0	20	0	0	0	484	0
0.6<VS≤0.7	0	11	0	0	2611	0	0	69	0
0.5<VS≤0.6	0	85	7	0	1816	10	0	2	0
0.4<VS≤0.5	0	215	109	0	0	30	0	0	0
0.3<VS≤0.4	0	6	197	0	113	16	0	0	0
0.2<VS≤0.3	0	0	40	0	0	0	0	0	0
0.1<VS≤0.2	0	0	0	0	0	0	0	0	0
0<VS≤0.1	0	0	0	0	0	0	0	0	0

Then it becomes possible to draw a line as seen in Table 6.7 to decide about the relative seismic safety of buildings such that the ones below the line are assumed as safe whereas the ones above the line are assumed as unsafe and transferred to final stage of evaluation for a more detailed analysis.

Although out of the scope of this study, the obtained damage state probabilities can also be used as inputs to the calculation of various types of building related loss like direct social losses (casualties), direct economic losses (building repair and replacement cost, building contents loss, business inventory loss, building repair time/ loss of function, relocation expenses, loss of income, rental income loss, etc.) and even indirect economic losses. More detailed information about earthquake loss estimation analysis can be obtained from HAZUS Technical Manual (National Institute of Building Sciences, 1999).

CHAPTER 7

SUMMARY AND CONCLUSIONS

7.1 SUMMARY

This study has been conducted to provide fragility information of low–rise and mid–rise RC frame structures in Turkey. Consequently, structural vulnerability considering Turkish construction practice state and building inventory is examined in this study.

Different levels of seismic hazard intensity are involved by employing three ground motion sets. PGV is selected as earthquake hazard intensity parameter and 60 ground motion records are grouped into three ground motion sets based on PGV values which range between 0–20 cm/s, 20–40 cm/s, and 40–60 cm/s.

The seismic design of 3, 5, 7, and 9–story analytical models are carried out according to the current codes and design spectrum obtained from three ground motion sets. Finally, the analytical models are formed according to the specific characteristics of construction practice and the observed seismic performance after major earthquakes in Turkey. Hence, three building subclasses are introduced as poor, typical, and superior reflected by analytical models with different material properties, construction qualities, and hysteretic model parameters. In order to consider uncertainty in structural input parameters, Latin Hypercube Sampling Method is used.

Structural capacity is determined in terms of limit states in this study. Since realistic limit state determination is an issue of fragility curve determination, a comprehensive study is conducted in terms of stiffness index, ductility and damage on structural members to obtain probabilistic limits states.

The demand statistics in terms of MIDR are obtained by nonlinear time–history analysis of analytical models that simulate poor, typical and superior structural subclasses with 3, 5, 7, 9–story.

PGV values and corresponding MIDR values are used to get the hazard vs. demand relationship and the probability of exceeding each limit state is found. Lognormal fit is assumed to obtain fragility curves that visualize fragility functions.

Final part of the study is devoted to the application of the generated fragility information for the RC frame structures considered. A fragility–based evaluation procedure is proposed as an alternative to the procedures used for the seismic vulnerability assessment of actual RC frame buildings in Turkey. It is also discussed how to interpret the output of this simple procedure and use as an input for other studies. For this purpose, Fatih district in Istanbul is selected as the study region with a large building stock consisting of low–rise and mid–rise RC frame buildings.

7.2 CONCLUSIONS

Based on the discussions of this study and the fragility curves obtained, following conclusions and results can be drawn:

- There are different methodologies to develop fragility curves. The resulting curves are strongly dependent on the choices made for the analysis method, structural idealization, seismic hazard identification and the damage models used. These choices can cause significant discrepancies in the vulnerability

predictions by different researchers, even in the cases where similar structural types and the same seismicity information are employed.

- The variability in the material characteristics in terms of concrete strength, steel yield strength, concrete modulus of elasticity and steel modulus of elasticity affect the structural variability. Besides, hysteretic behavior is a significant parameter. In this study, mass and damping are also considered as random variables.
- In this study, the main parameters affecting structural fragility are considered as number of stories, structural deficiencies; which are quantified as superior, typical, or poor subclass, and ground motion intensity level.
- Among all the uncertainties that affect the fragility curves record–to–record variability is the most dominant. Structural variability is generally small when compared to record–to–record variability.
- Probabilistic limit states are essential in fragility studies, in which the single–valued (deterministic) limit states can not be obtained with much confidence and the quantification of limit states directly affect the resulting fragility.
- The generated fragility curves are novel in the sense that such curves have not been developed yet for Turkish RC building inventory with detailed analysis and tools (nonlinear time–history analysis, MDOF models, material variability and probabilistic limit states).
- Structural damage shifts from low to high levels with decreasing structural subclass quality. Especially for high PGV values, this distinction is much more pronounced. Overall, the inherent characteristics of considered RC buildings (degrading behavior, rapid evolution of damage after initiation, etc.) are reflected in fragility curves, and in turn damage state probabilities.
- Structural damage seems to increase with the number of stories for superior, typical, and poor building subclasses. Hence, structures with more number of stories but of same subclass seem to be more vulnerable to seismic action as also stated by some other researchers.

- The generated fragility information can be employed for the vulnerability or seismic safety evaluation analyses of actual RC frame structures and also in loss estimation studies that is going to be conducted in Turkey in near future.

7.3 RECOMMENDATIONS FOR FUTURE STUDIES

The typical characteristics of Turkish low–rise and mid–rise RC frame buildings are reflected by the generated fragility curves in this study. Therefore, the curves can be employed for estimation of damage and losses in risk scenarios involving earthquake prone regions in Turkey. Nevertheless, some further investigations could be conducted. Since this study is limited to 3, 5, 7, and 9–story RC in–situ cast moment resisting frame buildings, future fragility studies can be conducted for masonry buildings, shear wall buildings, pre–cast RC buildings and structures with different number of stories. Besides, some irregularities in plan and elevation can be considered. Infill walls can be also included into the analytical models. Ground motion records can be selected not only using PGV but also other ground motion parameters like PGA, S_a, and S_d.

REFERENCES

- ACI Committee 318. (2002). ACI 318–02, Building Code Requirements for Structural Concrete. American Concrete Institute, Detroit.
- Akkar, S. and Özen, Ö. (2005). Effect of peak ground velocity on deformation demands for SDOF systems. *Earthquake Engineering and Structural Dynamics*, 34, 1551–1571.
- Akkar, S., Sucuoğlu, H., and Yakut, A. (2005). Displacement–based fragility functions for low and mid–rise ordinary concrete buildings, *Earthquake Spectra*, 21(4), 901–927.
- Ang, A.H.–S. and Cornell, C.A. (1974). Reliability Bases of Structure Safety and Design, *Journal of Structural Engineering*, ASCE, Vol.100, No.9, pp.1755–1769.
- Applied Technology Council. (1985). Earthquake Damage Evaluation Data for California. ATC–13, Redwood City, California
- ASCE (American Society of Civil Engineers). (2000). NEHRP Guidelines for the Seismic Rehabilitation of Buildings, FEMA 273, Washington D.C.
- ASCE (American Society of Civil Engineers). (2000). Prestandard and Commentary for the Seismic Rehabilitation of Buildings, FEMA 356, Washington, DC.
- Atalay, M.B. and Penzien, J. (1975). The seismic behavior of critical regions of reinforced concrete components as influenced by moment, shear and axial force, *Technical Report EERC–UCB 75–19*, University of California, Berkeley, California.
- Aydoğan V. (2003). Seismic vulnerability assessment of existing reinforced concrete buildings in Turkey, *M.S. Thesis*, Middle East Technical University, Ankara.

- Ayyub, B.M., and Lai, K–L. (1989). Structural reliability assessment using Latin hypercube sampling, *Proc., 5th Int. Conf. on Struct. Safety and Reliability, ICOSSAR'89*, Vol. 2, ASCE, New York, 1177–1184.
- Barron–Corvera, R. (2000). Spectral Evaluation of Seismic Fragility of Structures, *PhD Thesis*, Development of Civil, Structural and Environmental Engineering, State University of New York at Buffalo, N.Y.
- Baykal, H. and Kırçıl, M.S. (2006). Fragility Analysis of R/C Frame Buildings on Firm Sites*, Paper No. 8NCEE–000688, 100th Anniversary Earthquake Conference*, San Francisco, California.
- Booth, E., Spence, R. and Bird, J. (2004). Building Vulnerability Assessment using Pushover Methods – A Turkish Case Study. *Proceedings of an International Workshop on Performance–Based Seismic Design Concepts and Implementation*, Bled Slovenia, pp. 397–408.
- Building Seismic Safety Council. (2000). NEHRP Recommended Provisions for Seismic Regulations for New Buildings& Other Structures, FEMA 368, Washington, DC.
- Calvi, G.M. (1999). A displacement–based approach for vulnerability evaluation of classes of buildings. *Journal of Earthquake Engineering*, 3 (3), 411–438.
- Camelo, V.S., Beck, J.L. and Hall, J.F. (2001). "Dynamic Characteristics of Woodframe Structures", Consortium of Universities for Research in Earthquake Engineering, Richmond, CA.
- Cardona, O.D. and Yamin, L.E. (1997). Seismic Microzonation and Estimation of Earthquake Loss Scenarios: Integrated Risk Mitigation Project of Bogota, Colombia, *Earthquake Spectra* Vol.13 (4), 795–815.
- Chong, W.H. and Soong, T.T. (2000). Sliding Fragility of Unrestrained Equipment in Critical Facilities, *Technical Report MCEER 00–0005*, Buffalo, New York.

- Collins, K.R., Wen, Y.K., and Foutch, D.A. (1996). Dual–level design: a reliability–based methodology, *Earthquake Engineering and Structural Dynamics*, Vol.25, 1433–1467.
- Computers and Structures Inc. (2002). SAP 2000, Nonlinear, Version 8.08, Structural Analysis Program, Computers and Structures, Inc., Berkeley, CA.
- Constantinou, M.C., Tsopelas, P., Hammel, W., and Sigaher, A.N. (2000). New Configurations of Fluid Viscous Dampers for Improved Performance, *Passive Structural Control Symposium*, Tokyo Institute of Technology, Yokohama, Japan.
- Corvera, R.B. (2000). Spectral Evaluation of Seismic Fragility of Structures, *Ph.D. Dissertation*, State University of New York at Buffalo.
- DiPasquale, E. and Çakmak, A.S. (1987). Detection and assessment of seismic structural damage. *Technical Report NCEER–87–0015*, State University of New York, Buffalo, NY.
- Dymiotis, C., Kappos, A.J. and Chryssanthopoulos, M.K. (1999). Seismic Reliability of RC Frames with Uncertain Drift and Member Capacity, *Journal of Structural Engineering*, ASCE, Vol.125, No.9, pp. 1038–1047.
- Ellingwood, B. (1977). Statistical Analysis of RC Beam Column Interaction, *Journal of Structural Engineering ASCE*, Vol.103, pp.1377–1388.
- Ellingwood, B., Galambos, T.V., MacGregor, J.G., and Cornell, C.A. (1980). Development of a Probability–Based Load Criterion for American National Standard A58, *National Bureau of Standards*, Washington, DC.
- Elnashai, A.S. and Borzi, B. (2000). Deformation–based Analytical Vulnerability Functions for RC Bridges, *Engineering Seismology and Earthquake Engineering Report No. ESEE 00–6*, Imperial Collage, London, UK.

- Erberik, M.A. and Çullu, S. (2006). Assessment of Seismic Fragility Curves for Low– and Mid–Rise Reinforced Concrete Frame Buildings using Düzce Field Database. *NATO Science Series, Advances in Earthquake Engineering for Urban Risk Reduction*, pp.151–166.
- Erberik, M.A. and Elnashai, A.S. (2003). Seismic Vulnerability of Flat-Slab Structures. *Technical Report, Mid–America Earthquake Center DS–9 Project*, University of Illinois at Urbana–Champaign.
- Erberik, M.A. and Elnashai, A.S. (2004). Fragility Analysis of Flat–slab Structures, *Engineering Structures*, Vol.26, 937–948.
- Erberik, M.A. and Elnashai, A.S. (2006). Loss estimation analysis of flat–slab structures. *ASCE Natural Hazards Review 7*.
- Erberik, M.A. and Sucuoğlu, H. (2004). Seismic energy dissipation in deteriorating systems through low–cycle fatigue, *Earthquake Engineering and Structural Dynamics*, Vol.33, pp. 49–67.
- Erduran, E. (2005). Component based seismic vulnerability assessment procedure for RC buildings. *PhD Thesis*, Middle East Technical University, Ankara, Turkey.
- Ersoy, U. and Özcebe, G. (2001). Betonarme, *Evrim Yayınevi*, İstanbul.
- Ghobarah, A. (2004). On Drift Limits Associated with Different Damage Levels. *Proceedings of an International Workshop on Performance–Based Seismic Design Concepts and Implementation*, Bled Slovenia, pp. 321–332.
- Ghobarah, A., Aly, N.M., and El–Attar, M. (1997). Performance Level Criteria and Evaluation. *Proceedings of the International Workshop on Seismic Design Methodologies for the Next Generation of Codes*, Bled Slovenia, 207–215.
- Ghobarah, A., Aly, N.M., and El–Attar, M. (1998). Seismic Reliability Assessment of Existing Reinforced Concrete Buildings, *Journal of Earthquake Engineering*, Vol.2, No.4, pp.569–592.

- Goel, R.K. and Chopra, A.K. (1997), Period formulas for moment resisting frame buildings, *Journal of Structural Engineering* ASCE 123 (11), 1454–1461.
- Hueste, M.B. and Bai, J.W. (2004). Impact of Retrofit on the Seismic Fragility of a Reinforced Concrete Structure, Paper No.1163, *13th World Conference on Earthquake Engineering*, Vancouver.
- Hwang, H. and Huo, J.R. (1997). Chapter 7.b: Development of Fragility Curves for Concrete Frame and Shear Wall Buildings, Loss Assessment of Memphis Buildings, *Technical Report NCEER 97–0018*, 113–137.
- Ibarra, L. (2003). Global Collapse of Frame Structures under Seismic Excitations, *PhD Thesis*, Stanford University, CA.
- Iman, R.L. and Conover, W.J. (1982). Sensitivity Analysis Techniques: Self–teaching Curriculum, *Nuclear Regulatory Commission Report, NUREG/CR–2350, Technical Report SAND81–1978*, Sandia National Laboratories, Albuquerque, NM.
- Iman, R.L., Helton, J.C., and Campbell, J.E. (1981a). An Approach to Sensitivity Analysis of Computer Models, Part 1, *Journal of Quality Technology*, Vol.13, No.3, pp. 174–183.
- Iman, R.L., Helton, J.C., and Campbell, J.E. (1981b). An Approach to Sensitivity Analysis of Computer Models, Part 2, *Journal of Quality Technology*, Vol.13, No.4, pp. 232–240.
- Japan International Co–operation Agency and Istanbul Metropolitan Municipality. (2002). The Study on a Disaster Prevention / Mitigation Basic Plan in Istanbul including Seismic Microzonation in the Republic of Turkey*, Final Report,* Tokyo–Istanbul.
- Jeong, S.H. and Elnashai, A.S. (2004). Parametrized Vulnerability Functions for As–built and Retrofitted Structures. PEER Report 2004/05*, Proceedings of International Workshop on Performance–Based Seismic Design Concepts and Implementation*, Bled Slovenia, pp. 185–196.

- Julian, E.G. (1955). Discussion of Strength Variations in Ready–mixed Concrete, by A.E. Cummings, *ACI Structural Journal*, Vol.51, No.12, pp.772–778.
- Kalkan, E. and Gülkan, P. (2004). Site–Dependent Spectra Derived From Ground Motion Records in Turkey, *Earthquake Spectra*, Vol. 20 (4), 1111–1138. Earthquake Engineering Research Institute.
- Karaesmen, E. (2002). Öncesiyle Sonrasıyla Deprem, *Atılım Üniversitesi Yayınları*, Ankara.
- King, S.A., Kiremidjian, A.S., Basöz, N., Law, K., Vucetic, M., Doroudian, M., Oloson, R.A., Eidinger, J.M., Goettel, K.A., and Horner, G. (1997). Methodologies for Evaluating the Socio–Economic Consequences of Large Earthquakes, *Earthquake Spectra*, Vol.13 (4), 565–585.
- Kırçıl, M.S. and Polat, Z. (2006). Fragility analysis of mid–rise RC frame buildings, *Engineering Structures 28* (2006) 1335–1345.
- Kwon, O.S. and Elnashai, A.S. (2004) Sensitivity of Analytical Vulnerability Functions to Input and Response Parameter Randomness, *Proceedings of 13th World Conference on Earthquake Engineering*, Vancouver, Canada.
- Lee, T.H. and Mosalam, K.M. (2003). Sensitivity of seismic demand of a reinforced concrete shear–wall building, Applications of Statistics and Probability in Civil Engineering, *Der Kiureghian, Madanat & Pestana (eds)*, pp. 1511–1518.
- Lee, T.H. and Mosalam, K.M. (2004). Probabilistic Fiber Element Modeling of Reinforced Concrete Structures, *Computers and Structures*, 2004, Vol. 82, No. 27, pp. 2285–2299.
- Limniatis, A. (2001). Seismic Behavior of Flat–Slab RC Structures, *MSc. Dissertation*, Civil Engineering Department, Imperial College of Science, Technology and Medicine.
- McKay, M.D., Conover, W.J., and Beckman, R.J. (1979). A Comparison of Three Methods for Selecting Values of Input Variables in the Analysis of Output from a Computer Code, *Technometrics*, Vol.21, pp. 239–245.

- McVerry, G.H. (1979). Frequency Domain Identification of Structural Models for Earthquake Records, Report No EERL 79–02, California Institute of Technology, Pasadena, California.
- Ministry of Public Works and Settlement. (1998). Turkish Seismic Code, Specifications for Structures to Be Built in Disaster Areas, Ankara, Turkey.
- Mirza, S.A. and MacGregor, J.G., (1979). Variability of Mechanical Properties of Reinforcing Bars, *Journal of Structural Engineering* ASCE, Vol.105, No.ST5, pp.921–937.
- Mirza, S.A., Hatzinikolas, M., and MacGregor, J.G. (1979). Statistical Descriptions of Strength of Concrete*, Journal of Structural Engineering*, ASCE, Vol.105, No.ST6, pp.1021–1036.
- Mosalam, K., Ayala, G., and White, R. (1997). Chapter 7.c: Development of Fragility Curves for Masonry Infill – Concrete Frame Buildings, Loss Assessment of Memphis Buildings, *Technical Report NCEER 97–0018*, 139–158.
- Mostafa, E.M.S. (2003). Seismic fragility and cost–benefit analysis of structural and non–structural systems*. PhD Dissertation*, Cornell University.
- Naeim, F. (2001). The Seismic Design Handbook, Second Edition. Kluwer *Academic Publishers Group*, 825 pages.
- National Institute of Building Sciences. (1999) HAZUS Technical Manual (3 volumes), prepared for Federal Emergency Management Agency, Washington DC.
- Newmark, N.M. (1959). A method of computation for structural dynamics, *ASCE Journal of the Engineering Mechanics* Division 85 (EM 3), 67–94.
- Orhunbilge, N. (1997). Örnekleme Yöntemleri ve Hipotez Testleri, *İ.Ü. İşletme Fakültesi Yayınları*, İstanbul.

- Özcebe, G., Ersoy, U., Tankut, T., Akyüz, U., Erduran, E., Keskin, S., and Mertol, C. (2002). Mevcut Betonarme Binaların Deprem Güvenliklerinin Arttırılması, *ECAS 2002 Uluslararası Yapı ve Deprem Mühendisliği Sempozyumu*, Ankara.
- Özcebe, G., Yücemen, M.S., Aydoğan, V., and Yakut, A. (2003). Preliminary Seismic Vulnerability Assessment of Existing Reinforced Concrete Buildings in Turkey – Part I: Statistical Model Based on Structural Characteristics, *Seismic Assessment and Rehabilitation of Existing Buildings*, NATO Science Series IV/29, pp. 29–42.
- Özcebe, G., Yücemen, M.S., Yakut, A., and Aydoğan, V. (2003). Seismic Vulnerability Assessment Procedure for Low–to–Medium–Rise RC Buildings, *Middle East Technical University Civil Engineering Department Structural Engineering Research Unit* Technical Report No. 2003/2, Ankara.
- Park, Y.J. and Ang, A.H.S. (1985). Mechanistic seismic damage model for reinforced concrete, *Journal of Structural Engineering* ASCE, 111(4), pp. 722–739.
- Phan, L.T., Todd, D.R., and Lew, H.S. (1993). Strengthening Methodology for Lightly Reinforced Concrete Frames, *Technical Report* NISTIR 5128, Building and Fire Research Laboratory, Gaitersburg, Maryland.
- Porro, B. and Schraft, A. (1989). Investigation of Insured Earthquake Damage". Natural Hazard, Vol.2, 173–184.
- Porter, K.A. (2002), Chapter 21, Seismic Vulnerability, *Handbook of Earthquake Engineering*, W.F. Chen and C.R. Scawthorn, eds., CRC Press, Boca Raton, FL.
- Porter, K.A., Beck, J.L., and Shaikhutdinov, R.V. (2002). Sensitivity of Building Loss Estimates to Major Uncertain Variables. *Earthquake Spectra*, Volume 18, No. 4, pages 719–743.
- Rossetto, T. and Elnashai, A.S. (2003). Derivation of Vulnerability Functions for European Type RC Structures Based on Observational Data, *Engineering Structures* Vol.25 (10), 1241–1263.

- Rubinstein, R.Y. (1981). Simulation and the Monte Carlo Method, *Wiley*, 278 pages.
- Saatçioğlu, M. and Özcebe, G. (1989). Response of reinforced concrete columns to simulated seismic loading. *ACI Structural Journal* 86 (1), pp. 3–12.
- SEAOC. (1995). Performance Based Seismic Engineering of Buildings, *Vision 2000 Committee*, Structural Engineers Association of California, Sacramento, California.
- Singhal, A. and Kiremidjian, A.S. (1996). Method for Probabilistic Evaluation of Seismic Structural Damage. *Journal of Structural Engineering* ASCE, 122(12), pp. 1459–1467.
- Singhal, A. and Kiremidjian, A.S. (1997). A Method for Earthquake Motion–Damage Relationships with Application to Reinforced Concrete Frames, *Technical Report* NCEER 97–0008, Buffalo, NY.
- Sinozuka, M., Feng, M.Q., Kim, H.K., and Kim, S.H. (2000). Nonlinear Static Procedure for Fragility Curve Development, *Journal of Engineering Mechanics*, Vol. 126 (12), 1287–1295.
- Sözen, M.A. (1981). Review of Earthquake Response of RC Buildings with a View to Drift Control, *State–of–the–Art in Earthquake Engineering*, Kelaynak Press, Ankara, Turkey.
- SPD. (2003). PEER Structural Performance Database, *http://nisee.berkeley.edu/spd/*
- Sucuoğlu, H. and Nurtuğ, A. (1995). Earthquake ground motion characteristics and seismic energy dissipation. *Earthquake Engineering and Structural Dynamics* 24, 1195–1213.
- Sucuoğlu, H. and Erberik, M.A. (1998). Influence of ground motion intensity parameters on elastic response spectra. *11th European Conference on Earthquake Engineering*, Paris.

- Sucuoğlu, H. and Yazgan, U. (2003). Simple Survey Procedures for Seismic Risk Assessment in: Urban Building Stocks, *Seismic Assessment and Rehabilitation of Existing Buildings*, NATO Science Series IV/29, pp. 97–118.
- Sucuoğlu, H., Gülkan, P., Erberik, A., and Akkar, S., (1999). Measures of Ground Motion Intensity in Seismic Design, *Proceedings of the Uğur Ersoy Symposium on Structural Engineering*, 1999. Ankara.
- Tankut, T. (1999). Betonarme Yapıların Deprem Dayanımı Bakımından Değerlendirilmesi ve Güçlendirilmesi, *Deprem Güvenli Konut Sempozyumu*, Ankara.
- Trifunac, M.D. and Brady, A.G. (1975) A study on the duration of strong earthquake ground motion, *Bulletin of Seismological Society of America* 65, 581–626.
- Turkish Standards Institute. (1987). Design Loads for Buildings, TS 498, Ankara, Turkey.
- Turkish Standards Institute. (2000). Requirements for Design and Construction of RC Structures, TS 500, Ankara, Turkey.
- Uniform Building Code. (1997). International Conference of Building Officials, Whittier, California.
- Valles, R.E., Reinhorn, A.M., Kunnath, S.K., Li, C., and Madan, A. (1996). IDARC–2D Version 4.0: A Program for the Inelastic Damage Analysis of Buildings, *Technical Report* NCEER–96–0010, Buffalo, NY.
- Wen, Y.K., Ellingwood, B.R., Veneziano, D., and Bracci, J. (2003). Uncertainty Modeling in Earthquake Engineering. *MAE Center Project FD–2 Report*.
- Wen, Y.K., Ellingwood, G. T., and Bracci, J. (2003). Vulnerability Function Framework for Consequence–based Engineering, *Draft Report*, Project Title: DS–4, Vulnerability Functions, Mid–America Earthquake Center, University of Illinois at Urbana Champaign.

- Whitman, R.V., Reed, J.W., and Hong S.T. (1974). Earthquake Damage Probability Matrices, *Proceedings of the 5th World Conference on Earthquake Engineering*, Rome, 2531–2540.
- Wu, C.L. and Wen, Y.K. (2000). Earthquake Ground Motion Simulation and Reliability Implications, *Structural Research Series* No. 630. University of Illinois at Urbana–Champaign, June 2000.
- Wyss, G.D. and Jorgensen, K.H. (1998). A User's Guide to LHS: Sandia's Latin Hypercube Sampling Software, *Technical Report* SAND98–0210, Risk Assessment and Systems Modeling Department, Sandia National Laboratories, Albuquerque, NM.
- Yakut, A., Aydoğan, V., Özcebe, G., and Yücemen, M.S. (2003). Preliminary Seismic Vulnerability Assessment of Existing Reinforced Concrete Buildings in Turkey – Part II: Inclusion of Site Characteristics, *Seismic Assessment and Rehabilitation of Existing Buildings*, NATO Science Series IV/29, pp. 43–58

APPENDIX A

LEGEND ABBREVIATIONS

YIELD B1	:	Flexural yielding detected at first story beam
YIELD C1	:	Flexural yielding detected at first story column
YIELD B2	:	Flexural yielding detected at second story beam
YIELD C2	:	Flexural yielding detected at second story column
YIELD BT	:	Flexural yielding detected at top story beam
YIELD CT	:	Flexural yielding detected at top story column
FAIL B1	:	Flexural failure initiated at first story beam
FAIL INI	:	Flexural failure initiated at a story beam except first story

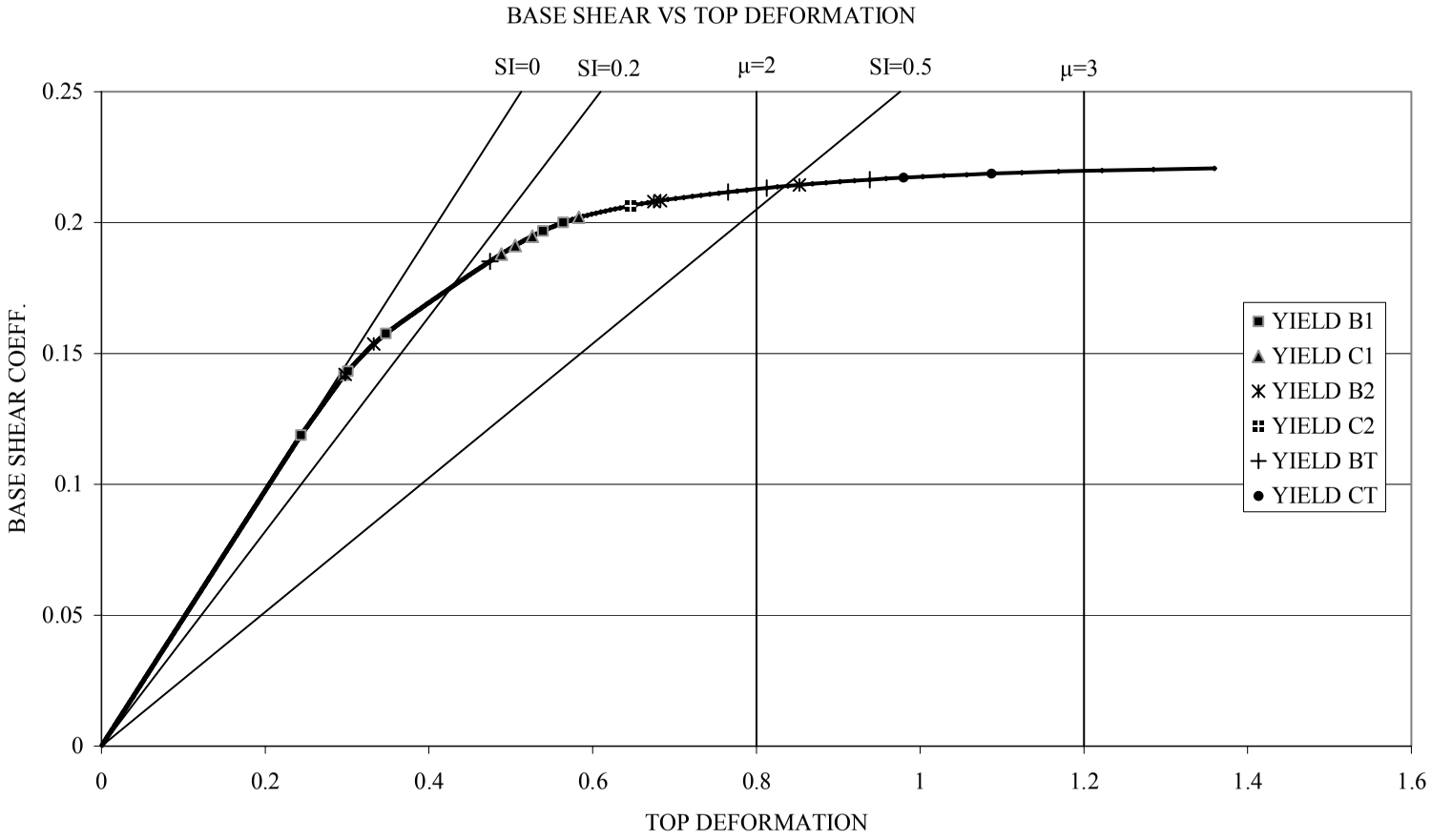

Figure A.1 Pushover curve and local response stages of MRF3–P

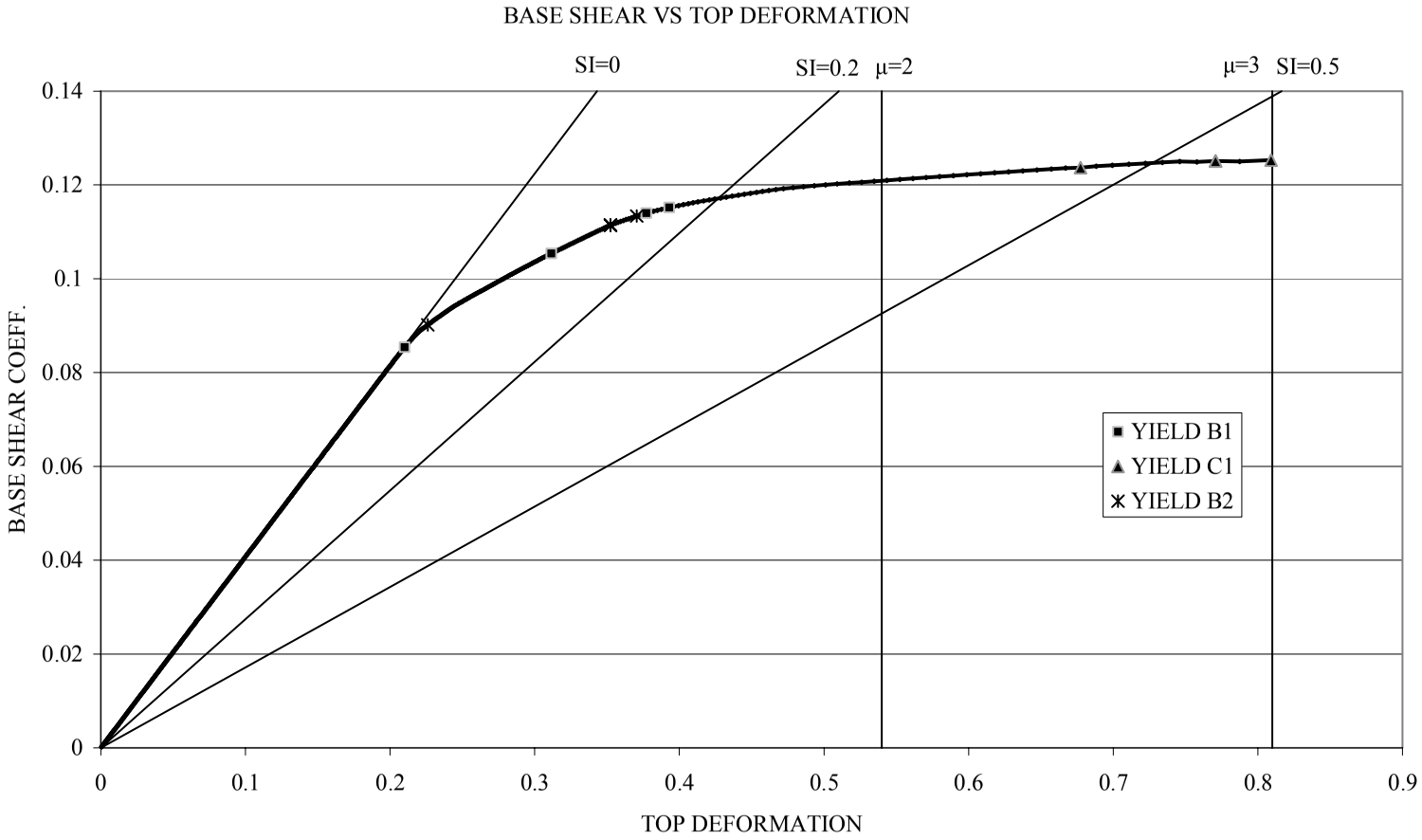

Figure A.2 Pushover curve and local response stages of MRF5–P

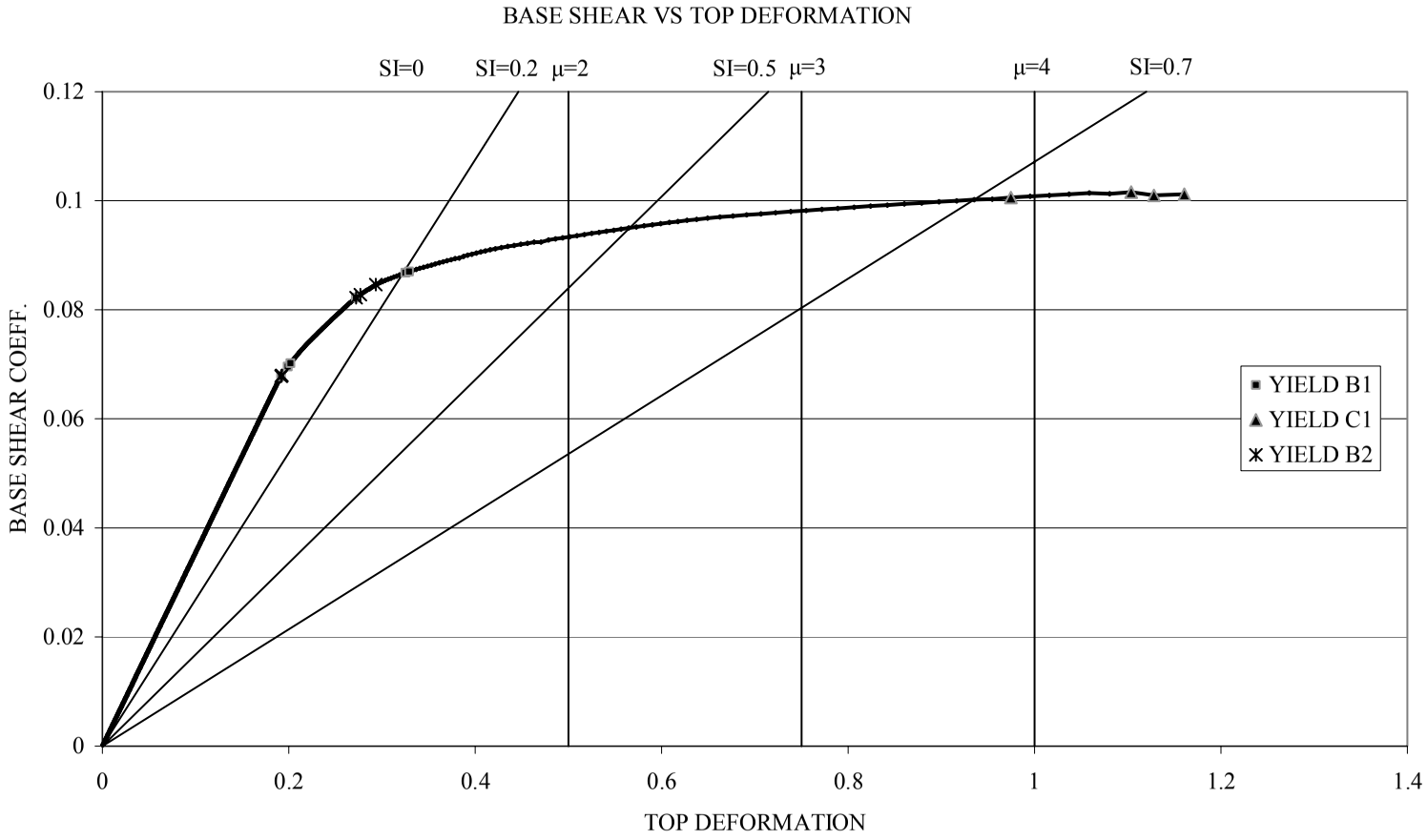

Figure A.3 Pushover curve and local response stages of MRF7–P

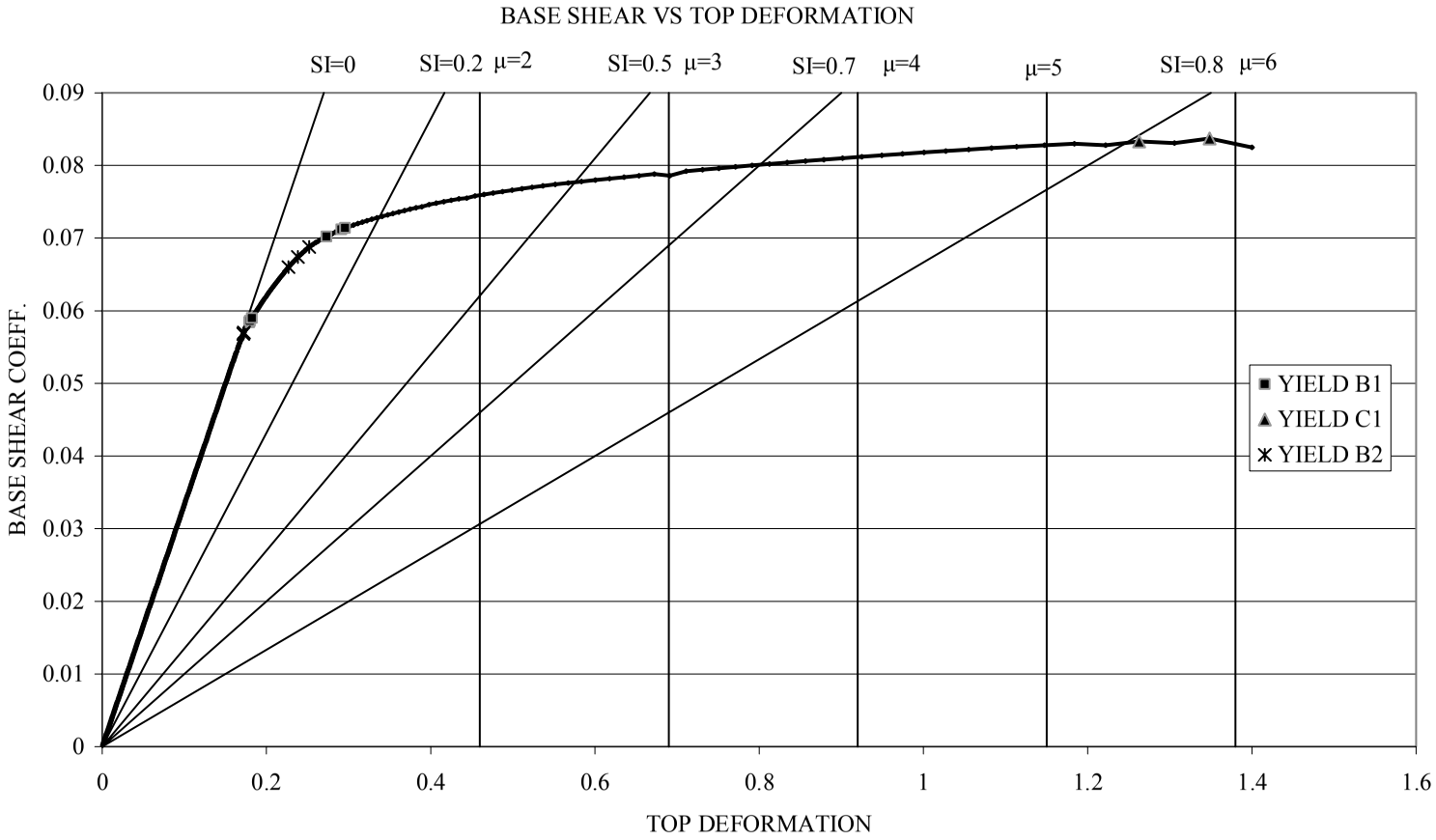

Figure A.4 Pushover curve and local response stages of MRF9–P

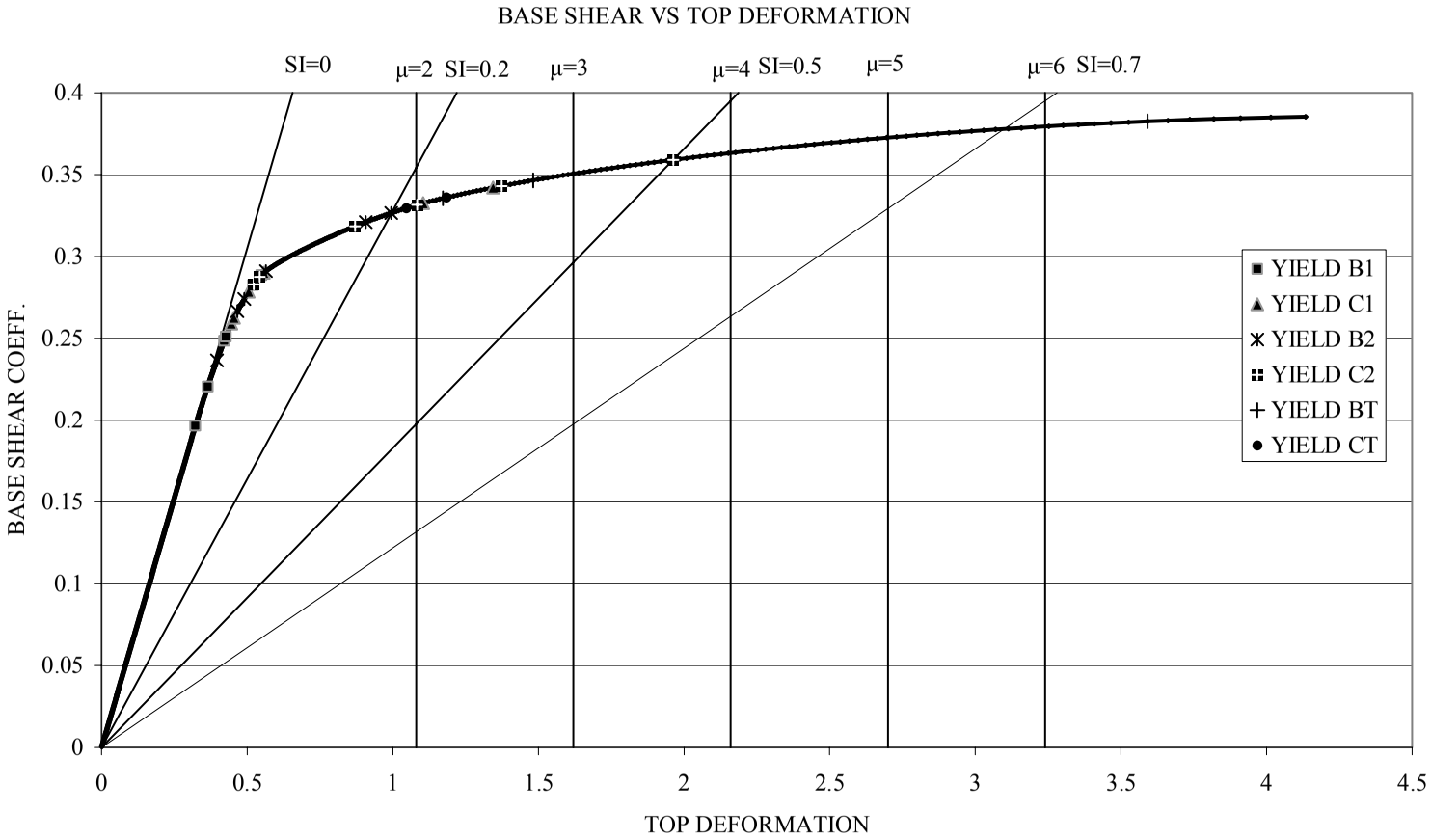

Figure A.5 Pushover curve and local response stages of MRF3–T

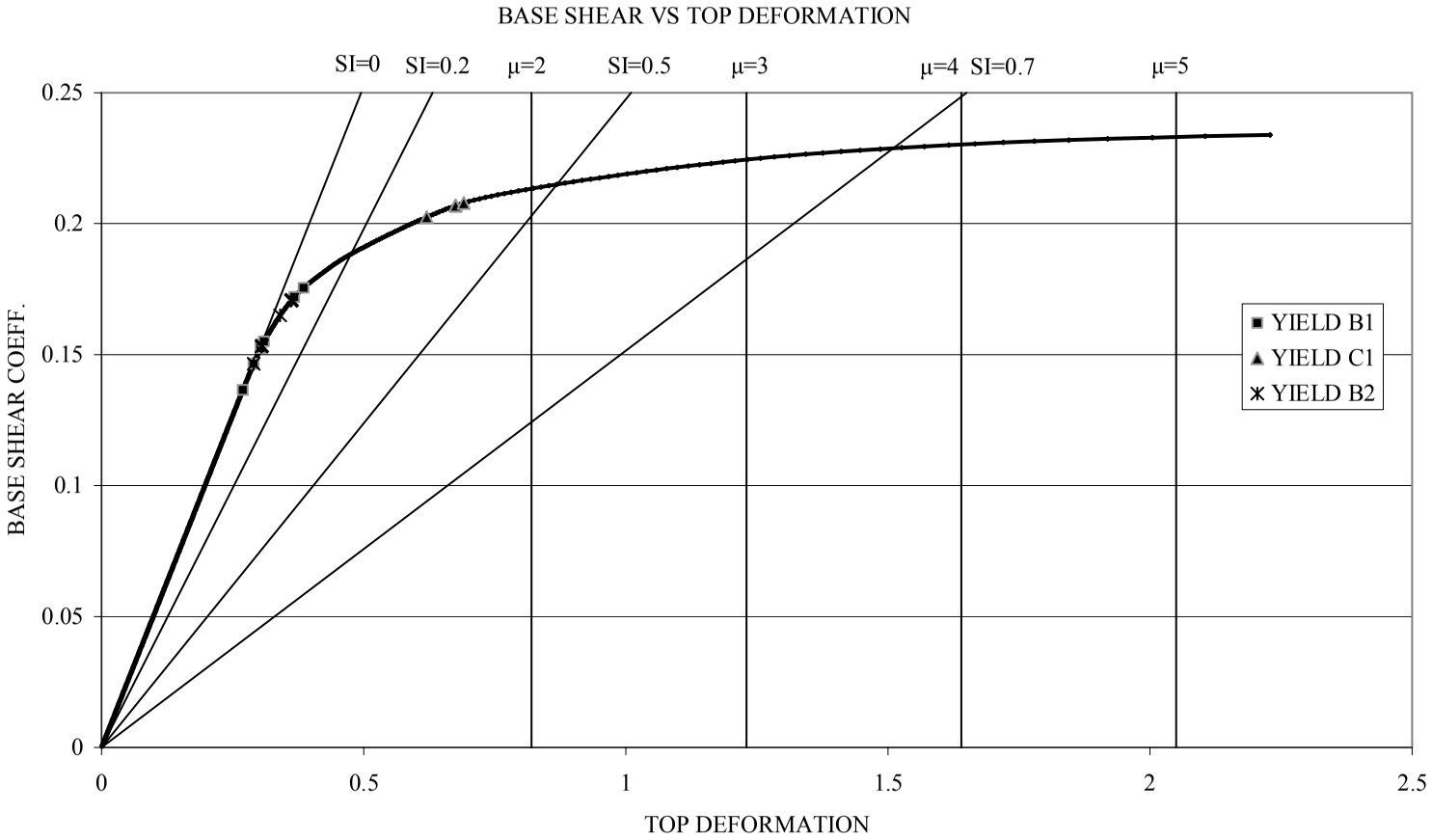

Figure A.6 Pushover curve and local response stages of MRF5–T

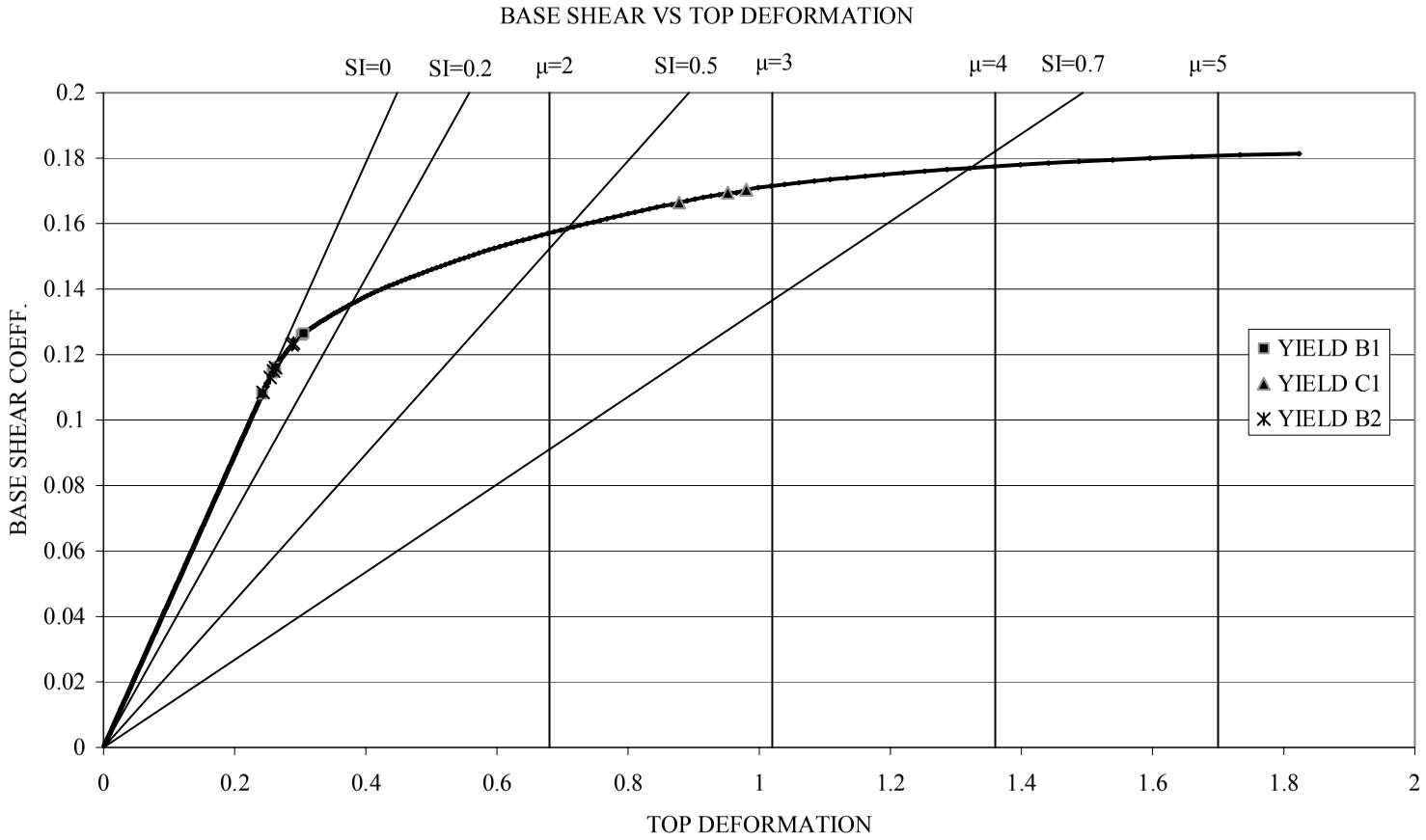

Figure A.7 Pushover curve and local response stages of MRF7–T

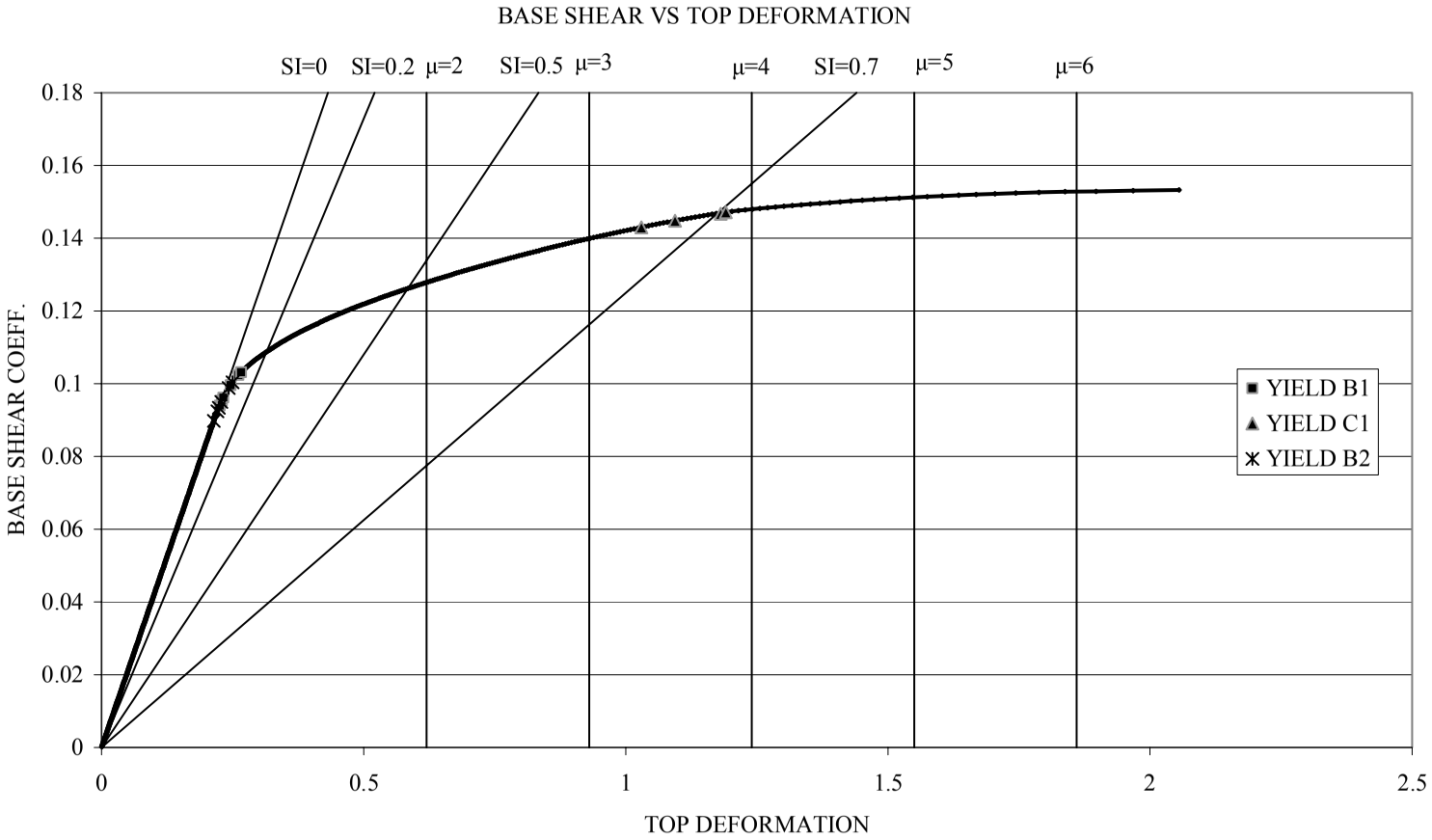

Figure A.8 Pushover curve and local response stages of MRF9–T

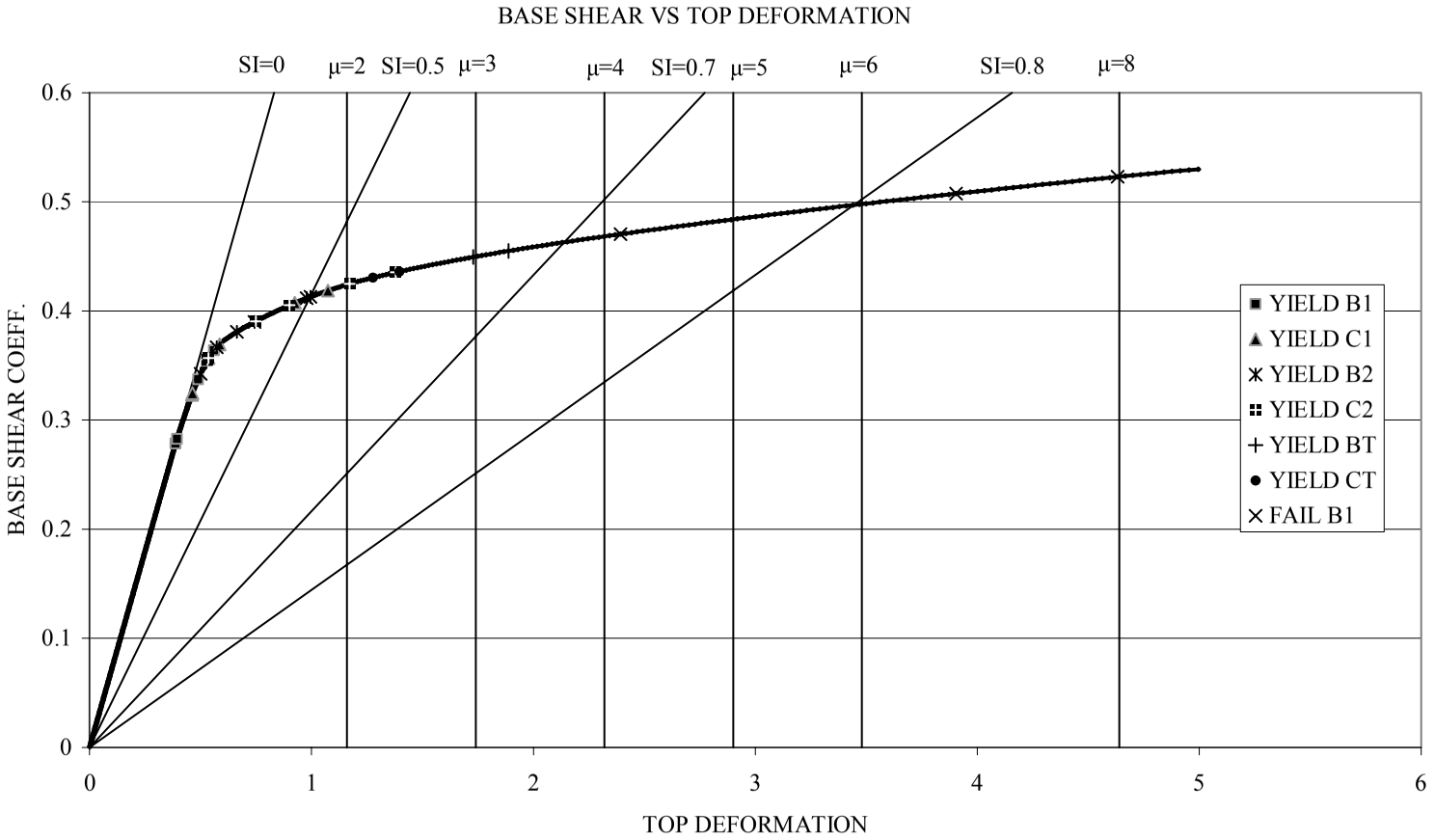

Figure A.9 Pushover curve and local response stages of MRF3–S

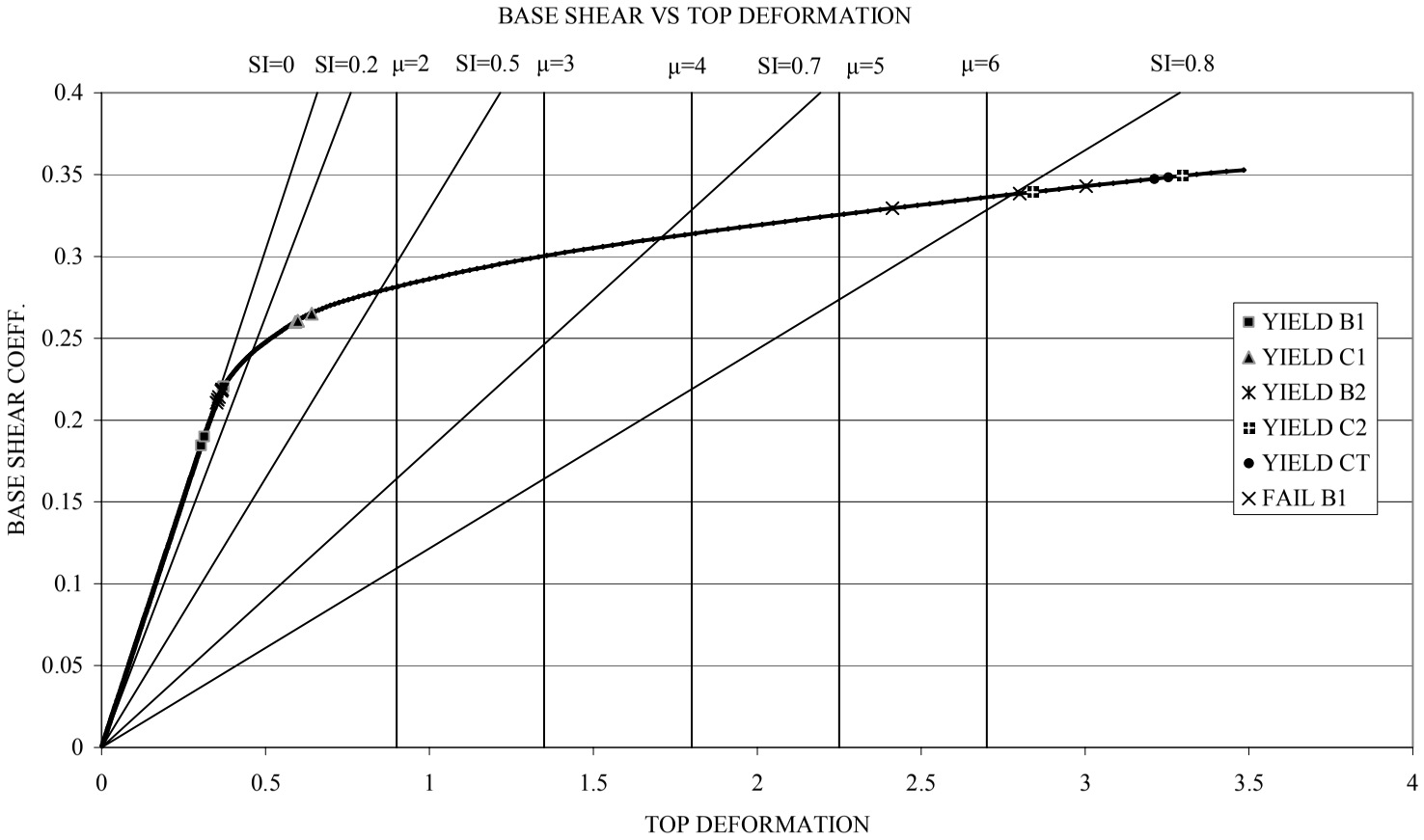

Figure A.10 Pushover curve and local response stages of MRF5–S

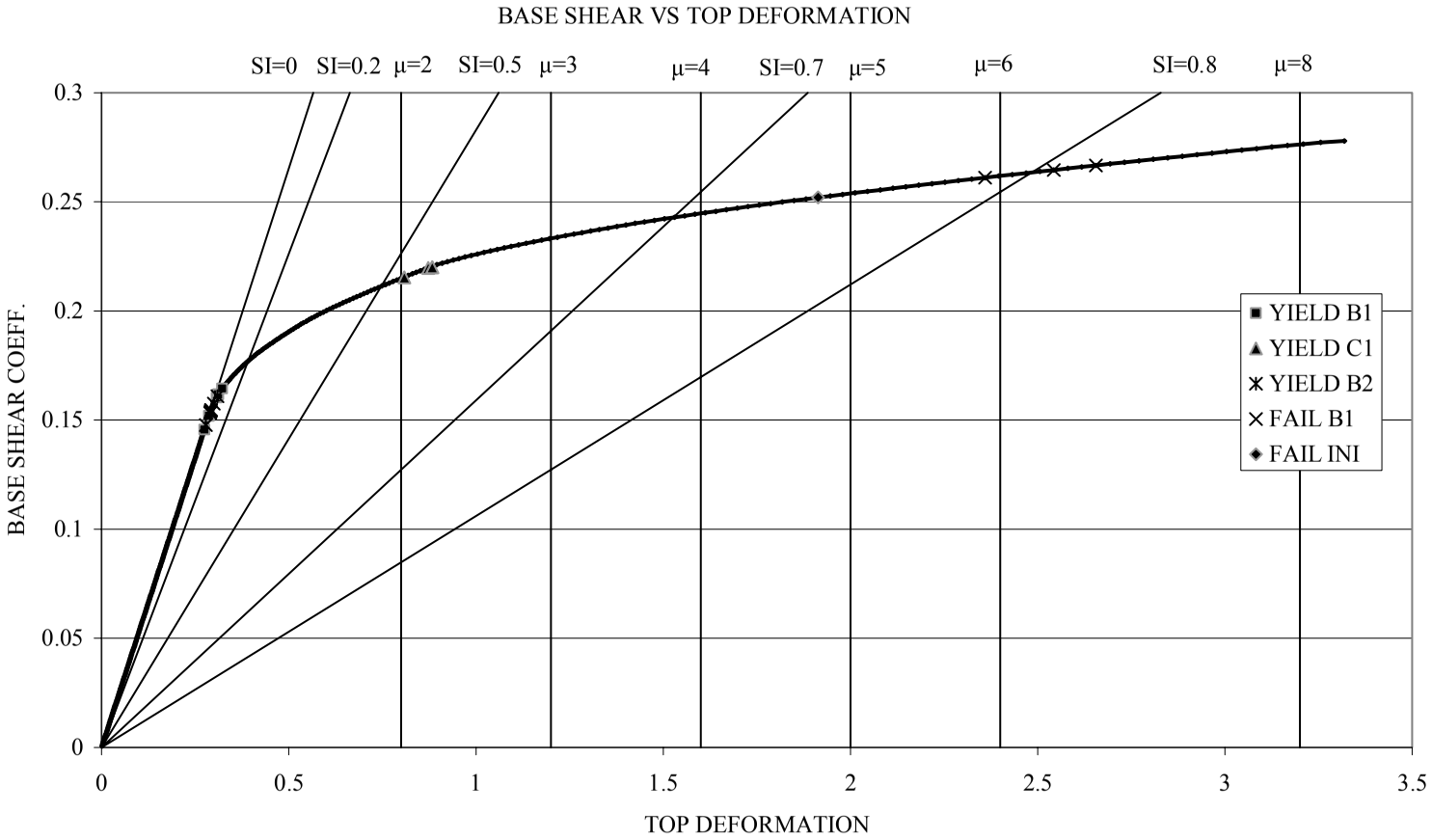

Figure A.11 Pushover curve and local response stages of MRF7–S

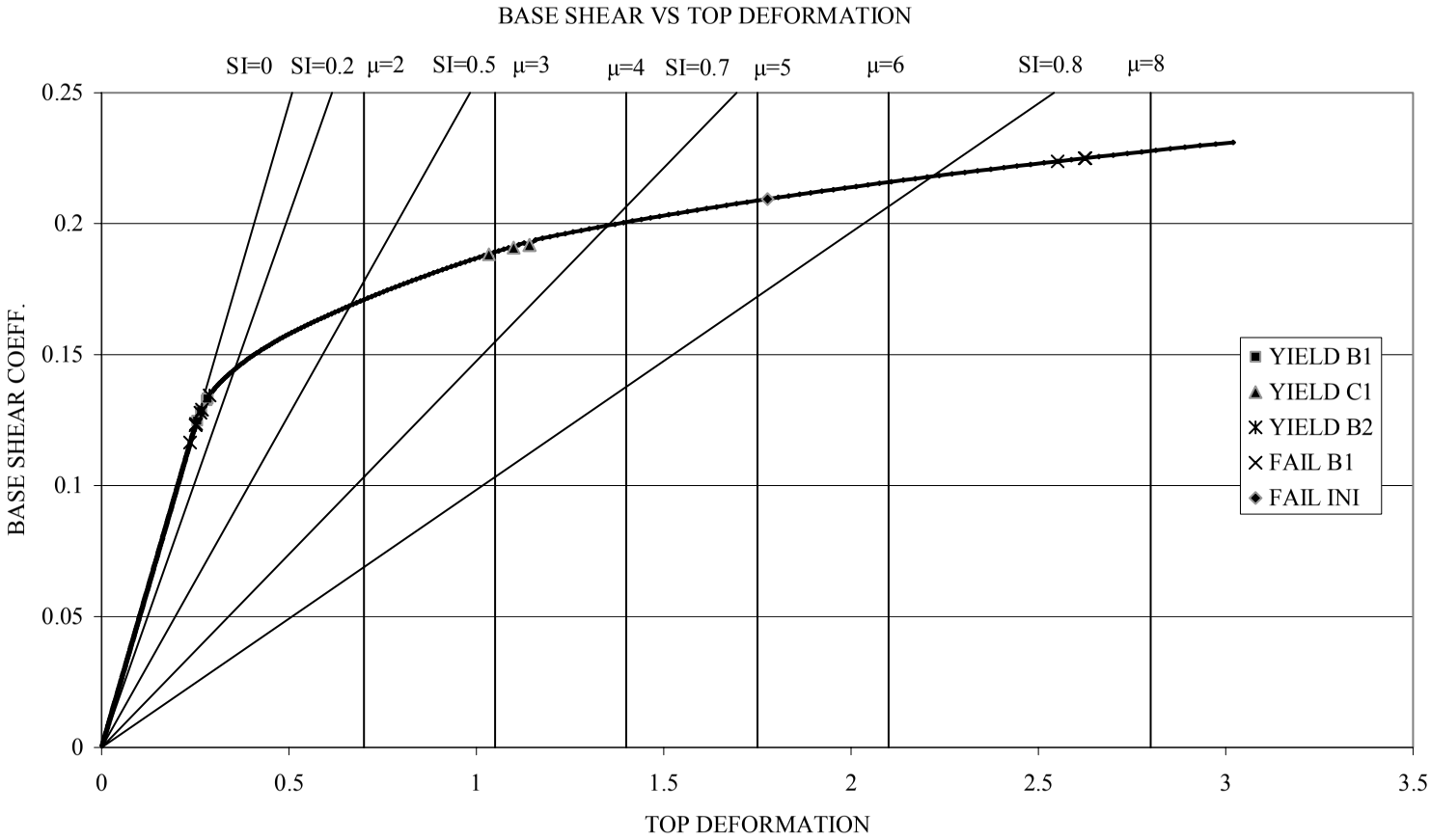

Figure A.12 Pushover curve and local response stages of MRF9–S

APPENDIX B

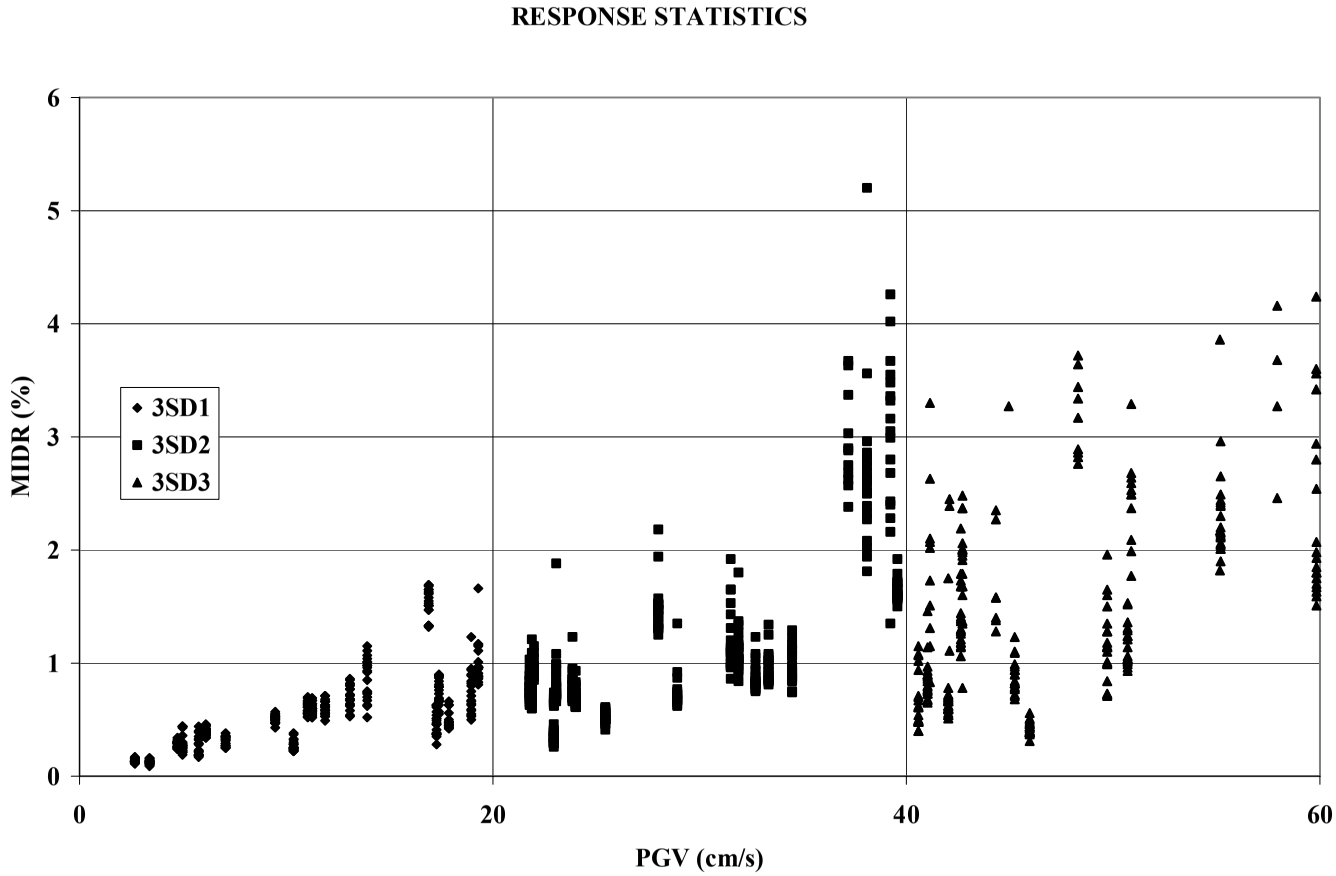

Figure B.1 Time–history results of MRF3–P

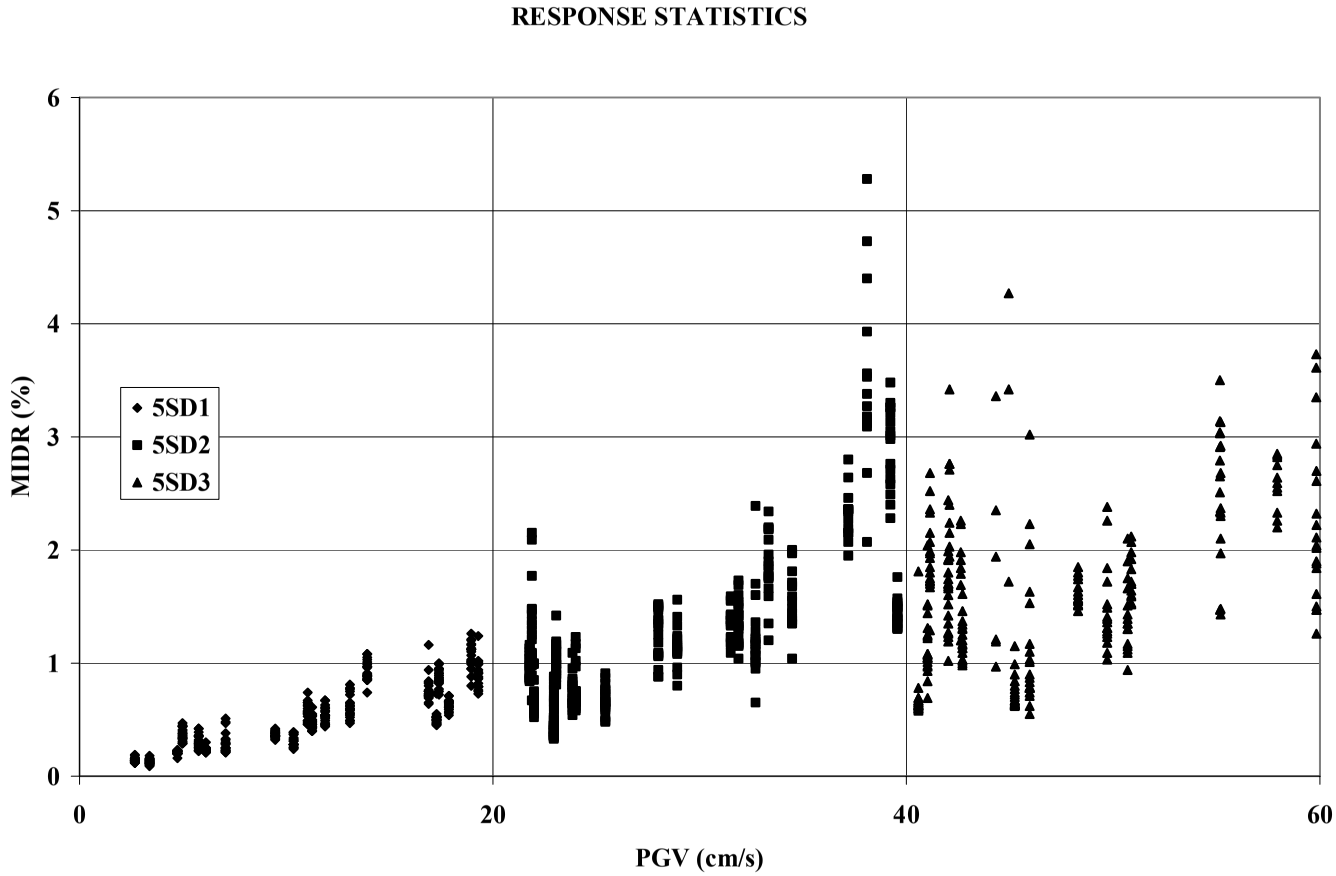

Figure B.2 Time–history results of MRF5–P

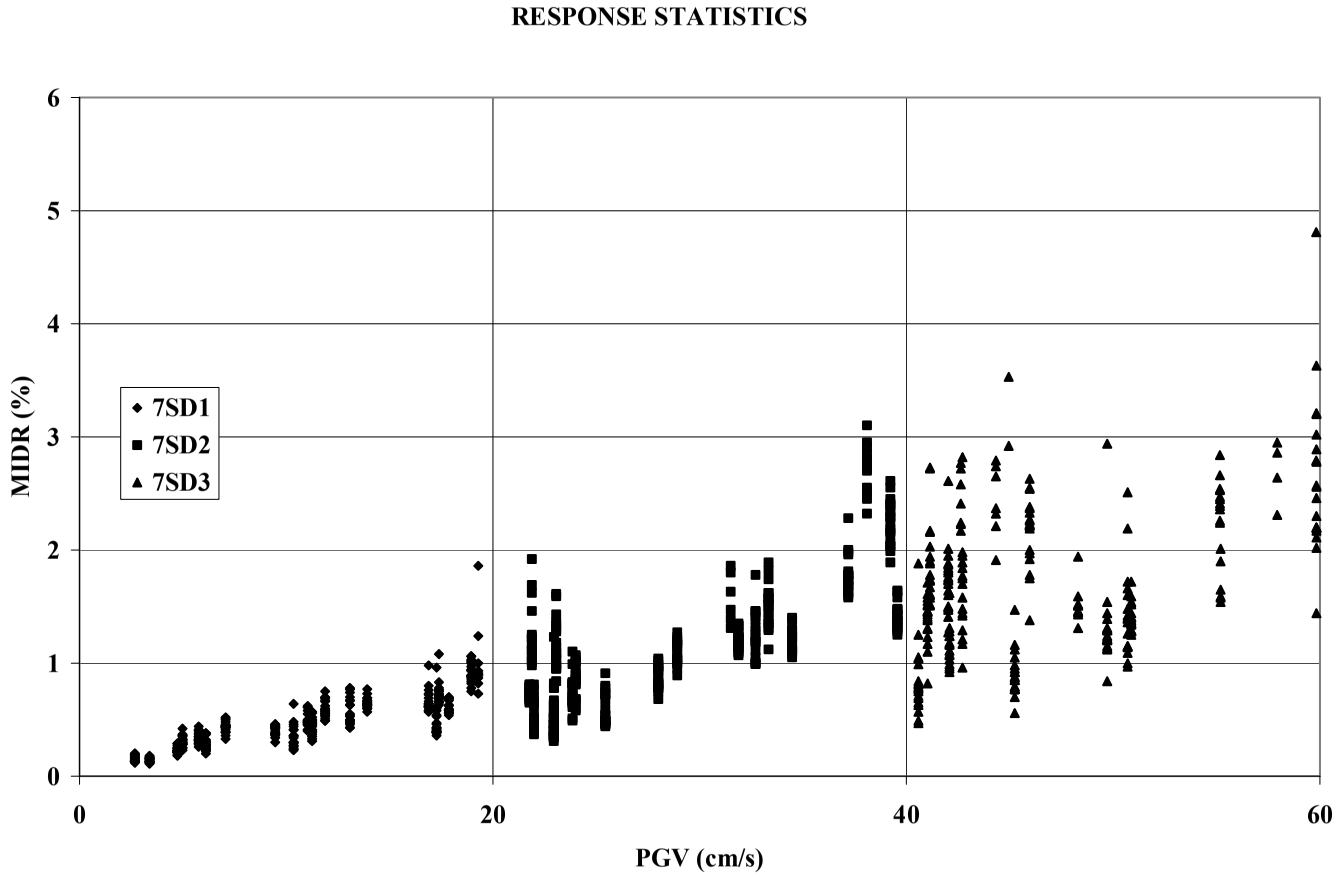

Figure B.3 Time–history results of MRF7–P

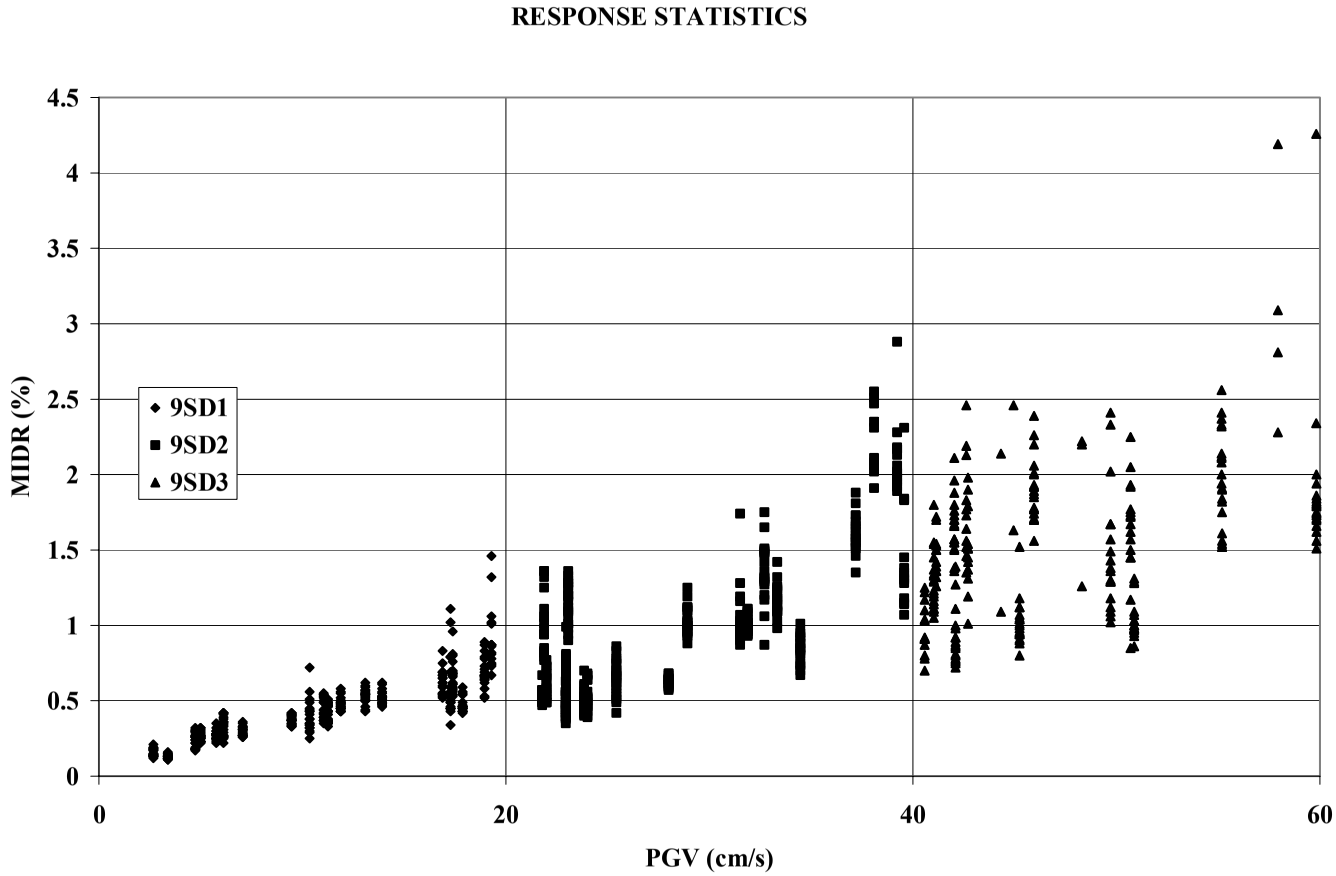

Figure B.4 Time–history results of MRF9–P

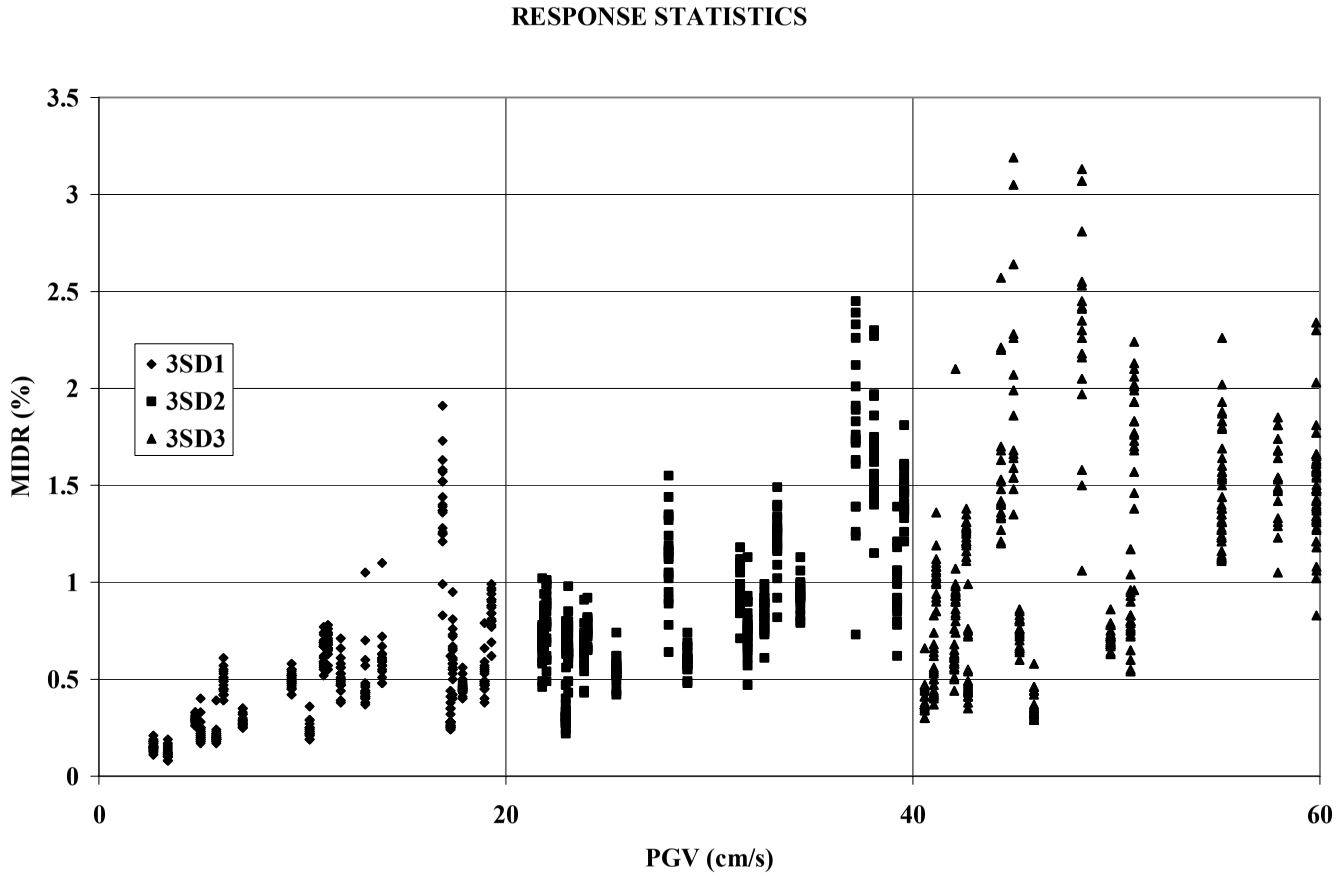

Figure B.5 Time–history results of MRF3–T

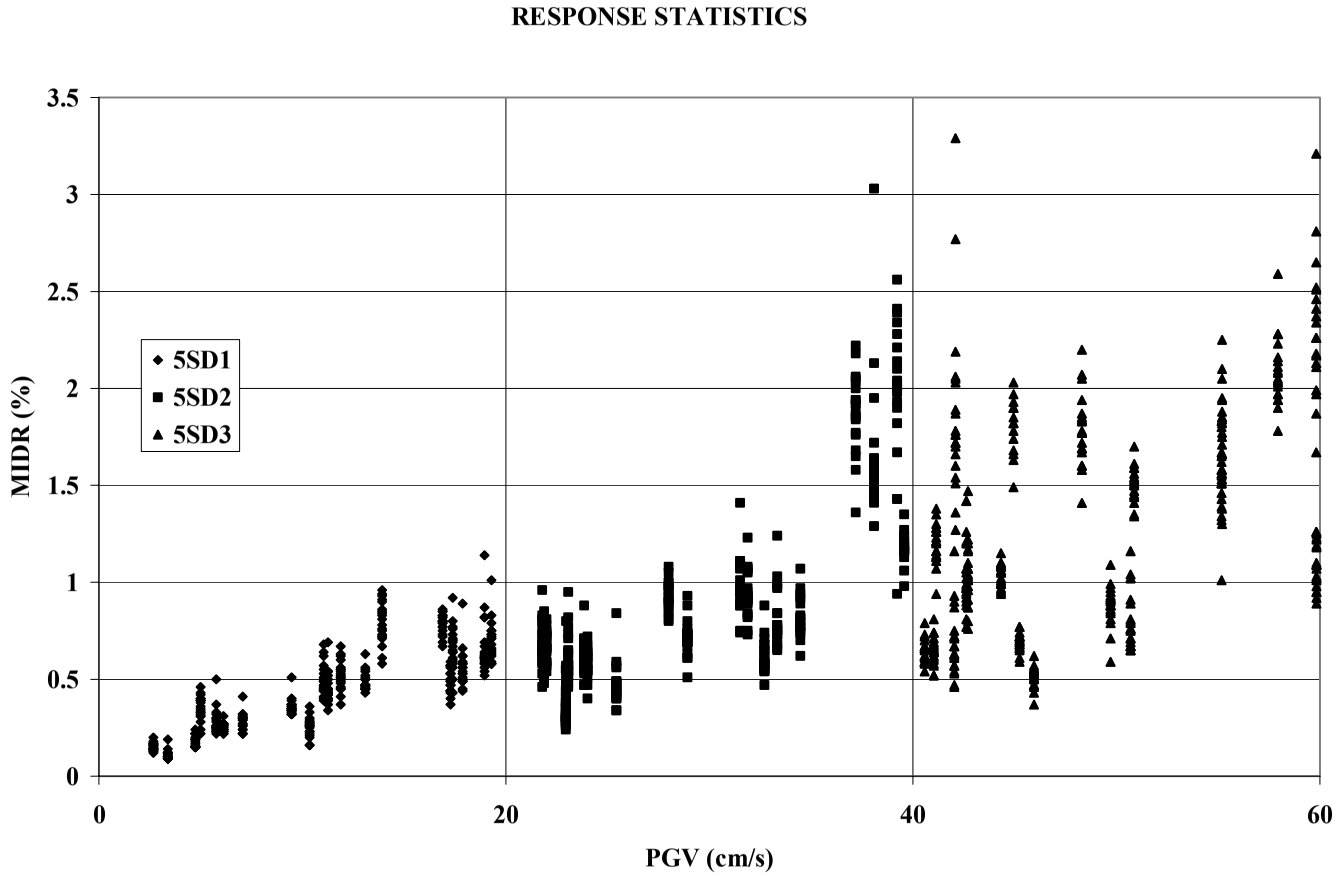

Figure B.6 Time–history results of MRF5–T

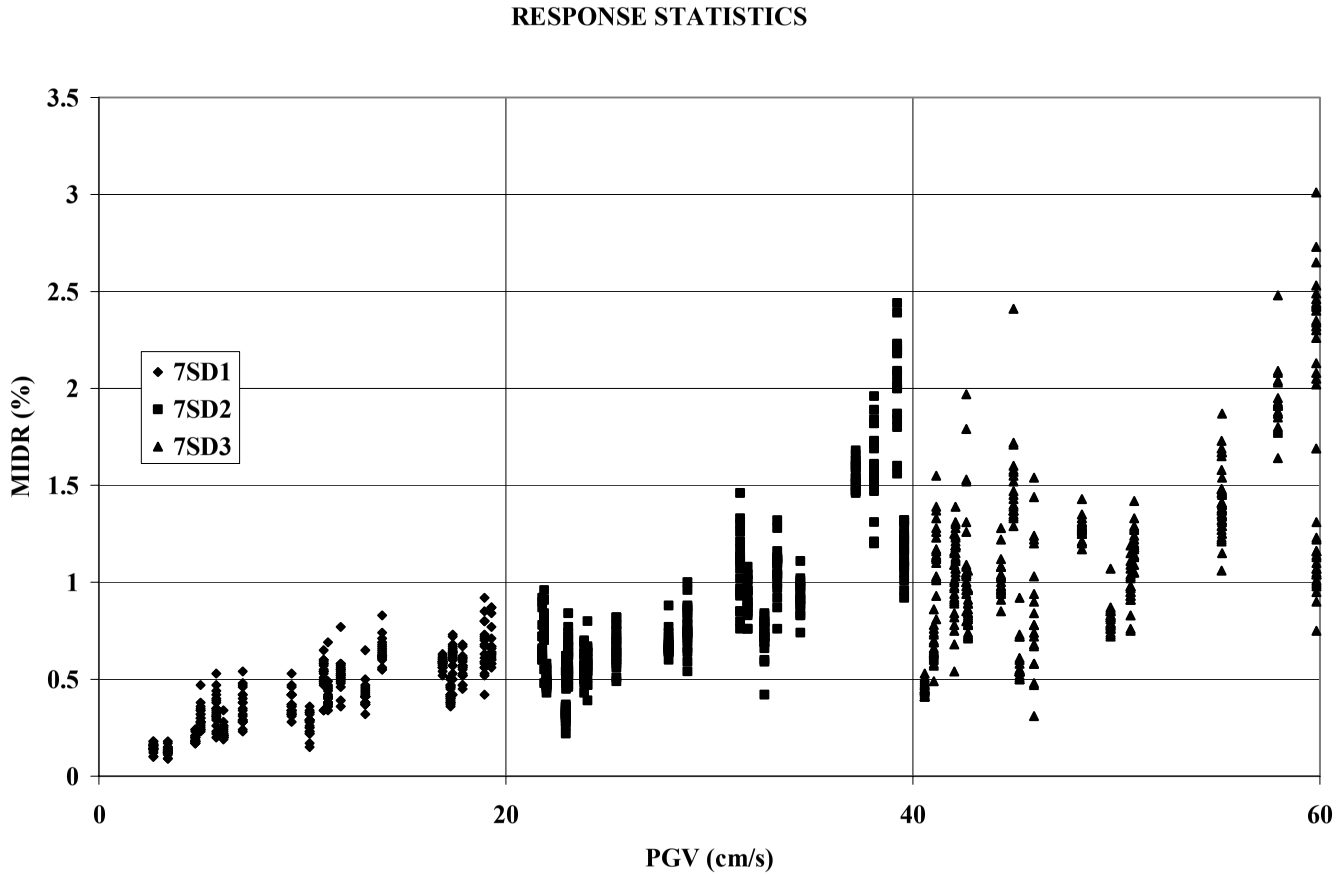

Figure B.7 Time–history results of MRF7–T

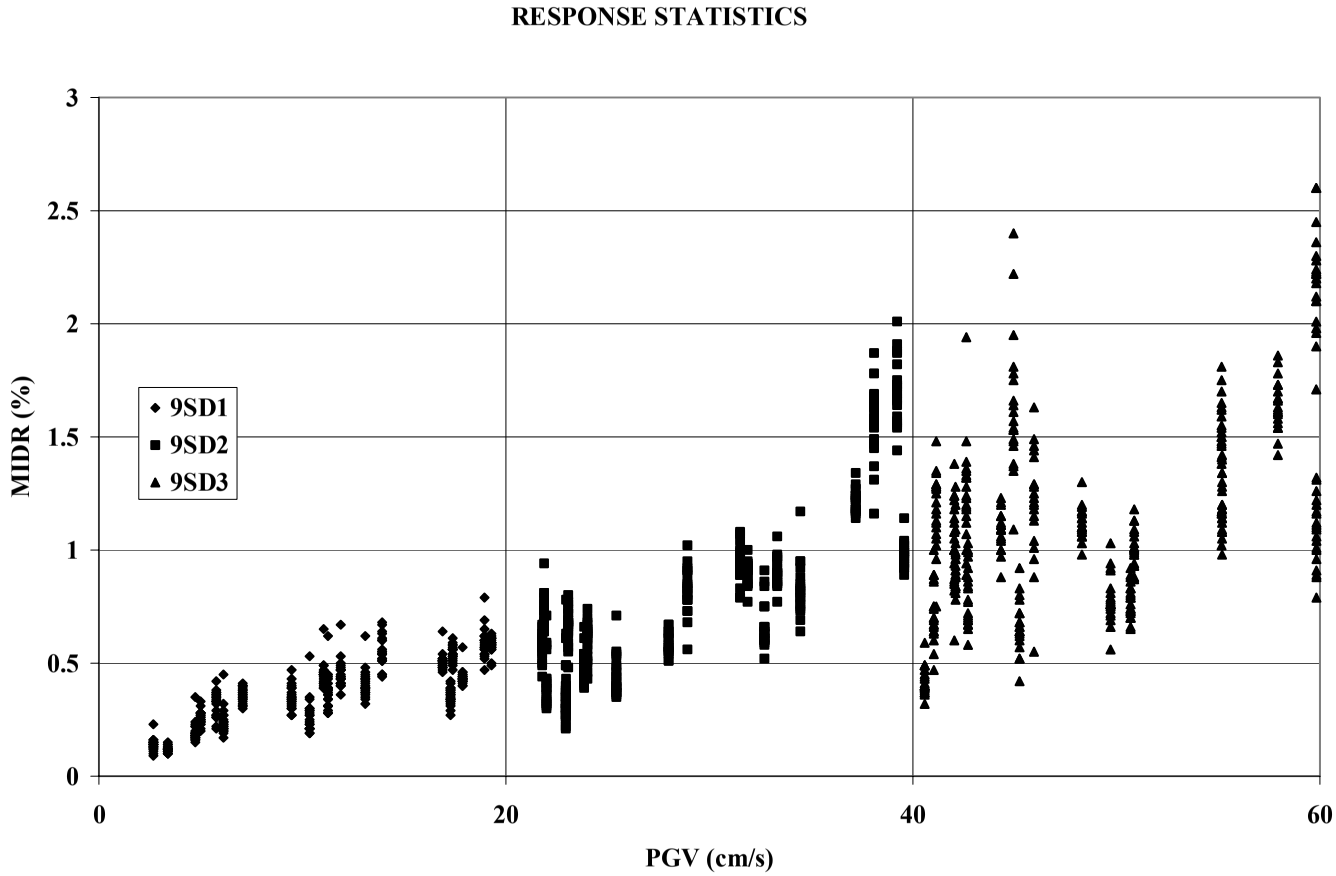

Figure B.8 Time–history results of MRF9–T

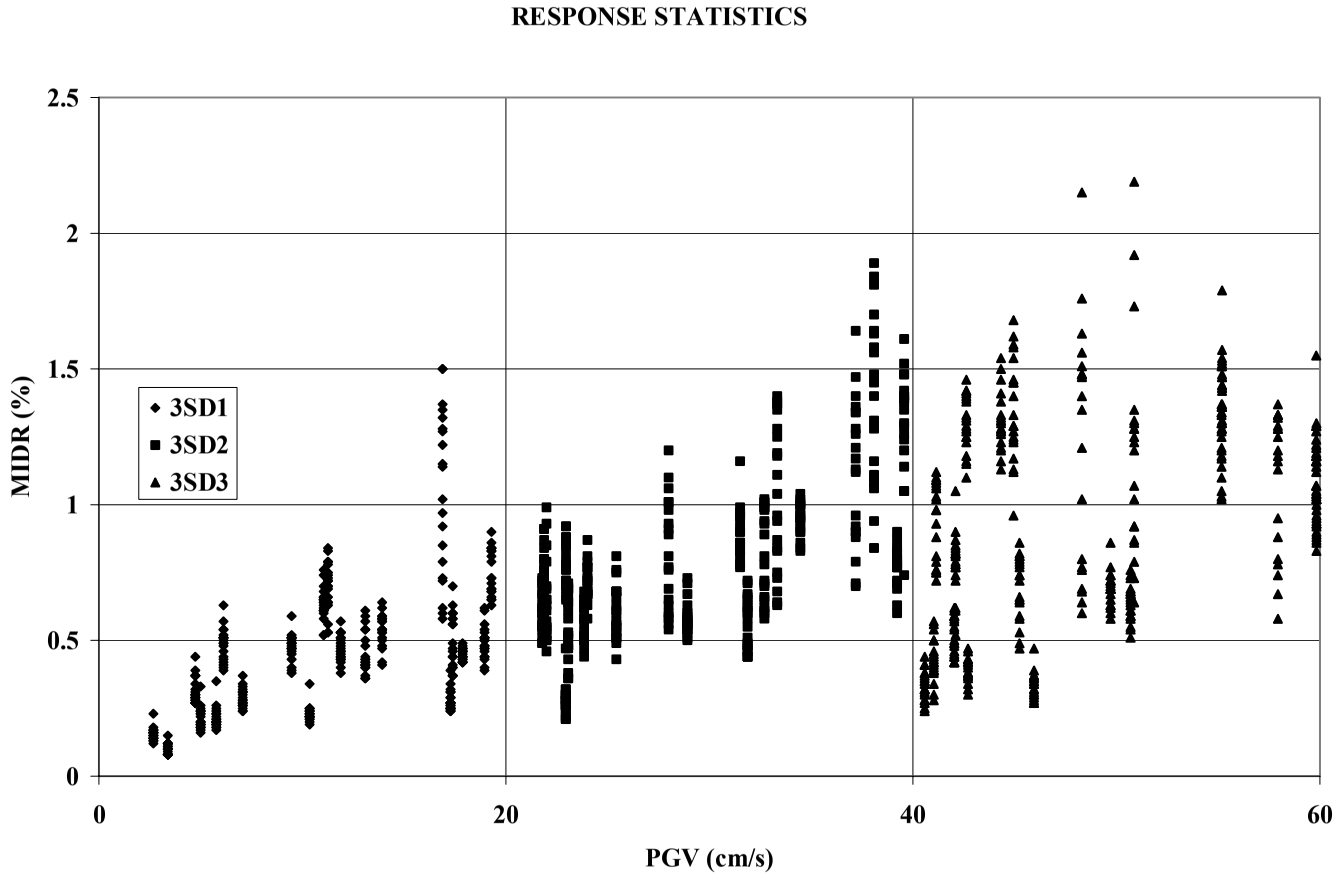

Figure B.9 Time–history results of MRF3–S

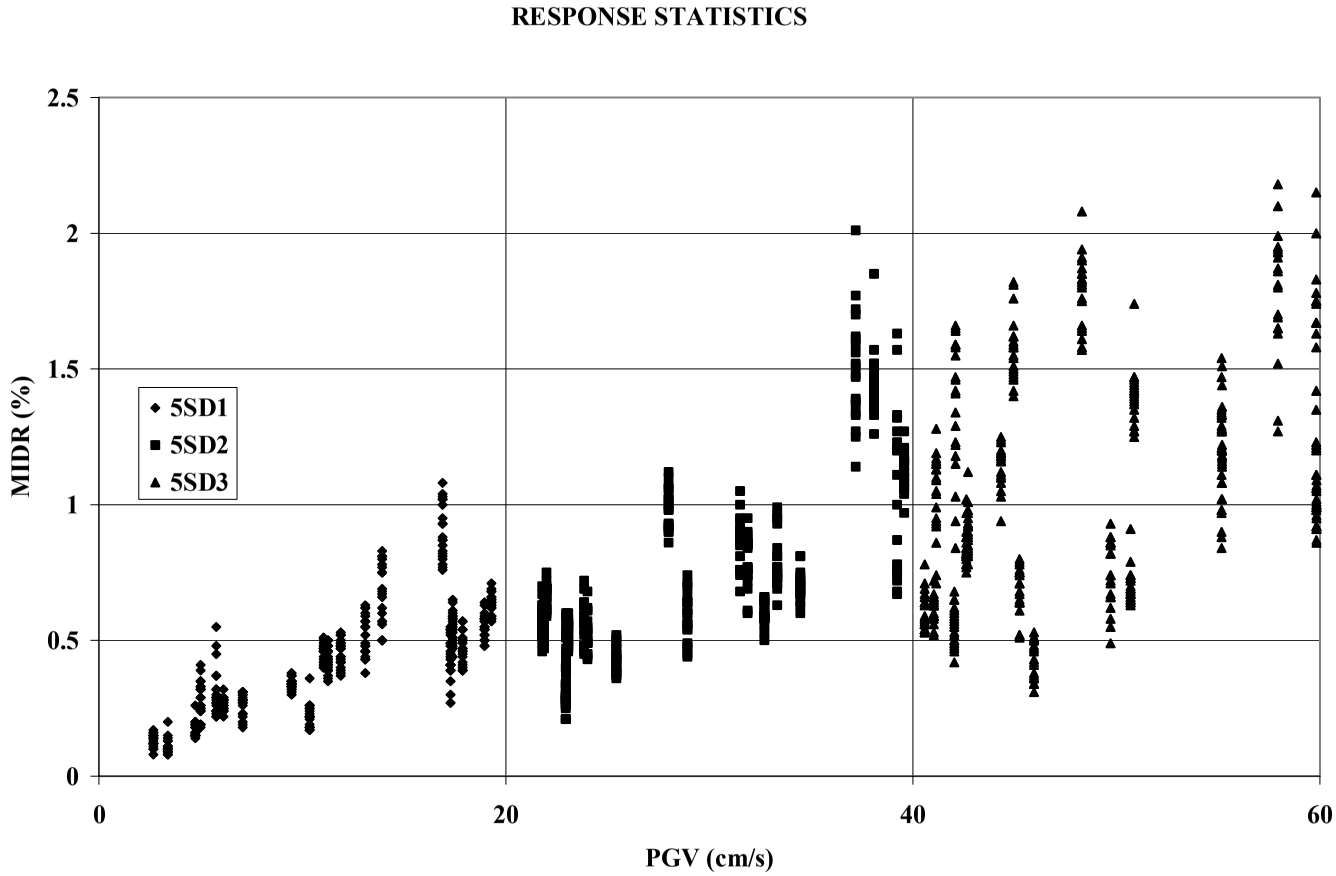

Figure B.10 Time–history results of MRF5–S

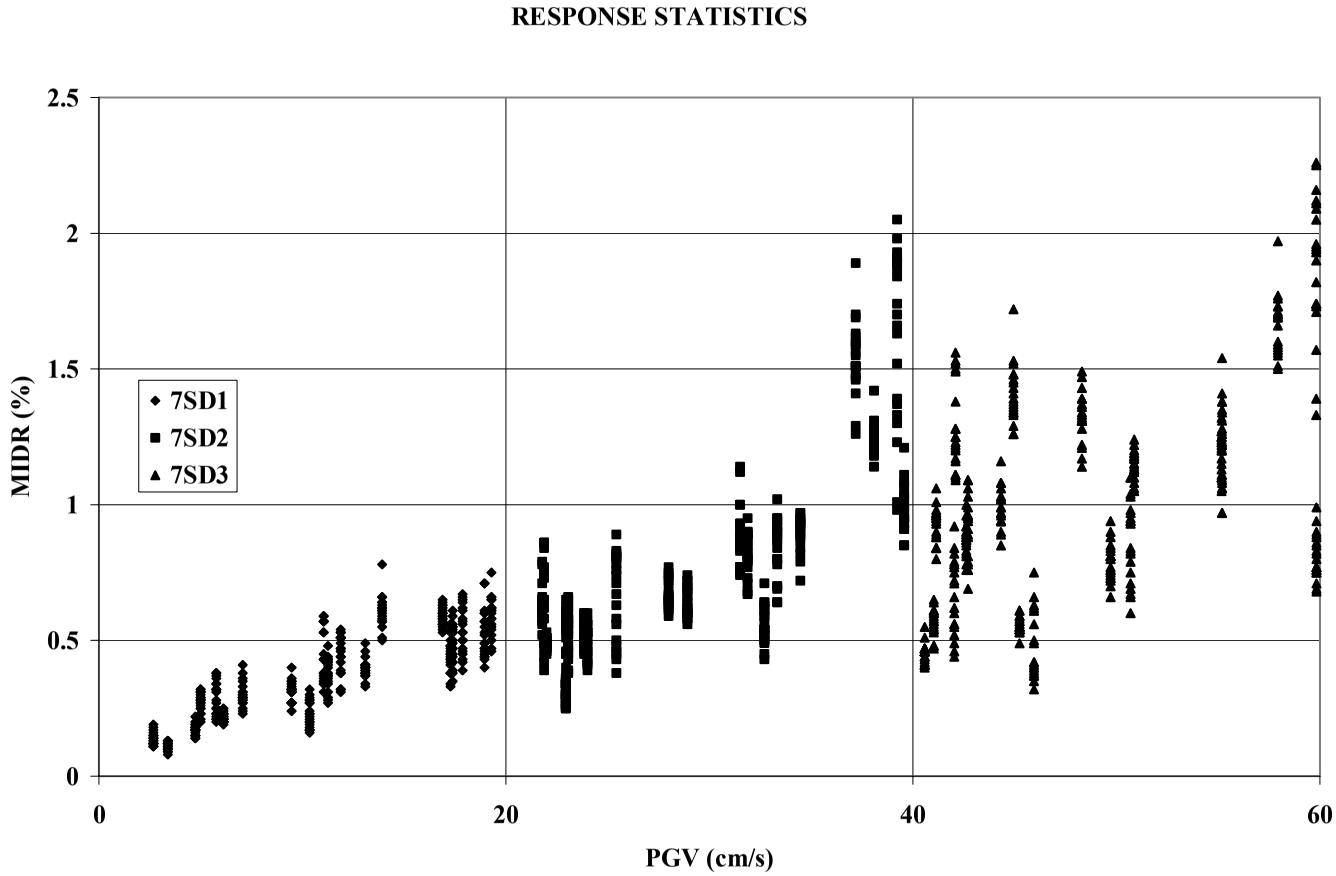

Figure B.11 Time–history results of MRF7–S

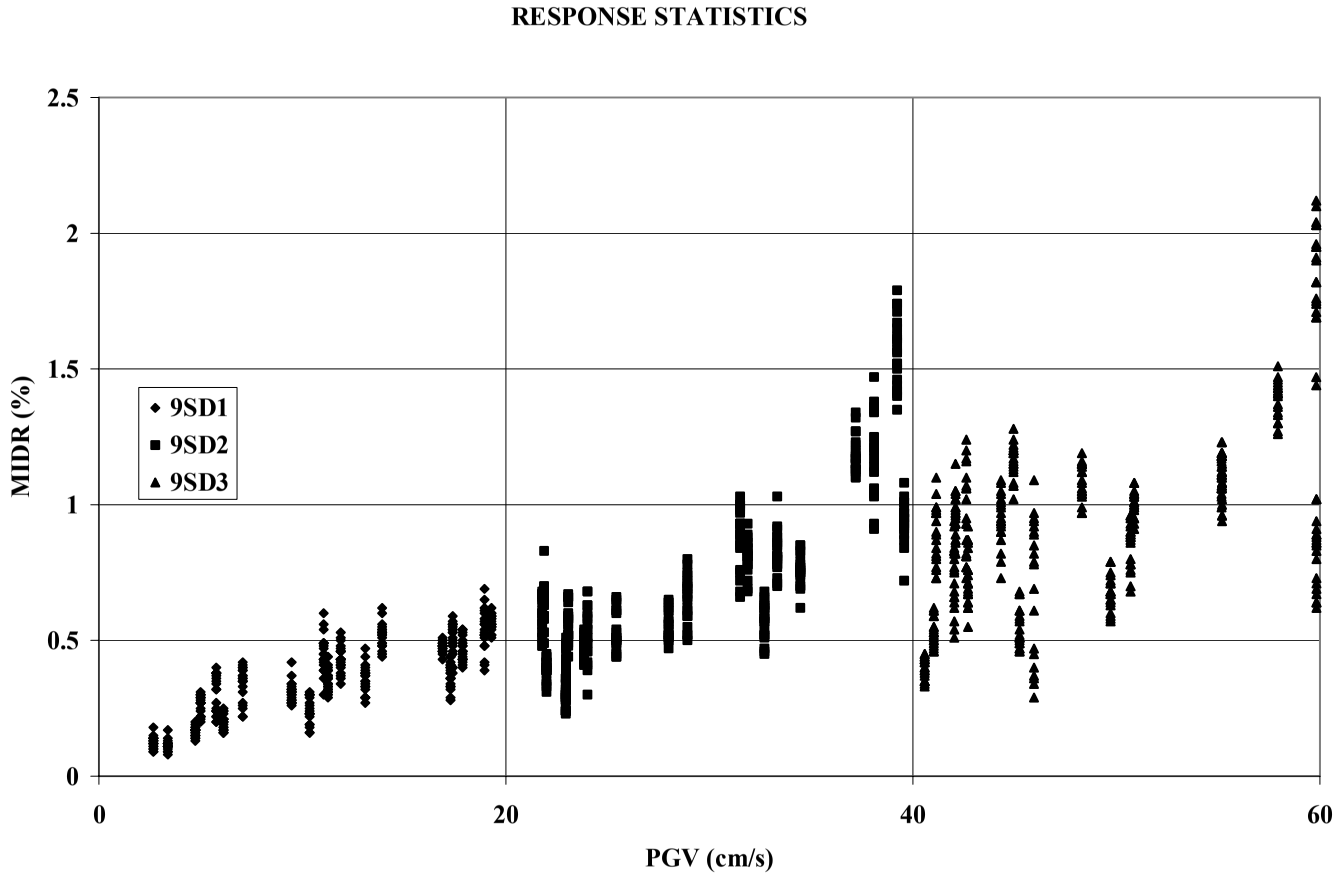

Figure B.12 Time–history results of MRF9–S